

The Synaptic RNAome - identification, interactions and intercellular transfer

Dissertation

for the award of the degree
“Doctor rerum naturalium”
of the Georg-August-Universität Göttingen

within the *IMPRS for Neurosciences*,
of the Göttingen Graduate Center for Neurosciences, Biophysics and Molecular Biosciences (GGNB)

submitted by
Robert Epple
born in Leipzig, Germany

Göttingen 2021

Thesis Committee:

Prof. Dr. André Fischer

German Center for Neurodegeneration, Göttingen

Dr. Camin Dean

Charité - Berlin University of Medicine, Berlin

Prof. Dr. Tiago Outeiro

Department of Experimental Neurodegeneration, Göttingen

Members of the Examination Board:

Prof. Dr. Martin Göpfert

Department of Cellular Neurobiology, Schwann Schleiden Research Center, Göttingen

Prof. Dr. Sarah Köster

Georg-August-University Göttingen, Institute for X-Ray Physics, Göttingen

Prof. Dr. Ralf Heinrich

Department of Cellular Neurobiology, Georg-August-University Göttingen, Göttingen

Date of oral examination: March, 2nd, 2021

Table of contents

Abstract.....	1
General Introduction	2
Synapses as the basic units of neuronal information.....	2
Synaptic weights.....	3
Changing the synaptic weights - local translation.....	5
RNAome regulation.....	6
Isolation of synaptic RNA.....	8
Scope of this thesis.....	10
Chapter 1 - The coding and small-non-coding hippocampal synaptic RNAome.....	11
Author contributions.....	11
Abstract.....	12
Acknowledgements	13
Introduction.....	13
Results.....	14
Discussion.....	23
Material and Methods.....	27
Notes	33
References.....	34
Supplementary material.....	38
Addendum.....	40
Chapter 2 - Studying the effects of locally inhibiting a miRNA.....	44
Introduction.....	44
Material and Methods.....	45
Results.....	46
Discussion.....	48

Chapter 2.1 Intercellular RNA transport.....	49
Chapter 3 - Astrocytes transfer RNAs to neurons for translation.....	51
Author contributions.....	51
Abstract.....	52
Introduction.....	53
Results.....	54
Discussion.....	65
Material and methods.....	71
Notes and acknowledgements.....	78
References	79
Supplementary material.....	85
Supplementary figures	90
Discussion.....	92
Importance of local translation in diseases	92
Identification of synaptic RNAs	92
Advantages of SNIDER.....	93
Interaction of synaptic RNAs.....	94
Intercellular origin of synaptic RNAs.....	95
InSUREns.....	97
Means of RNA transport.....	97
ADEVs as a way to transfer RNAs.....	98
Extracellular vesicle internalization mechanisms.....	98
lncRNAs in ADEVs.....	99
Synaptic tagging.....	100

Outlook and possible improvements.....	102
1) InSUREns modifications and use cases.....	102
2) ADEVs - open questions.....	102
3) Extending the regulatory network with more ncRNAs.....	103
4) Combining 4TU tagging and SNIDER.....	103
List of Abbreviations.....	105
Bibliography.....	106
Acknowledgements.....	113
Declaration.....	114

Abstract

Synaptic plasticity is how neurons adapt to new stimuli and necessitates changes in synaptic weight. For these changes to be durable, local translation in neurites, and at pre- and post-synapses is required. Current methods do not capture the pool of local RNAs in its entirety and focus mainly on mRNAs. Here, I focused on wide-scale interactions between non-coding RNAs and mRNAs at hippocampal synapses; data were collected from synaptosomes and an advanced microfluidic culture system. This new method, SNIDER (**SyNapse Isolation Device** by **R**efined Cutting), was developed to obtain pure neuronal, neurite-localized RNAs; it works by precisely cutting the synaptic compartment of microfluidic chambers, yielding more mRNAs than synaptosome isolation. I also used SNIDER to study the effects of KCl stimulation on the local RNAome. In another experiment, synapses were locally perfused with an inhibitor of miR-9-5p, an abundant microRNA in synaptosomes that is linked to neuronal development as well as dendrite morphology. Surprisingly, after isolation of inhibited synapses with SNIDER, I found the local transcriptome to be unchanged - even though miR-9-5p inhibition produced clear effects in neuronal somata. Our findings, taken together with existing literature, suggested a glial origin of synaptic miR-9-5p. Astrocytes are highly abundant glia cells and their end feet often engulf the pre- and postsynapse to form the tri-partite synapse. To study astrocyte to neuron RNA transfer, I designed a novel method, InSUREns (**I**ntercellularly **S**hipped and **U**ptaken **R**NAs **E**nsnared), whereby astrocytic RNAs were labeled with 4-thiouracil and neuronal ribosomes were labeled with HA-tags. By applying a double pull-down strategy, astrocytic RNAs that were transported into neurons for translation can then be identified. Astrocyte-derived extracellular vesicles (ADEV) were investigated as the means of RNA transportation. Indeed, ADEV internalization took place over the whole neuronal cell body, including neurites. ADEVs furthermore contained many RNAs that were identified via InSUREns. Additionally, many lncRNAs were present in ADEVs that are known to interact with synaptic RNAs. These data suggest an important role of ADEVs in supplying neuronal and synaptic RNAs. Finally, a hypothesis is developed, how astrocytic RNAs could form the synaptic tag in the synaptic tagging and capturing model.

Introduction

Neurons have a problem. They have long axons and dendrites - extensions that can protrude dozens of micrometers, sometimes even centimeters away from the nucleus. Between axons and dendrites synapses are formed, the processing units of all brain activity. Yet, much like any other compartment of the cell, the axon and the dendritic tree need to be supplied with proteins. What is more, these proteins have to be available upon specific time points in order to facilitate the molecular changes that occur during learning.

This logistical challenge is not unlike that of furniture retailers. In both cases, there are several far-dispersed places where certain products are in demand. In case of the furniture retailer, ready-to-assemble furniture can be delivered to customers' homes, where clients are building the furniture when and however it suits them best. By outsourcing the actual manufacturing, the retailer saves costs and time.

Similarly, neurons can transport the blueprints - mRNAs - for proteins into their axons and dendrites, where they are locally translated into proteins, far away from the nucleus. As a result, the timing and amount of protein synthesis is only dependent on the immediate surrounding of the synapse, invaluable to implement learning at high resolution. Studies could even show that this local production of key synaptic proteins is crucial for facilitating a memory (Huber et al., 2000; Vickers et al., 2005).

Synapses as the basic units of neuronal information

When we publicly talk about neuroscience, the focus often lies on the function of neurons themselves, as a whole. But neurons cannot go anywhere; their position is locked and their fate sealed, as they are unable to divide. The often-heard term plasticity however implies something underlying the cellular structure of the brain that is capable of transforming.

With neurons stuck in place, plasticity can only happen at synapses; here information processing is actualized and fine-tuned. Every neuron connects between 1000 and 10,000 other neurons. Some of those connections are hard-wired and form during development, especially those that connect distant brain areas with one another, like sensory cortices with thalamus or hippocampus and amygdala. Other synapses are being so weak that throughout childhood and adolescence they are pruned, due to not being stimulated frequently enough. Most synapses are refined and formed throughout our life.

To become what we call a person, our environment causes our neurons to imprint itself with heuristic instructions in the form of synaptic circuitries, to predict situational outcomes and to adapt our behavior in order to maximize the desired outcome.

Personality, so all our characteristics that describe our reaction to situational circumstances, is shaped in this way. Fortunately, most of those traits are not set in stone once they are formed and can be changed. Remarkable recoveries after brain damage, successful psychotherapy and the true mastering of a craft are the most impressive testaments to the ability to change one's circuitry.

Synaptic weights

Neurons fire or they do not. This central dogma for neurobiology, termed all-or-nothing response, means that all inputs result either in no outgoing response from that neuron or in the neuron reacting with an ion overshoot, producing a distinct, reinforced electric potential that travels along the axon and leads to the stimulation of other neurons in return; the so-called action potential.

But between all and nothing is a lot of space – namely all the thousands of inputs have to be subjected to enough stimulation in a very short time to trigger an action potential. How strong each input should be weighed in is determined by many factors at each synapse; the number and type of neurotransmitter receptors, voltage-dependent ion channels, membrane size, distance from the soma, shape and size of the cytoskeletal scaffold for synaptic proteins and many more.

All these factors make up the synaptic weight and all weighted inputs summed up determine whether an action potential shall be induced or not. And finally, all action potentials comprise what we describe as neural activity.

We can see that a myriad of intermediate stages exists, where the summation of input is not zero but still below prompting an all-or-nothing response. Thus, changing even a single synaptic weight can tip the scales and potentially trigger the neuron into developing an action potential.

To understand this on a molecular scale, we have to understand the architecture of synapses. A synapse consists of two parts; pre-synapses are located along the axon of a neuron, whereas post-synapses are located in dendrites. Information in the brain flows primarily over the chemical synapse; a small cleft between the pre-synapse of the transmitting cell and the post-synapse of the receiving cell.

Provided there is an action potential in the axon, synaptic vesicles, filled with neurotransmitters, are being released from the pre-synapse into the cleft. Upon release these neurotransmitters bind receptors at the post-synaptic membrane, causing them to open, so that ions can flow in and out of the post-synapse. This ion flow in return creates excitatory post-synaptic potentials that are summed up in the post-synaptic neuron as described above.

At any existing synapse that process happens at an individual baseline level. If the frequency and amplitude of neurotransmitter release stays the same, this synapse is in homeostasis (Fig 1, left and middle).

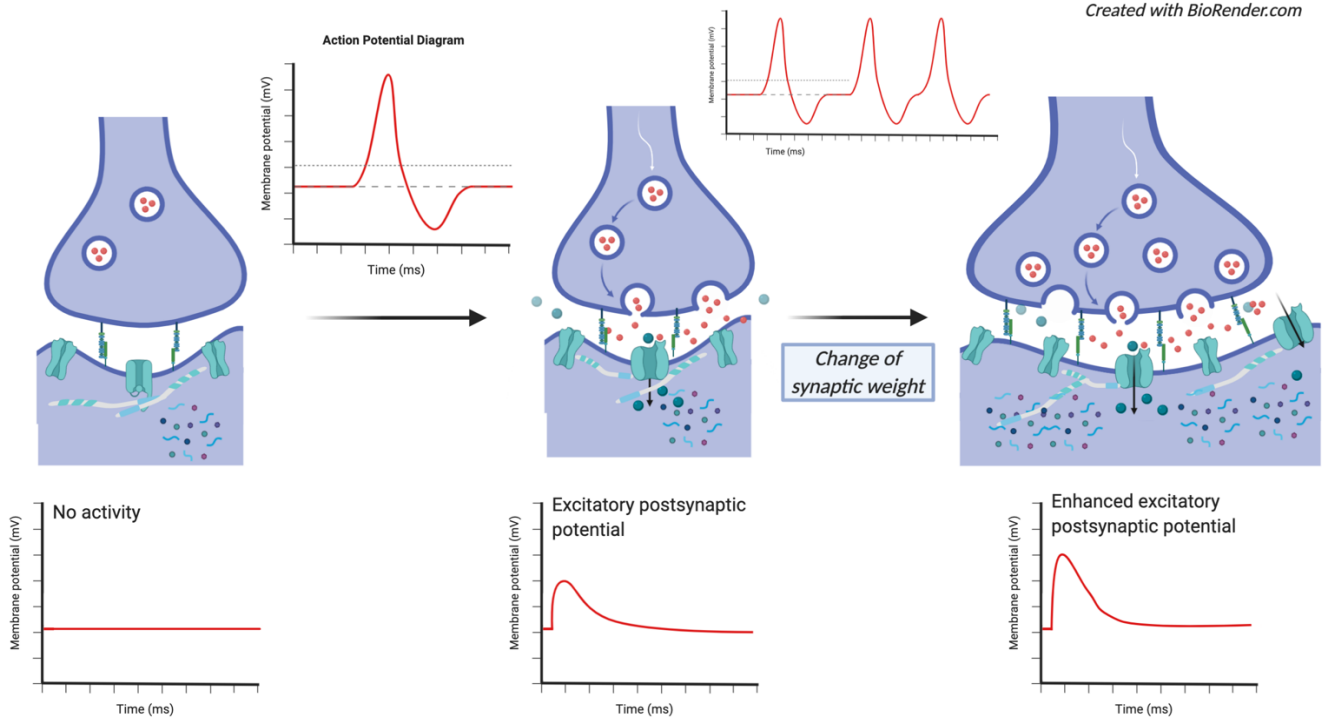


Fig 1: Depiction of the consequences of synaptic weight increase. Each synapse has a certain size, number of receptors and other factors determining the strength to which an incoming signal (action potential) is passed down to the soma (small inlet). When action potentials arrive in rapid succession this can lead to a reconfiguration of the molecular makeup of a synapse, resulting in a changed post-synaptic potential.

If, however, the frequency of action potentials that arrive at the pre-synapse is significantly higher, the synapse undergoes several changes; both synaptic compartments grow in size, more synaptic vesicles are present at the pre-synapse, more receptors are being inserted into the post-synaptic membrane and the cytoskeletal scaffold is increased. All those changes result in an increase of the excitatory post-synaptic potentials (Fig 1, right). When we say plasticity, we mean changes of synaptic weights according to new or altered stimuli.

Likewise, if the action potentials arrive at lower frequencies, the synaptic weight is weakened by essentially the opposite of all described mechanisms and thus the excitatory post-synaptic potentials are thereby reduced (not depicted).

Interestingly, newer studies suggest a certain number of discrete synaptic weights, rather than a continuous spectrum. This concept is called gradation and estimates about the exact number of discrete weights range from 10 (Liu et al., 2017) to 26 (Bartol et al., 2015).

Changing the synaptic weights - local translation

Most biological processes are being executed by proteins, including enzymatic reactions, metabolite conversion and structuring of the organism. Similarly, many proteins are involved in changing the synaptic weight; but how is the neuron regulating its proteome to respond adequately to plasticity events?

In part, the overall transcription program of the cell is altered by epigenetic modifications to the histones and DNA, ensuring the maintenance of altered synaptic weights by the appropriate amount of protein synthesis. Nonetheless protein supply at the changing synapse needs to happen fast. Action potentials arise in the order of milliseconds, synapse changing neuronal activity in the order of seconds and minutes.

To overcome this problem, we find that neurons provide mRNAs to synaptic regions, where protein synthesis occurs locally (Fig 2, left). This special form of translation is not happening evenly distributed over the whole dendrite but - depending on the model - either in a few hot spots in dendritic branches (Rangaraju et al., 2017) or by complexes that patrol across the whole tree (Doyle and Kiebler, 2011) (Fig 2, right).

All molecules required for this - ribosomes, tRNAs, ncRNAs and mRNAs - are present directly at those translational hotspots (Higa et al., 2014; Kosik, 2016; Wang and Bao, 2017; Wu et al., 2016).

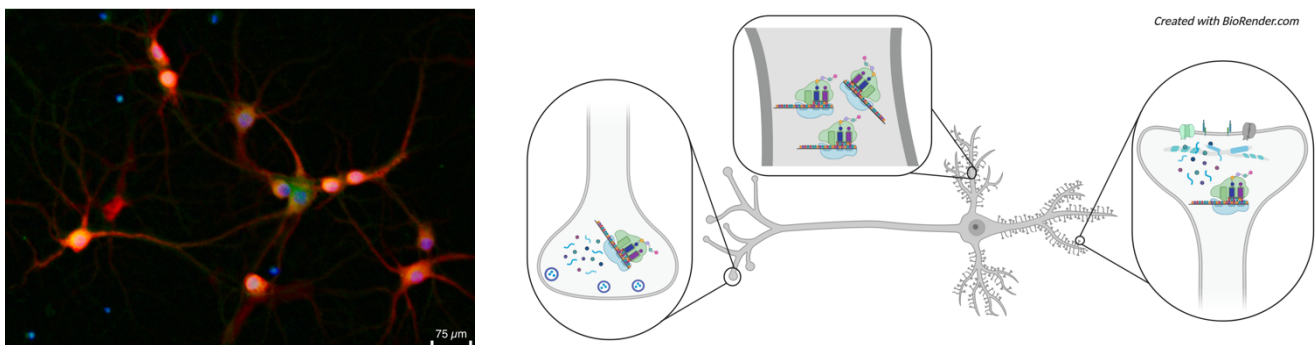


Fig 2: Local translation along neurites and axons. Left: puromycin (A1113803, Gibco) staining for 30min depicts spots of protein synthesis across neurites (red: puromycin, green: Camkk2)¹. Right: scheme showing the three different spots for local translation; pre-synapse, post-synapse and dendritic tree. In all those locations translating ribosomes have been observed.

¹ Antibodies used; Puromycin: primary (MABE343, Merck), secondary (A-21052, Invitrogen)
Camkk2: primary (ab96531, Abcam), secondary: (ab150077, Abcam)

It is of utmost importance to state that local translation is not a fallback mechanism or a supportive source of proteins, but essential for plasticity. Early studies could show that when local protein synthesis was impaired, the learning effect would not take place (Kang and Schuman, 1996) and that the necessary short-term morphological changes to the dendritic spine rely likewise on local translation (Bosch et al., 2014).

Additionally, last year it was proposed that aggregation of psychiatric disease-related proteins inside dendrites impairs local translation and as a consequence cognitive function deteriorates (Endo et al., 2020).

Finally, a computational model was built to simulate spread of proteins depending on the translational location (Fonkeu et al., 2019). This study found that experimentally observed patterns of RNA distribution - with accumulations of mRNAs and proteins at synapses - could be simulated well with local translation.

RNAome regulation

Before gene transcription can result in proteins, cells have a multitude of regulatory pathways to adjust mRNAs; parameters that decide amount, isoform, time and localization of protein synthesis. Many regulatory pathways are mediated by other RNAs: microRNAs (miRs), circular RNAs, long-non-coding RNAs (lncRNAs) and several others. These RNAs are not encoding proteins themselves, and thereby are summarized as non-coding RNAs (ncRNAs). Since mRNAs and ncRNAs are produced in a single-stranded manner, they have the ability to hybridize with one another at many positions.

mRNAs have seed region on their 3' untranslated regions (UTR), where miRs can bind - this effectively results in two different outcomes; either degradation of mRNA through protein complexes, or inhibition of its translation. At the same time, other ncRNAs can influence that interaction by binding miRs, preventing them from targeting mRNAs (Fig 3). Most miRs can target dozens or hundreds of mRNAs, likewise most mRNAs are targeted by dozens or hundreds of miRs.

Those interactions are of great relevance to local translation, as they can quickly change - especially when new RNAs are introduced to the local pool or when local RNAs themselves are modified, e.g., by the synaptic demethylases (Walters et al., 2017). These quick changes could render synaptic mRNAs suddenly available for translation.

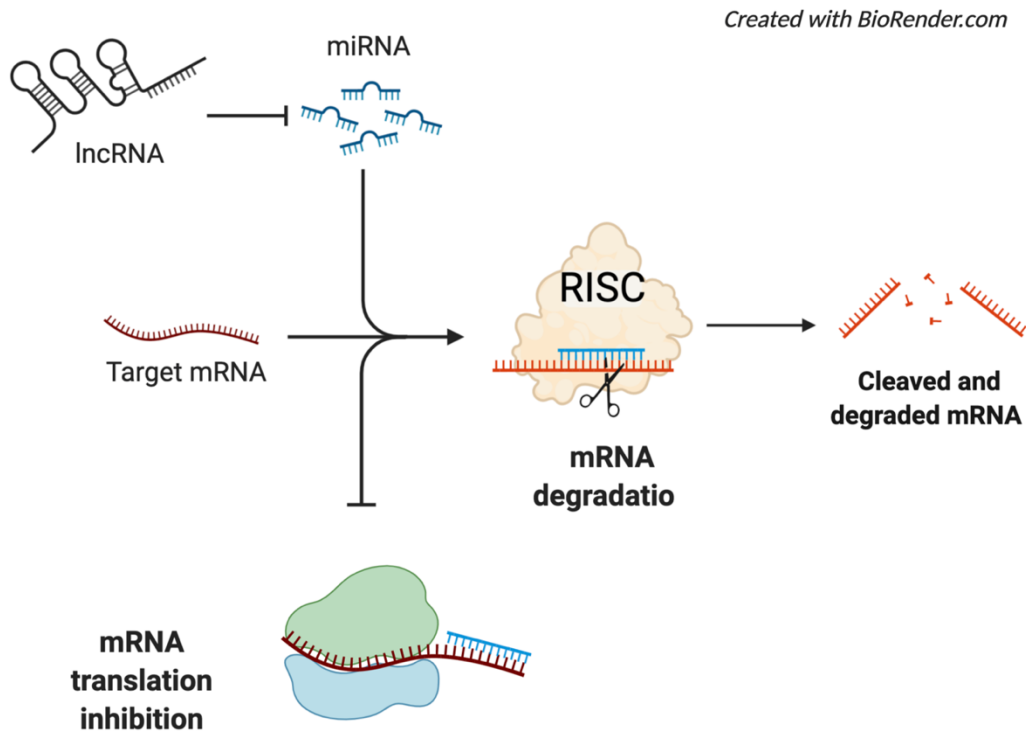


Fig 3: RNA - RNA regulatory networks. mRNAs can be bound by small ncRNAs, most notably miRs; resulting in either disintegration or translational inhibition.

Researchers are just beginning to describe functional relationships between the small RNAome and the RNAome at the synapse. For example, a recent paper proves that local activity at spines is coupled to the maturation of a plasticity-related miR in close vicinity (Sambandan et al., 2017). Moreover, miRs are released by pre-synaptic neurons in an active manner over exocytosis and endocytosis pathways (Xu et al., 2013). The group of Harlow extended that view by detecting tRNA fragments (trfRNA) and miRs inside synaptic vesicles (Li et al., 2015).

Many of those interactions are not understood yet, and often this is due to insufficient datasets of small and total RNA of the same samples.

Isolation of synaptic RNA

As early as in the 1960s *in vitro* labeling techniques demonstrated that protein synthesis happens in neurites (Giuditta et al., 1968; Koenig, 1967). Since then, several techniques have been devised to allow subcellular investigations.

The first systematic exploration of neurites started with the dissection and examination of the giant squid axon (Giuditta et al., 1980). Similarly, the neuropil of CA1 was micro-dissected to sequence neurite RNAs (Cajigas et al., 2012). Synaptosomes on the other hand are obtained by using gradient ultracentrifugation; under immense centrifugal forces it is possible to sever axonic terminals from the axon itself. Thanks to the hydrophobic properties of the bilipid membrane, the severed membrane of the axon terminals closes right after the separation, preserving proteins and RNAs inside. Post-synaptic densities (PSD) are often also isolated, since neuexin and neuroligin proteins connect both synaptic membranes over the synaptic cleft. Hence, when the membrane also closes around the PSD, then some post-synaptic RNAs and proteins are isolated, too.

There are two general approaches for *in vitro* isolations. The first uses hanging inserts, where neurons are cultured on a porous membrane, with pores fine enough to allow the outgrowth of neurites. By swiping the underside of the membrane, it is possible to obtain axonal and dendritic RNAs.

The second approach utilizes compartmentalized chambers. Beginning with Campenot chambers, axons were spatially isolated; while the cell body would grow in the main compartment of the chamber, only axons would extend under the barriers into neighboring compartments (Campenot, 1977). By doing so, studies of the effects of neuronal growth factors could be done, without the factors diffusing into the main compartment.

Each of the discussed methods has its own strengths and weaknesses. The neuropil cutting is restricted to parts of the brain, where anatomically there are long stretches of neurites. Furthermore, it is difficult to control for the purity of the yielded material. Synaptosomes take several hours to be acquired, which increases the chance of RNA degradation. Hanging inserts do not allow for sufficient visual control of formed synapses. It is also quite likely that hanging neurites would accumulate molecules from the soma - driven by diffusion and gravity - that do not resemble the genuine neurite RNAome. In Campenot chambers the thickness of the barriers favors the outgrowth of axons, making it difficult to study physiological synapses.

For a complete picture of synaptic RNAs, one has to also consider that, as of now, all published methods underrepresent the post-synaptic RNAome: synaptosomes only contain post-synaptic densities and therefore only RNAs that are stuck in them, hanging inserts cannot verify if synapses on their downside are actually forming and Campenot chambers create only few isolated dendrites. In the case of neuropil preparations, inclusions from surrounding cells can end up in the final sample. To correct for this, usually all genes that are not supposed to be at the synapse are being filtered out, hence *a priori* assumptions bias the results.

In continuation of the *in vitro* approach by Campenot, new designs have been suggested, among them the widely used design by Taylor and colleagues (Taylor et al., 2010). This chamber introduces two neuronal pools, connected by hundreds of parallel running microgrooves. Somata cannot pass through these microgrooves, but extend their neurites from both sides into the microgrooves, where functional synapses are formed. Slightly offset to one pool runs a perpendicular perfusion channel through all microgrooves allowing the temporally and spatially precise pharmaceutical manipulation of synapses, without affecting the somata; a feature hitherto not possible.

By further advancing this design, it should be possible to create a new method of isolating the synaptic RNAome.

Scope of this thesis:

Synapses are the basic unit of information processing in the brain. It is thus highly interesting to disentangle the molecular mechanisms underlying synaptic plasticity. Local translation is a key process in changing synaptic weights long-term. Only by identifying the individual RNAs involved, will it be possible to recognize patterns and to formulate hypotheses about the roles of each transcript. To that end, I aimed to dissect the synaptic RNAome.

1) *Characterizing of the hippocampal synaptic RNAome*

The hippocampus is a key area for memory formation. So far, a combined catalogue of mRNAs and non-coding RNAs (ncRNAs) at hippocampal synapses has been missing. Especially, for miRNAs the available microarray data is limited and most works focus on single miRs.

Thus, my aim was to create such a database. To achieve this, I used two different techniques - synaptosomes and a new technique (SNIDER) that I developed to isolate pure neuronal RNAs from all neurites. Samples were prepared using next generation sequencing (NGS), which additionally allowed me to identify synaptic lncRNAs.

2) *Using SNIDER to study the effects of locally inhibiting a miRNA*

In our synaptosome preparations miR-9-5p was the second highest expressed miR. I, therefore, delivered miR-9-5p inhibitor to neuronal cultures by packaging them into lipid nanoparticles. Uptake of the inhibitor in normal cultures lifted the inhibition of miR-9-5p and, as a result, more Camkk2, a known target of miR-9-5p, was translated. By using the perfusion channel of the microfluidic chamber, I inhibited miR-9-5p locally I inhibited miR-9-5p locally to investigate the effects on the local transcriptome level.

3) *Investigating the intercellular transfer of RNAs*

As I discovered through Chapter 1 and 2, RNAs can be transferred from astrocytes to neurons. I reasoned that this could be true for many mRNAs as well. In order to detect all shipped RNAs, I devised a novel method to label all astrocytic RNA and all neuronal ribosomes. Both necessary constructs were delivered via AAVs into a primary neuronal culture. I identified several thousand shipped RNAs and further enquired whether astrocyte-derived extracellular vesicles (ADEVs) could be a possible route for transfer. To that end, I labelled ADEVs to study their uptake and sequenced the RNAs inside.

Chapter 1 - The coding and small-non-coding hippocampal synaptic RNAome

Detailed Author contribution of Robert Epple (R.E.):

Conceptual work

- Concept development and establishment of SNIDER
- Experimental design of the KCl stimulation experiment

Experimental work

- Performing total and small RNA sequencing for microfluidic chambers
- Assisting the synaptosome collection
- Imaging

Data analysis

- Analysis was done in close cooperation with Prof. Dr. Andre Fischer and Dr. Dennis Krüger
- Comparing the astrocytic exosome miRs with our dataset
- Overlaps of datasets

Data presentation

- Figure 2 A-C, Figure 5 A and Figure S1
- Manuscript editing

Copyright notice:

Accepted for publication by Molecular Neurobiology.

Reprinted here is the preprint found on BioRxiv (Epple, 2020)

Copyright © 2021 The authors, some rights reserved; exclusive licensee Springer, Molecular Neurobiology.

The coding and small-non-coding hippocampal synaptic RNAome

Robert Eppel¹, Dennis Krüger^{1,2}, Tea Berulava¹, Gerrit Brehm^{3, 4}, Rezaul Islam¹, Sarah Köster^{3, 4} & Andre Fischer^{1,4,5*}

¹Department for Systems Medicine and Epigenetics, German Center for Neurodegenerative Diseases (DZNE), Von Siebold Str. 3a, 37075, Göttingen, Germany

²Bioinformatics Unit, German Center for Neurodegenerative Diseases (DZNE), Von Siebold Str. 3a, 37075, Göttingen, Germany

³Institute for X-Ray Physics, University of Göttingen, Göttingen, Germany

⁴Cluster of Excellence "Multiscale Bioimaging: from Molecular Machines to Networks of Excitable Cells" (MBExC), University of Göttingen, Germany

⁵Department of Psychiatry and Psychotherapy, University Medical Center Göttingen, Germany

*corresponding author: andre.fischer@dzne.de (ORCID: [0000-0001-8546-1161](https://orcid.org/0000-0001-8546-1161))

Abstract

Neurons are highly compartmentalized cells that depend on local protein synthesis. Thus, messenger RNAs (mRNAs) have been detected in neuronal dendrites and more recently also at the pre- and postsynaptic compartment. Other RNA species, such as microRNAs, have also been described at synapses where they are believed to control mRNA availability for local translation. Nevertheless, a combined dataset analyzing the synaptic coding and non-coding RNAome via next-generation sequencing approaches is missing. Here we isolate synaptosomes from the hippocampus of young wild type mice and provide the coding and non-coding synaptic RNAome. These data are complemented by a novel approach to analyze the synaptic RNAome from primary hippocampal neurons grown in microfluidic chambers. Our data show that synaptic microRNAs control almost the entire synaptic mRNAome and we identified several hub microRNAs. By combining the *in vivo* synaptosomal data with our novel microfluidic chamber system, we also provide evidence to support the hypothesis that part of the synaptic microRNAome may be supplied to neurons via astrocytes. Moreover, the microfluidic system is suitable to study the dynamics of the synaptic RNAome in response to stimulation. In conclusion, our data provide a valuable resource and hint to several important targets for future experiments.

Keywords: mRNA, microRNA, lncRNA, snoRNA, synapse, synaptosomes, gene-expression, RNA-sequencing

Acknowledgments

RE is a member of the international Max Planck Research School (IMPRS) for Neuroscience, Göttingen. We thank Mike Zippert and Reinhard Hildebrandt for the construction of SNIDER. This work was supported by the following third-party funds to AF: the ERC consolidator grant DEPICODE (648898), funds from the German research foundation (DFG) SFB1286 (B06) and funds from the German Center for Neurodegenerative Diseases (DZNE). SK is supported by the DFG via SFB1286 (B02). AF and SK are supported by funds from the DFG under Germany's Excellence Strategy - EXC 2067/1 390729940.

Introduction

Neurons are highly compartmentalized cells that form chemical synapses and the plasticity of such synapses is a key process underlying cognitive function. In turn, loss of synaptic integrity and plasticity is an early event in neuropsychiatric and neurodegenerative diseases. Synapses are usually far away from the soma, which raises the question how neurons ensure the supply of synaptic proteins. Theoretical considerations and a substantial amount of data show that mRNAs coding for key synaptic proteins are transported along dendrites to synaptic compartments, where they are locally translated into proteins (Doyle & Kiebler, 2011) (Kosik, 2016) (Holt *et al*, 2019) (Fonkeu *et al*, 2019) (Biever, 2020). Hence, several studies investigated the synaptic RNAome via different approaches. For example, early *in situ* hybridization experiments demonstrated the localization of specific mRNAs to synapses (Garner *et al*, 1988). In addition, microarray and RNA-seq techniques were used to study the synapto-dendritic (Cajigas *et al*, 2012) (Ainsley *et al*, 2014) (Farris *et al*, 2019), synapto-neurosomal (Most *et al*, 2015) and more recently also the synaptosomal RNA pool of the mouse brain (Chen *et al*, 2017) (Hafner, 2019). However, compared to mRNAs, there is comparatively less knowledge about the non-coding RNAome at synapses. The best known non-coding RNAs are microRNAs which are 19-22 nucleotide long RNA molecules regulating protein homeostasis via binding to a target mRNA thereby causing its degradation or inhibition of translation (Gurtan & Sharp, 2013). Several microRNAs have been implicated with synaptic plasticity and were identified at synapses where they have been linked to the regulation of mRNA stability and availability for translation (Smalheiser, 2014) (Weiss *et al*, 2015) (Rajman & Schratt, 2017) (Sambandan *et al*, 2017). The combined analysis of the synaptic microRNA/mRNAome is however lacking and knowledge about other non-coding RNA species is rare. Another issue is that the methods used so far to study synaptic RNAs from tissue samples do not allow to distinguish between RNAs produced by the corresponding neurons and RNAs that might be transferred to synapses from other cell types. This question is becoming increasingly important, since there is emerging evidence for inter-cellular RNA transport and data supporting the hypothesis that for example glia cells provide neurons with RNA (Sotelo *et al*, 2014) (Jose, 2015).

In this study we isolated synaptosomes from the hippocampus of mice and performed from the same preparation total and smallRNA-sequencing. To complement these data and address the question about the origin of synaptic RNAs we developed a novel microfluid chamber that not only allowed us to grow primary hippocampal neurons that form synapses in a pre-defined compartment (Taylor *et al*, 2010), but enabled us to isolate the synaptic compartments from these chambers using a novel device we call SNIDER (**SyNapse Isolation Device by Refined Cutting**) followed by RNA-sequencing. We also show that this novel microfluid chamber is suitable to assay the dynamics of the synaptic RNAome in response to stimulation. In conclusion, our experiments allowed us for the first time to build a high-quality synaptic microRNA/mRNA network and suggest key synaptic RNAs, including lncRNAs and snoRNAs, for future mechanistic studies in the context of the healthy and diseased brain.

Results

The hippocampal coding and non-coding synaptosomal RNAome

We isolated high-quality synaptosomes from the hippocampus of 3 months old mice, and processed the corresponding RNA for total and small RNA-sequencing (**Fig 1A**). After quality control for high confidence transcripts, we could detect 234 mRNA, 6 lncRNAs (excluding sequences that code for predicted genes), 65 microRNAs and 37 SnoRNAs (**Fig 1B, tables S1, 2, and 3**). GO-term analysis revealed that the mRNAs reflect exclusively the pre-and post-synaptic compartment (**Fig 1C**) confirming the quality of our data. Functional pathway analysis showed that the mRNAs found in our synaptosomal preparations represent key pathways linked to synaptic function and plasticity (**Fig. 1D**). We also observed a substantial amount of highly abundant microRNAs present in our synaptosomal preparations (**Table S2**) and wanted to understand the synaptic regulatory mRNA-microRNA network. To this end, we applied a novel bioinformatic approach and first generated the mRNA-network using the mRNAs detected at synapses, intersected this network with the synaptic microRNAome and asked if any of mRNAs within the network represent confirmed microRNA targets. Our data revealed that the 98% of the synaptic mRNAome is targeted by 95% of the synaptic microRNAs (**Fig 1E, F**). These data suggest that the synaptic microRNAome plays an important role in local mRNA availability. We detected a number of hub microRNAs and especially microRNA-27b-3p, microRNA-22-3p, the cluster consisting let-7b-5p, let-7c-5p and let-7i-5p as wells as microRNA-181a-5p, microRNA-9-5p and microRNA-124-5p appear as central regulators of the synaptic mRNA pool (**Fig 1F**).

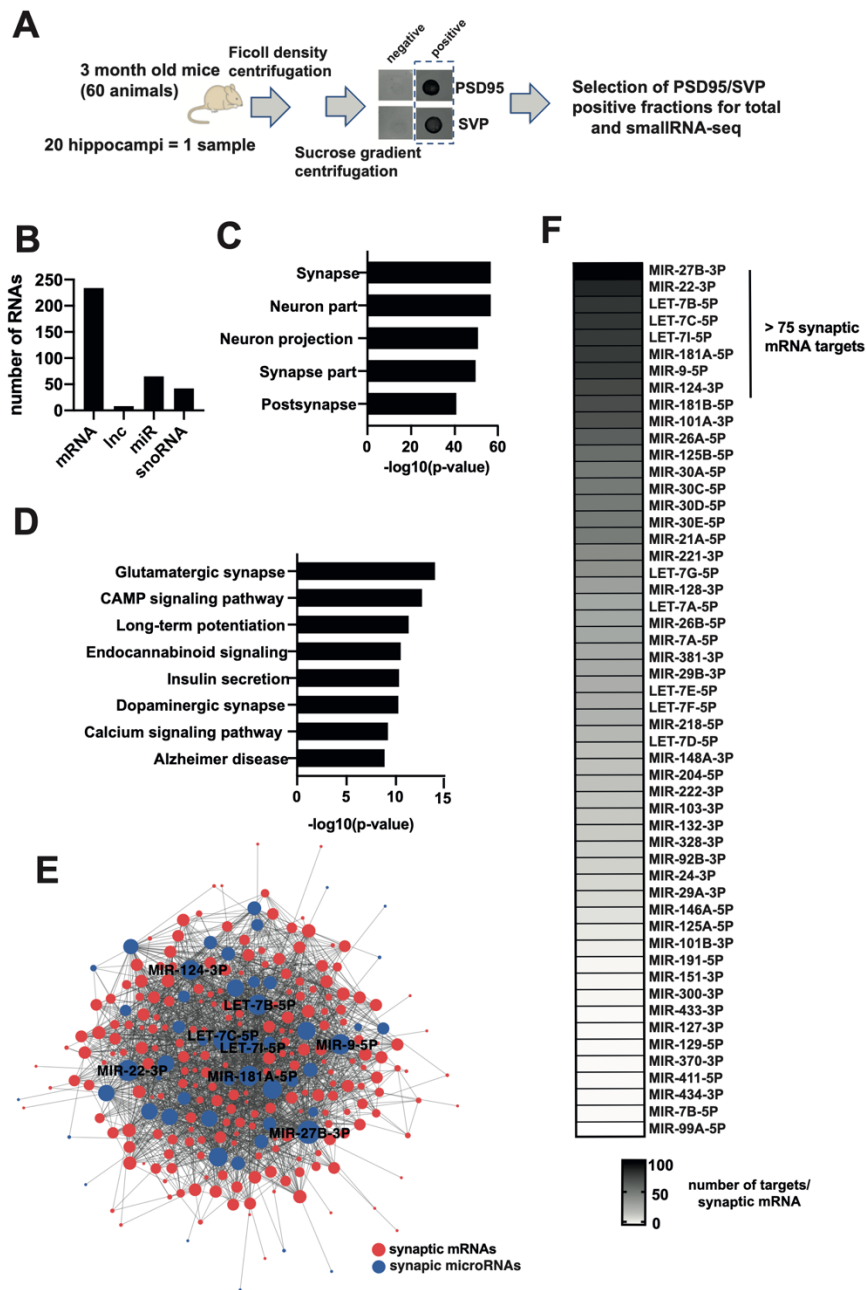


Figure 1: The coding and small-non-coding RNAome of hippocampal synaptosomes. **A.** Experimental scheme. **B.** Bar graph showing the detected RNA species. **C.** GO-analysis showing that the identified mRNAs represent the synaptic compartment. **D.** KEGG-pathway analysis showing that the synaptic mRNAome consists of transcripts that are essential for the function of hippocampal synapses. **E.** microRNA-mRNA interaction network of the synaptic RNAome. Red circles represent the identified mRNAs that form a highly connected network, while blue circles indicate the detected microRNAs. Only the names of the top hub microRNAs are shown. **F.** Heat map showing the synaptic microRNAome ranked by their confirmed mRNA targets that were found at synapses.

Comparison of the hippocampal synaptosomal coding and non-coding RNAome to primary hippocampal neurons

Compartmentalized microfluidic chambers have been developed to study the pre- and postsynaptic compartments of neurons. In these chambers, neurons grow their neurites into microgrooves and form synapses in a narrow compartment, the perfusion channel (Taylor *et al.*, 2010). We hypothesized that such microfluidic chambers would be a *bona fide* complementary approach to study the synaptic RNAome via RNA-sequencing. Moreover, since the synapses formed within the perfusion channel of such chambers are not in contact with any other neural cell type, this approach would also allow us to address the question to what extent synaptically localized RNAs originate from the corresponding cell or may have been shuttled from neighboring glia cells, a process that has been specifically proposed for synaptic microRNAs (Prada *et al.*, 2018). However, a reliable approach to isolate synapses and corresponding RNA for subsequent sequencing from the perfusion channel of such microfluidic chambers did not exist. Therefore, we generated a modified microfluidic chamber that allowed us to cut the perfusion channel to harbor the corresponding synapses followed by the isolation of RNA. Thus, we grew mouse hippocampal neurons in these chambers (**Fig 2A**). For reproducible cutting we employed a newly-devised instrument we call SNIDER (**SyNapse Isolation Device by Refined Cutting**) (**Fig 2B, C**) and isolated RNA for total and smallRNA sequencing. When comparing the transcriptome obtained from the perfusion channel, with corresponding data generated from RNA isolated from primary hippocampal neurons grown in normal culture dishes, we observed the expected enrichment for a specific subset of RNAs, representing about 12% of the entire transcriptome (**Fig 2D**). In more detail, the transcriptome of the perfusion chamber consisted of 1460 mRNAs, 199 lncRNAs, 54 microRNAs and 57 highly expressed snoRNAs of which 22 were also detected in synaptosomes. (**Fig 2E, Supplemental tables S4, 5, 6**). GO-term analysis revealed that the identified mRNAs represent the synaptic compartment, which is in line with our data obtained from the adult mouse hippocampus (**Fig 2F**) and further supports the feasibility of our approach. Functional pathway analysis confirmed that the detected mRNAs code for key synaptic pathways and reflect the high energy demand of synapses (oxidative phosphorylation). This is also the reason why pathways such as Alzheimer's, Huntington's and Parkinson's disease are identified (**Fig 2G**), since key genes de-regulated in these diseases are linked to mitochondria function. The direct comparison of the hippocampal synaptic mRNAome from the adult mouse brain and the mRNAome from primary neurons revealed that almost all mRNAs detected from *in vivo* synaptosomes, are also found in primary neurons grown in microfluidic chambers (**Fig 2H**), confirming 219 mRNAs as a high-quality and reproducible synaptic mRNAome. The GO-terms and functional pathways linked to these 219 mRNAs are identical to the data shown in Fig 1C&D. The 1244 mRNAs that were specifically observed in microfluidic chambers represent also the synaptic compartments and pathways linked to oxidative phosphorylation, synaptic vesicle cycle and metabolic processes and may therefore reflect the difference of the synaptic RNAome in the adult brain and cultured primary neurons (**Fig 2I**).

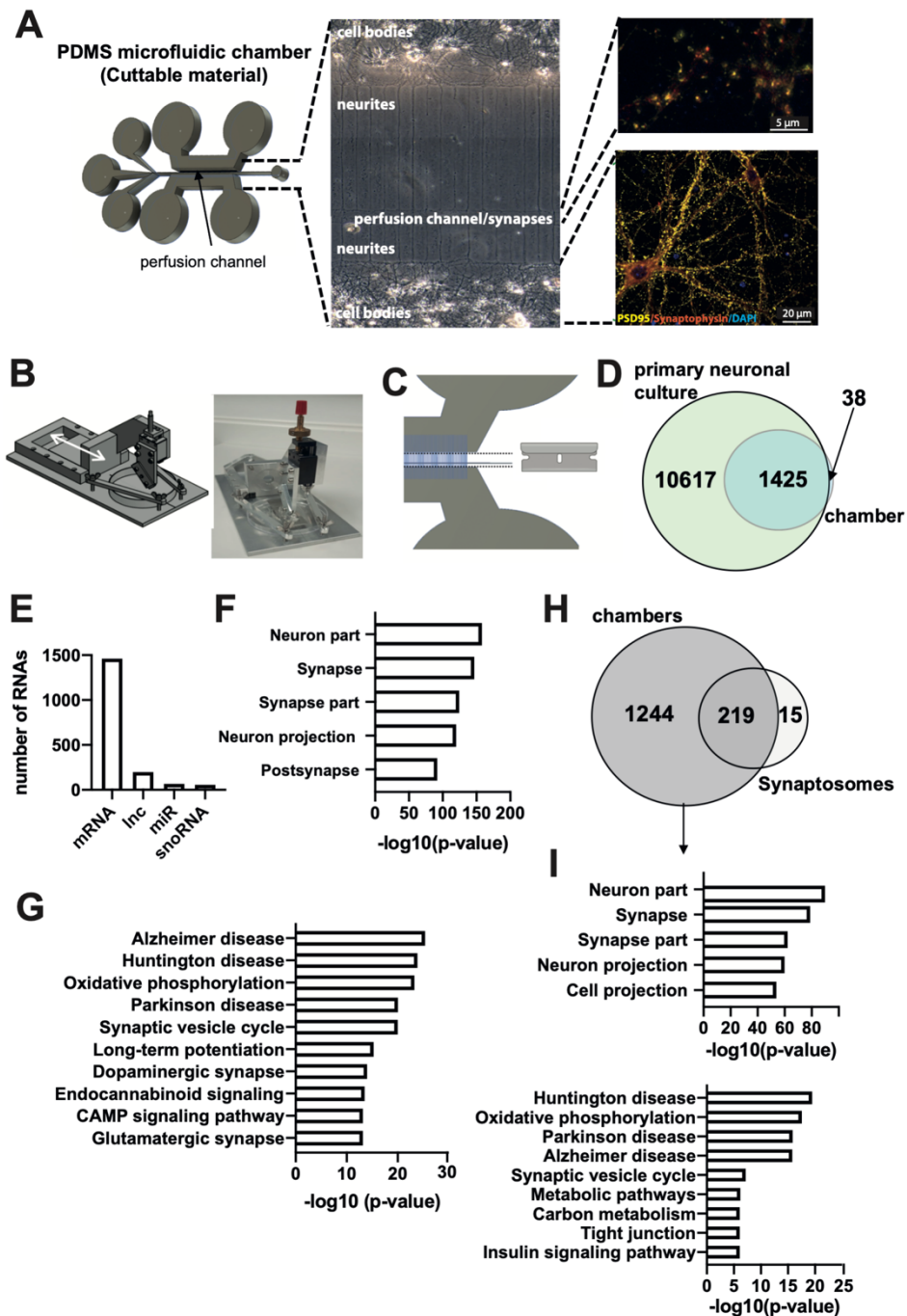


Figure 2: Analyzing the synaptic RNAome in microfluidic chambers via RNA-sequencing. **A.** Microfluidic chambers built from PDMS. Left panel shows the scheme of the microfluidic chamber indicating the perfusion channel in which most of synapses form. The principle is based on chambers first reported by Taylor and colleagues (Taylor et al., 2010) but has been substantially modified (See Fig S1 for more details). The middle panel shows the bright-field image of neurons growing in these chambers and the right panel shows immunostaining for PSD-95 and Synaptophysin within the perfusion channel (upper image) and the part of the chambers that contains the cell bodies (lower image). **B** Scheme and image showing our newly devised tool for cutting the perfusion channel from the microfluidic chambers, named SNIDER. **C.** Schematic illustration of the cutting of the microfluidic chambers.

D. Venn diagram showing the comparison of the total RNA-seq data obtained from primary hippocampal cultures grown in normal dishes (primary neuronal culture) and corresponding data obtained from the perfusion channel isolated from microfluidic chambers in which primary hippocampal neurons were grown. **E.** Bar chart showing the detected RNA species. **F.** GO-analysis showing that the identified mRNAs represent the synaptic compartment. **G.** KEGG-pathway analysis showing that the synaptic mRNAome consists of transcripts that are essential for the function of hippocampal synapses. **H.** Venn diagram showing the overlap of mRNAs detected in hippocampal synaptosomes and in microfluidic chambers. **I.** Upper panel: GO-analysis showing that the 1244 mRNAs specifically detected in microfluidic chambers represent the synaptic compartment and “cell projection”. Lower panel: KEGG-pathway analysis of the same dataset.

In addition, “neuronal projection” is detected as a significant GO-term, most likely indicating the fact that unlike synaptosomal preparations, the perfusion channel still contains some neurites. This might also explain that much more lncRNA, namely 199 annotated lncRNAs, are detected in the microfluidic chambers. Pathway analysis suggest that these lncRNA are mainly linked to mRNAs that control processes associated with oxidative phosphorylation and synaptic plasticity while comparatively few microRNAs seem to be regulated by the synaptic lncRNAs (**Fig S2**). Similar to the *in vivo* data, we found 54 highly expressed microRNAs (**Table S5**).

To further study the mRNA/microRNA network, we used the same approach as described for the synaptosomal data. Our data reveals that the 88% of the synaptic mRNAome in microfluidic chambers is targeted by 45 (83%) synaptic microRNAs (**Fig 3A**). Taken together, our data from hippocampal synaptosomes and the novel microfluidic chamber strongly suggest that the synaptic transcriptome is under tight control of a local microRNA network. Comparison of the *in vivo* synaptic microRNAome to the data obtained from the microfluidic chambers revealed 17 microRNAs that were commonly identified at synapses, while 37 microRNAs were specific to the chambers and 48 microRNAs were only found in the *in vivo* data from hippocampal synaptosomes (**Fig 3B**). When we generated the synaptic microRNA/mRNA network for the commonly detected 17 synaptic microRNAs and 219 mRNAs (see Fig 2G), we observed that this core synaptic microRNAome controls 80 % (179 of 219) of the core mRNAome (**Fig 3C**).

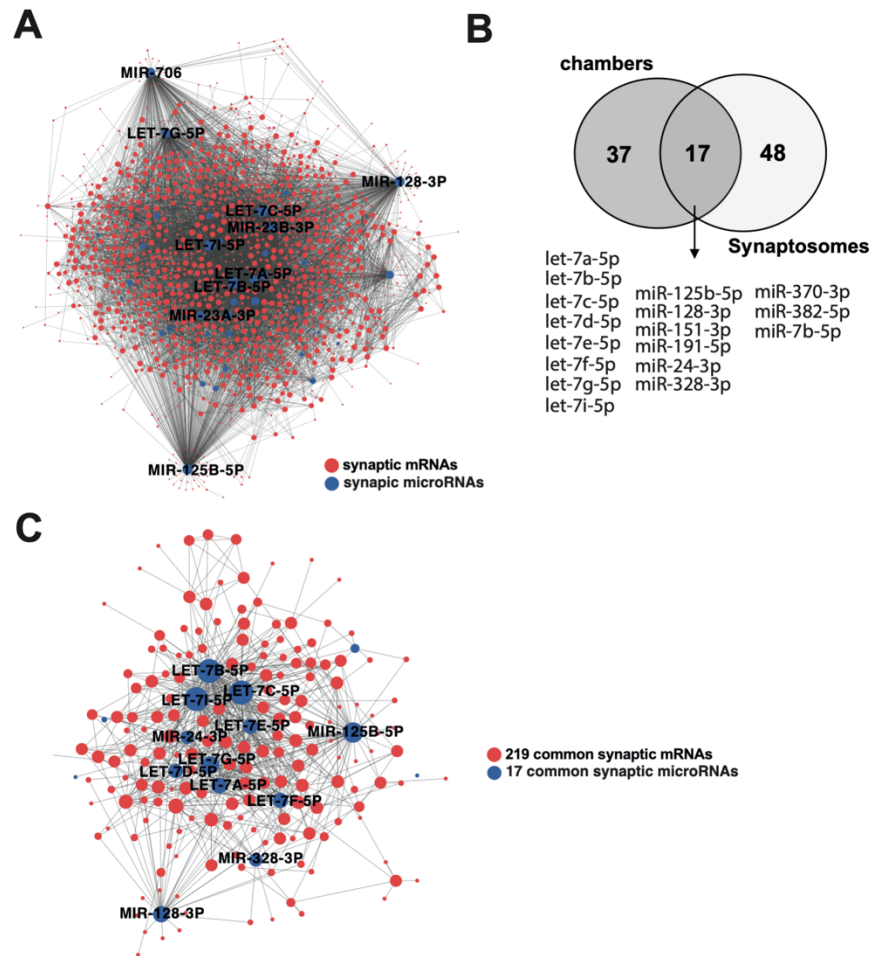


Figure 3: A core synaptic microRNAome. **A.** microRNA-mRNA interaction network of the synaptic RNAome detected in microfluidic chambers. Red circles represent the identified mRNAs that form a highly connected network, while blue circles indicate the detected microRNAs that control this network. Only the names of the top hub microRNAs are shown. **B.** Venn diagram comparing microRNAs detected in microfluidic chambers (Chambers) and synaptosomes. **C.** microRNA-mRNA interaction network of the 219 synaptic mRNAs commonly detected in synaptosomes and microfluidic chambers and the 17 commonly detected microRNAs. Only the names of the top hub microRNAs are shown.

Evidence for astrocytic microRNA transport to synapses

The finding that 37 microRNAs are exclusively found in synapses from primary neurons is likely due to the difference between *in vivo* brain tissue and primary neuronal cultures and a similar trend has been observed at the level of the mRNAs (see Fig 2G). More interesting is the observation that 73%, namely 48 out 65, of the microRNAs detected in hippocampal synaptosomes are not found in microfluidic chambers (see Fig 3B), which is in contrast to the mRNA data in which almost all of the synaptosomal mRNAs are also found in synapses of the primary neuronal cultures grown in microfluidic chambers (See Fig 2G).

These data may indicate that *in vivo* some of the synaptic microRNAs are not exclusively produced by the corresponding neuron but might be rather shuttled to synapses via other neural cell types. In fact, movement of microRNAs between cells is an accepted mechanism of intra-cellular communication (Jose, 2015). Prime candidate cells to support synapses with microRNAs are astrocytes that form together with neurons tripartite synapses. A prominent mechanism that mediates RNA transport amongst neuronal cells is intracellular transport via exosomes (Smythies & Edelstein, 2013). Thus, we compared a previously published dataset in which microRNAs from astrocytic exosomes were analyzed via a TAQman microRNA-array (Jovičić *et al*, 2013).

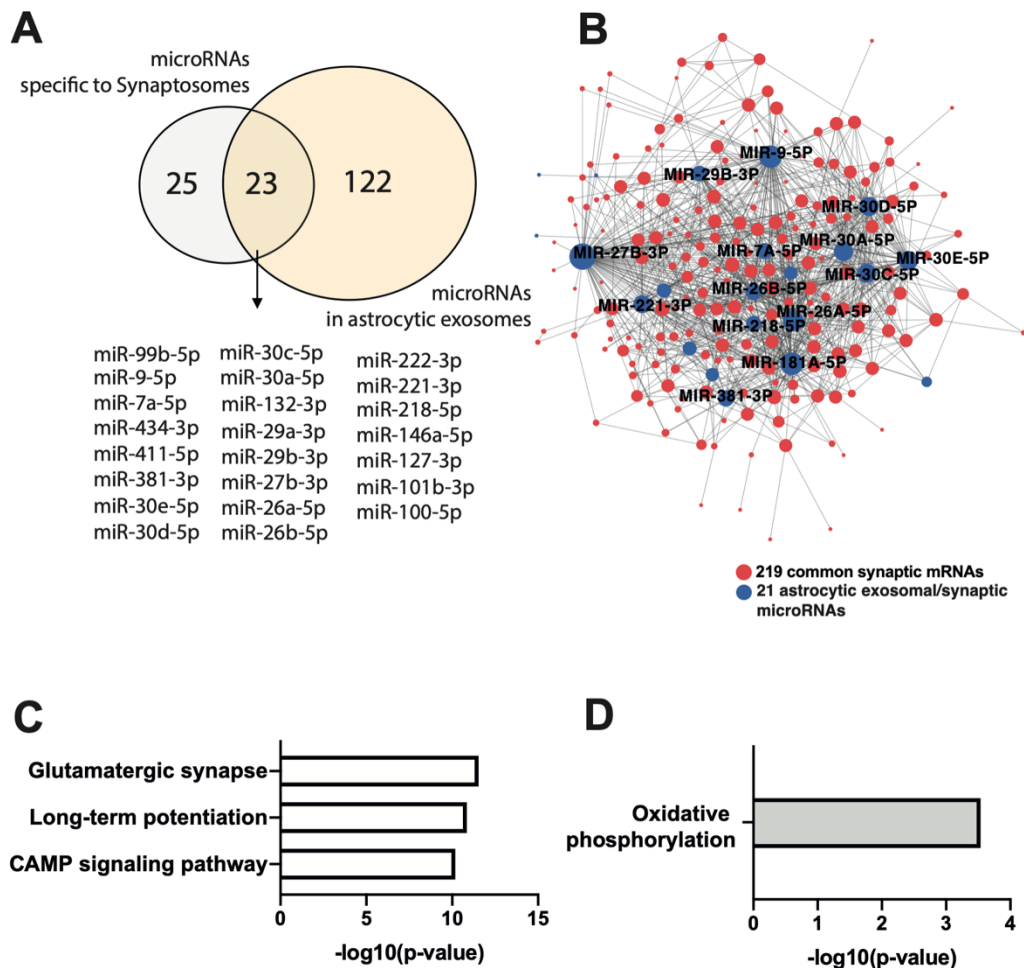


Figure 4: Comparing microRNAs from astrocytic exosomes to the synaptic RNAome. **A.** Venn diagram comparing the 48 microRNAs exclusively detected in synaptosomes to the list of microRNAs found in astrocytic exosomes. **B.** microRNA-mRNA interaction network showing that 203 of the commonly detected 219 mRNAs and 21 of the 23 microRNAs found in synaptosomes and astrocytic exosomes form an interaction network. Only the names of the top hub microRNAs are shown. **C.** KEGG-pathway analysis of the 203 mRNAs within the network. **D.** KEGG pathway analysis of the 16 common synaptic mRNAs that are not targeted by the overlapping microRNAs shown in (A).

Indeed, 50% of the microRNAs exclusively detected in hippocampal synaptosomes have also been described in exosomes released from astrocytes (**Fig 4A**). When we asked if these 23 microRNAs have mRNA targets detected in synaptosomes we observed that 21 of these microRNAs target in total 197 out of the commonly detected 219 synaptic RNAs (**Fig. 4B**), which is further confirmed by functional pathway analysis showing that the 21 microRNAs control synaptic genes linked to the glutamergic synapse, LTP and cAMP signaling (**Fig. 4C**). It is interesting to note that the synaptic mRNAs not targeted by any of the 21 microRNAs represented functional pathways linked to oxidative phosphorylation (**Fig. 4D**).

Table 1: Synaptic microRNAs detected in cognitive diseases

Synaptic microRNA	Disease	Literature (PMID)
mmu-miR-7a-5p#	Depression	32304043
mmu-miR-125b-5p*	Alzheimer's disease	31240600
mmu-miR-30d-5p#	Schizophrenia	32304043
mmu-miR-29a-3p#	Alzheimer's disease; Schizophrenia	31240600; 32304043
mmu-miR-181a-5p#	Alzheimer's disease	31240600; 29121998; 32304043
mmu-miR-30a-5p#	Schizophrenia	32304043
mmu-miR-125a-5p	Alzheimer's disease	31240600
mmu-let-7d-5p*	Schizophrenia	32304043
mmu-miR-99b-5p#	Alzheimer's disease	29121998
mmu-miR-26b-5p#	Schizophrenia	32304043
mmu-let-7e-5p*	Alzheimer's disease	29121998
mmu-miR-29b-3p#	Schizophrenia	32304043
mmu-miR-30e-5p#	Schizophrenia	32304043
mmu-miR-24-3p*	Schizophrenia	32304043
mmu-miR-330-5p	Depression/Bipolar disease	32304043
mmu-miR-146a-5p#	Alzheimer's disease	31240600; 31437718
mmu-miR-132-3p#	Alzheimer's disease	24014289; 31240600

1: ranked by expression level in synaptosomes (top to down)

*also detected in synaptic compartment of primary neurons grown in microfluidic chambers

#also detected in astrocytic exosomes

Synaptic microRNAs are linked to neurodegenerative and neuropsychiatric diseases

So far, our data support the view that the synaptic microRNAome plays an important role in neuronal function. To further strengthen this notion, we decided to ask whether synaptic microRNAs might be particularly de-regulated in cognitive diseases. To this end we performed a literature search and curated a list of 71 microRNAs that were found to be de-regulated in post-mortem human brain tissue, blood samples or model systems for Alzheimer's disease, depression, bi-polar disease or schizophrenia. Comparison of this dataset with our findings from synaptosomes revealed 17 synaptic microRNAs that are de-regulated during cognitive diseases of which 4 are also found in the microfluidic chambers and 11 were also detected in astrocytic exosomes, representing an interesting pool of synaptic microRNAs for further studies (**Table 1**).

Microfluidic chambers are suitable to assay the synaptic RNAome upon neuronal stimulation

Our findings suggest that we can study the synaptic RNAome in a reliable manner using our modified microfluidic chambers in combination with SNIDER. This approach also provides a novel tool to study the neuronal-controlled synaptic RNAome in response to stimulation.

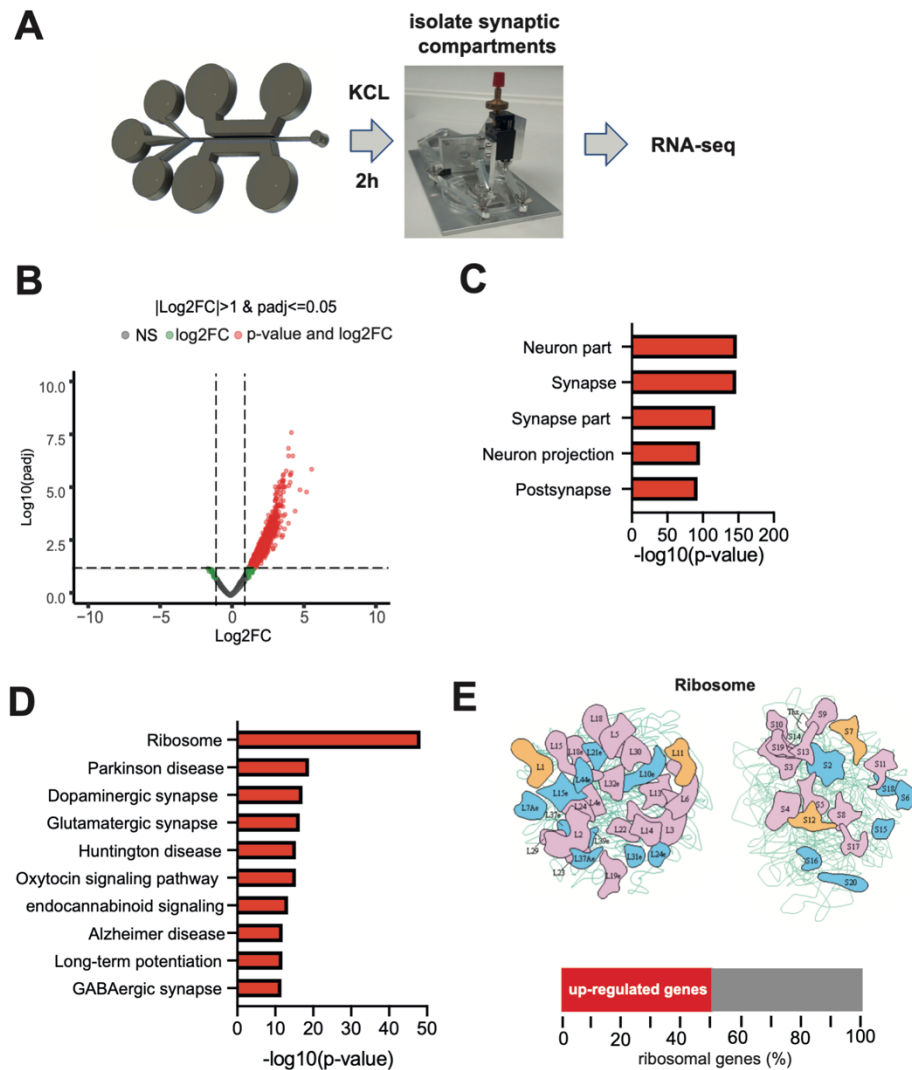


Figure 5: The synaptic mRNAome upon stimulation. **A.** Experimental scheme. **B.** Volcano plot showing a substantial up-regulation of synaptic RNAs upon KCL treatment. **C.** GO-analysis showing that the identified mRNAs represent the synaptic compartment. **D.** KEGG-pathway analysis showing that the changes of the synaptic mRNAome upon KCL treatment represent transcripts mainly linked to ribosomal function. **E.** Upper panel shows images of the KEGG pathway for “ribosome”. Colored subunits represent transcripts significantly increased. Lower panel: bar chart showing that 50% of the genes that comprise the “ribosome” KEGG-pathway are increased at the synaptic compartment upon KCL treatment.

To further evaluate this potential, we decided to expose primary hippocampal neurons grown in microfluidic chambers to KCl treatment followed by the isolation of the perfusion channel and RNA isolation for RNA-sequencing 2 h later (**Fig 5A**). Our analysis revealed a substantial number of mRNAs that were increased in the synaptic compartment (**Fig 5B, Table S7**). Since we can exclude that these mRNAs are shuttled from glia cells, they likely represent part of the transcriptional response and reflect mRNAs that were transported to synapses, which is feasible within the 2h time window after treatment. In line with this assumption the up-regulated RNAs exclusively represent the synaptic compartment (**Fig 5C**). Functional pathway analysis revealed a strong enrichment of RNAs coding for the ribosome (**Fig 5D**). In fact, 50% of all transcripts that correspond to the ribosomal subunits were increased at the synapse upon KCL treatment (**Fig 5E**).

Discussion

The synaptic RNAome

The aim of our study was to provide a high-quality dataset of the synaptic coding and small non-coding RNAome with a specific focus on microRNAs. Thus, our data represents an important resource for future studies. To the best of our knowledge our study also provides the first dataset which analyzes in parallel the coding, non-coding and small non-coding RNAome in hippocampal synapses via next-generation sequencing. Moreover, we used two different approaches in that we isolate hippocampal synaptosomes from the hippocampus of 3 months-old wild type mice and we developed a microfluidic chamber that in combination with a novel cutting device allowed us to isolate synaptic compartments for subsequent RNA-sequencing from primary hippocampal neurons.

This chamber combines the advantages of the currently used microfluidic chambers that allow the specific manipulation of synapses (Taylor *et al.*, 2010), with the ability to isolate the perfusion channel that harbors synaptic connections. Therefore, this novel microfluidic chamber will allow the specific manipulation of the synaptic compartment in combination with next-generation sequencing approaches and should be viewed as a suitable screening tool to study the dynamics of the synaptic RNAome. Feasibility of this approach was for example demonstrated by our finding that KCL treatment leads to substantial changes of the synaptic RNAome and future approaches will now employ more physiological manipulations and study the synaptic RNAome in disease models. It is noteworthy, that most of the mRNAs up-regulated at the synapse upon stimulation represent key components of the ribosome, which is in agreement with the importance of local mRNA translation (Holt *et al.*, 2019). In line with previous data, we identified a substantial number of mRNAs that almost exclusively represent the synaptic compartment and key signaling pathways linked to synaptic integrity and plasticity.

It is interesting to note that the mRNA coding for the amyloid-precursor protein (APP), a key factor in Alzheimer's disease (AD) pathogenesis, was also found at synapses (**see Table S1**).

To our knowledge, this observation has not been explicitly reported before but is in line with the physiological function of wild-type APP at synapses (Hefter *et al.*, 2020). Generally, we detected more mRNAs within the dataset obtained from primary neurons when compared to the synaptosomal preparation. This observation likely reflects the difference between the *in vivo* preparation of hippocampal tissue and cultured primary neurons. Another important consideration is that synapses likely differ depending on the distance to the soma, an issue that cannot be addressed when isolating synaptosomes, while the RNAome detected in the microfluidic chambers represent synapses that are most distant to the corresponding somata. Similar important is the fact that the preparation from the perfusion channel of our microfluid chamber still contains some neurites. Thus, the corresponding RNAome also includes dendritic mRNAs.

This view is supported by previous data in which the mRNA pool was analyzed from neuropil or synaptodendritic compartments. For example, 2550 mRNAs were detected in hippocampal neuropil from mice (Cajigas *et al.*, 2012), and 1875 mRNAs were identified when ribosome-bound mRNA was analyzed in the same region (Ainsley *et al.*, 2014). We observed only 234 mRNAs in hippocampal synaptosomes but we suggest that these mRNAs represent a high-quality dataset. Thus, we only report mRNAs that passed rigorous quality control and exhibit a substantial amount of sequencing reads. The quality of these data is further confirmed by the fact that almost all of the synaptosomal mRNAs, namely 219, are also detected within the RNA-seq dataset we obtained from the microfluidic chambers.

The most comparable mRNA dataset to our *in vivo* approach is a recent study that employed FACS to isolate synaptosomes from the mouse forebrain (Hafner, 2019) and also reported raw data on the generic synaptosomes. It is important to note that this study employed a different analysis pipeline and reported all transcripts that map with >25% of the read length when using the STAR-aligner tool, while we consider only transcripts that map with at least >66%. Nevertheless, we observed that the top 500 mRNAs reported by Hafner *et al.* almost completely overlapped with our dataset. Namely 209 of the 234 mRNAs that we reported for hippocampal synaptosomes are also found in the Hafner *et al.* dataset from mouse forebrain synaptosomes (**table S8**), further supporting the quality of our dataset and strengthening the view that synaptic mRNAs play a critical role in neuronal function.

We also report the detection of lncRNAs in datasets obtained from synaptosomes and microfluidic chambers but for now restricted the presented data to the currently annotated lncRNAs. We also detected lncRNAs that are currently still referred to as "predicted" and await further confirmation. Therefore, we encourage researchers to further explore our raw data as annotation of the genome improves. The presence of lncRNA in synaptosomes is in line with previous data (Chen *et al.*, 2017) but it is interesting to note that more lncRNAs were found in the microfluidic chambers when compared to the *in vivo* synaptosomes.

A similar trend has been observed for mRNAs and might be due to the fact that the RNA preparation from the microfluid chambers also contain some dendritic RNA. Our data suggest that the detected lncRNAs regulate processes associated with oxidative phosphorylation and synaptic plasticity and may also affected the function of selected microRNAs.

Although these observations need to be further studied, it is interesting to note that metastasis-associated lung adenocarcinoma transcript 1 (Malat1) appeared as one hub lncRNA at synapses. This is in line with a previous study showing that knocking down MALAT1 in hippocampal neurons decreases the number of synapses, although it has to be mentioned that the authors linked this finding to the role of MALAT1 on gene-expression control (Bernard *et al*, 2010). The presence of snoRNAs at synapses is also highly interesting and in line with a previous study that reported snoRNAs in synaptosomes (Smalheiser *et al*, 2014). Moreover, there was a substantial overlap of the snoRNAs detected in synaptosomes and in primary neurons (60% of the synaptosomal snoRNAs were also detected in microfluidic chambers).

Most of the commonly detected snoRNAs were of the C/D box (49%) or H/ACA-box type (17%) that regulate RNA-methylation and pseudouridylation of mainly ribosomal RNAs (Batkovič *et al*, 2020), which is in line with the presence of ribosomes at synapses (Holt *et al.*, 2019). However, we also identified snoRNAs that cannot be classified in either category (35%) that warrant further investigation. Some of the synaptic snoRNAs have been associated to additional processes and for example SNORD50, SNORD83B or SNOR27 have been linked to mRNA 3' processing and post-transcriptionally gene-silencing (Batkovič *et al.*, 2020), while SNORD115 affects mRNA abundance and is genetically linked to the Prader-Willi-syndrome, a rare genetic disease leading to intellectual disability (Cavaillé, 2017).

A synaptic mRNA/microRNA network

We detected a substantial number of microRNAs in hippocampal synaptosomes and in the microfluidic chambers. The presence of mature microRNAs at synapses is in line with previous reports that employed RT-PCR to study neurites of primary hippocampal neurons (Kye *et al*, 2007), micro-array-technology to analyze microRNAs in the synapto-neurosomes isolated from the forebrain of mice (Lugli *et al*, 2008) or more recently also smallRNA-sequencing and NanoString analysis of hippocampal neuropil or synaptosomes (Smalheiser *et al.*, 2014) (Sambandan *et al.*, 2017). Comparison of the dataset generated by Sambandan and colleagues revealed that out of the 65 microRNAs we detect, 57 were also reported in this previous study. These data further strengthen the view that microRNAs play an important role at synapses and suggest that our dataset represents a high quality synaptic microRNAome as a resource for future studies.

To the best of our knowledge, our study is the first that provides a synaptic coding and small non-coding RNAome from the same preparation thereby allowing us to address the role of the synaptic microRNAome at the systems level.

We used the data to develop a novel tool which is first fed with the mRNA data to parse multiple databases containing experimentally validated interactions and thereby building a high confidence mRNA network of the synapse (See methods for more details). We intersected this mRNA network with the confirmed targets of all microRNAs, which are detected within the same sample to build the synaptic microRNA/mRNA network.

Overall, our data suggest that up to 98% of the synaptic mRNAome is controlled by synaptic microRNAs, suggesting that essentially all synaptic localized mRNAs are potentially regulated via the synaptic microRNAs. Considering that mRNA transport to synapses is an energy-demanding and highly controlled process (Doyle & Kiebler, 2011) it is likely that synaptic microRNAs do not degrade their mRNA targets but rather control their availability for local translation, a question that should be studied in future experiments at the systems level. Another important observation is that many of the synaptic microRNAs are de-regulated in cognitive diseases (see table 1) that often start with synaptic dysfunction. In addition, there is increasing interest in circulating microRNAs as biomarkers for cognitive diseases (Rao *et al*, 2013) (Rupaimoole & Slack, 2017).

The fact that microRNAs have also been reported in synaptic vesicles (Xu *et al*, 2013) and in exosomes derived from neuronal cultures (Jain *et al*, 2019) suggest a potential path how pathological microRNA changes observed in the brain may also manifest in circulation. Hence, the various CNS clearance systems (Plog & Nedergaard, 2018) might transport such vesicles to the circulation, a hypothesis that should be further studied. In the same context, there is substantial data to suggest that microRNAs regulate biological processes across cell-types and even organs (Valadi H, 2007) (Jose, 2015). Intriguingly, in the perfusion channel of microfluidic chambers, which are free of any somata and only contain distal synapses and some neurites, substantially less microRNAs are existent than in the synaptosomes. These microRNAs significantly overlapped with the ones detected in exosomes released by astrocytes (Jovičić *et al.*, 2013).

It is therefore tempting to speculate that within the tripartite synapse astrocytes support synapses with additional microRNAs that help to control the synaptic mRNA pool. Support for this view stems also from the observation that the 3 most significant functional pathways controlled by the synaptosomal microRNAome are “Glutamatergic synapse”, “cAMP signaling” and “long-term potentiation”, which are identical to the top 3 pathways controlled by the microRNAs that are potentially shuttled to synapses via astrocytes. These data underscore the importance of the corresponding mRNA pool and may suggest that microRNAs supplied to synapses by other cell types might suppress translation of the most relevant local mRNAs rather than degrading a few selected RNAs.

Our data allowed us to identify a number of synaptic hub microRNAs (e.g., see Fig 1E and F) and the functional analysis of these microRNAs would be an important task for future studies. Of particular importance would be microRNAs that are de-regulated in cognitive diseases.

Support for this view stems from recent data on microRNA-181a-5p, a hub in our synaptic network, that is de-regulated in neurodegenerative and neuropsychiatric diseases (Stepniak *et al*, 2015) (Ansari, 2019) and was found to be processed at synapses upon neuronal activity (Sambandan *et al.*, 2017). The finding that most microRNAs of the let-7 family are highly abundant at synapses and control a large set of mRNAs is also interesting, since these microRNAs have been observed in several CNS-related pathologies (Derkow *et al*, 2018) while comparatively little is known on their role on the adult brain. Another hub microRNAs is miR-125b-5p that is de-regulated in Alzheimer's disease and causes memory impairment in mice when elevated in the hippocampus of mice (Banzhaf-Strathmann *et al*, 2014), yet its role at the synapse remains elusive. Similarly interesting is miR-128-3p, that is de-regulated in various neuropsychiatric and neurodegenerative diseases and recent data suggest that inhibition of microRNA-128-3p can ameliorate AD pathology (Liu *et al*, 2019).

In conclusion, our study provides the synaptic RNAome and is thus a valuable resource for future studies. Our data furthermore support the importance of synaptic mRNAs and microRNAs and we introduce a new microfluidic chamber that will allow researchers to combine the power of a specific analysis and manipulation of the synaptic compartment (Taylor *et al.*, 2010) with RNA-sequencing approaches.

Materials & Methods

Animals

Three months old male C57B/6J mice were purchased from Janvier Labs. All animals were housed in standard cages on 12h/12h light/dark cycle with food and water ad libitum. All experiments were performed according to the protocols approved by local ethics committee

Isolation of hippocampal synaptosomes for RNA-sequencing

To obtain sufficient RNA for sequencing of hippocampal synaptosomes we isolated the hippocampi from sixty 3-month-old wild type mice. Twenty bi-lateral hippocampi were pooled as 1 sample to obtain 3 independent samples that were further processed to isolate high-quality synaptosomes using a previously described protocol (Boyken *et al*, 2013). In brief, hippocampi were homogenized by 9 strokes at 900 rpm in sucrose buffer and centrifuged at 4° for 2min at 5000rpm (SS34). Supernatants were further centrifuged at 4° for 12min at 11000rpm. Pellets were loaded onto a Ficoll gradient and centrifuged at 4° for 35min at 22500rpm (SW41).

The interface between 13% and 9% Ficoll was washed by further centrifugation and then pelleted by 8700rpm for 12min in a SS34 rotor. Resuspended synaptosomes were then centrifuged on a sucrose gradient for 3h at 28000rpm (SW28). Finally, synaptosomes were fractioned via the Gilson Minipuls and 21 fractions were collected and analyzed by dot blotting.

For this, from each fraction, 2 μ l of sample were pipetted on nitrocellulose membrane, and dried for 5min. Blocking of unspecific signal was done by 5% low fat milk in TBST for 10 min. Antibodies against Synaptophysin and PSD95 were applied for 15min, then the membrane was washed three times for 3min each, in TBST with 5% milk. Secondary antibody was applied for 15min. Afterwards membrane was washed again three times with TBST without milk before being imaged. Only 5 fractions from each preparation showed a signal for synaptophysin and PSD95 ensuring the presence of high-quality synaptosomes and were therefore processed for total and small RNA-sequencing.

Production of microfluidic chambers

To isolate synapses and corresponding RNA for subsequent sequencing from the perfusion channel of currently employed microfluidic chambers (Taylor *et al.*, 2010) was not possible. Therefore, we generated a microfluidic chamber that allowed us to cut the perfusion channel by using polydimethylsiloxan (PDMS) for the chamber and the corresponding substrate (**Fig S1**). Pilot studies showed that unlike the commonly used microfluidic chambers (Taylor *et al.*, 2010), the usage of PDMS as a substrate to bind the chambers on allowed us to cut the perfusion channel. In more detail, the microfluidic chambers were designed using AutoCAD 2017.

The overall layout was similar to the version reported by Taylor and colleagues (Taylor *et al.*), yet for more yield of synaptic RNAs the length of the chamber was increased, with more microgrooves and a wider synaptic compartment to allow easier alignment during cutting. Layouts were translated into photolithography masks by Selba. Production of silicon wafers was done with two layers. The first layer was made by applying 2 ml Photoresist SU-8-2025 on 50.8mm diameter silicon wafers and running the spin coater with the following settings: 1.) 15 sec, 500 rpm, 100 ramp 2.) 100sec, 4000 rpm, 50 ramp. To prebake, wafers were put on a 65° heating plate for 1 min, then for 15min on a 95° heating plate. For depositing the first layer, the mask with the microgrooves pattern was inserted into the MJB4 mask aligner; exposure was set to 9 sec under light vacuum conditions. Afterwards wafers were postbaked at 65° for 1 min and 5 min at 95°C.

Subsequently 3 ml of the second photoresist SU-8-2050 were added on top and spread thin with the following spincoater protocol: 1.) 15 sec, 100 ramp, 500 rpm 2) 60 sec, 900 rpm, 50ramp. This time prebaking was done with 1min at 65° and minimum of 30min at 95°. The second layer was aligned to the microgrooves using the microscope of the mask aligner. UV light exposure lasted 19 sec, in the soft contact setting. After postbaking as described for the first layer, wafers were developed for 10min or more in mrDev600 with the aid of ultrasonication.

PDMS (SYLGARD™ 184 Silicone Elastomer Kit) was used to manufacture the chambers as well as the bottom substrates. Sylgard components were mixed 10:1, mixed with a 1ml pipette tip, poured over the wafers that were placed in 6cm diameter Petri dishes and very thinly (1-2mm high) onto 10cm dishes. Degassing was done for minimum 15 minutes in a desiccator under vacuum. Afterwards wafers and bottom parts were transferred to a 70° oven and cured for 2h.

Chambers and bottom parts were cut out by a scalpel, holes in the chambers were punched by biopsy punchers of 6mm and 8mm diameter and bottom parts were cut into smaller pieces to hold one chamber each. To clean off dust, the pieces off of dust they were placed in an ultrasonic bath for 10 min and then dried on a heatplate at 70°. PDMS can be bound to PDMS covalently under oxygen plasma conditions; a tesla-coil type device, the Corona plasma treater from Blackhole lab, was used to this end. The plasma treater was hovered slowly 2cm above the chambers (bottom side up), going back and forth to cover the whole area by discharges for 30sec, then the same was done to the bottom part. Thereupon both parts were brought together and pressed very slightly to ensure complete contact. Covalent bond forming was enhanced by placing the so assembled chamber in the oven at 70° for 10min. Subsequently chambers were filled with PBS or borate buffer to maintain hydrophilic properties. For chambers that were supposed to be imaged, chambers were not treated with plasma; rather chambers were assembled to the PDMS or glass substrate under the biosafety cabinet by simply pressing both pieces together.

Once assembled, chambers were brought to a biosafety cabinet and washed with 70% ethanol, then twice with water. Coating on PDMS worked best when done with 0.5 mg PDL in borate buffer overnight. Visual inspection under the microscope should make sure that no bubbles are present in the chambers. Great care needs to be taken when washing to not remove the coating. Liquid should be never removed with a suction pump sucking liquid directly from the channels, instead liquid should be removed by pointing the pipette at the wall of open reservoirs. Washing was done twice with PBS, 80µl per top reservoir, allowing for the liquid to flow into the down reservoir. Perfusion reservoirs were washed by applying 50µl in each well, one at a time and waiting for 5min in between. Once all PBS was removed from the open reservoirs 80µl of medium was added per top reservoir, allowing for the liquid to flow into the down reservoir. This process was repeated once, before chambers were left over night in the incubator before seeding, to ensure proper hydrophilicity. For easier handling always two chambers were put together in a 10cm dish, with two lids of 15ml falcon tubes filled with water next to them, to reduce the evaporation from the chambers themselves.

Primary hippocampal neuronal cultures

Pregnant CD1 mice were sacrificed under anesthesia by cervical dislocation at E16 or E17. Brains from embryos were extracted and their hippocampi collected. Processing was done using the Papain kit from Worthington, and cells were counted and diluted to a density of 5 Million per ml.

Seeding was done with the following pipetting scheme in order to make sure, most cells reach the microgrooves but do not enter them. 10µl of cell suspension containing 70.000 cells were injected in the channels from the top wells. We started with the axonal side. A second pipetting step with 5µl added to the channels from the bottom wells, after inspection of cells under the microscope. After 10 minutes, a similar seeding was performed for the dendritic side. One hour later each well was filled up to 100µl. The next day another 100µl were pipetted into each well.

Visual inspection under a microscope was necessary to do several rounds of seeding with decreasing volume to make sure the desired spread of cells was achieved. After two hours reservoirs of the chambers were filled up with medium to 100µl each, by pipetting an additional 70µl simultaneously in both reservoirs per side, while not adding more medium to the perfusion. We used Neurobasal Plus with GlutaMax, Penicilin/Strep and B27 Plus supplement for better viability. Parallel to chambers, normal 12-well dishes, coated with PDL in borate overnight and washed three times with water, were cultured at 260.000 cells per well; those served as standby cultures. Since medium evaporation can happen quickly in the chambers, every 2-3 days medium from these standby cultures was filtered by a 0.22µm syringe filter and then added to the chambers. For the KCl stimulation, around 50µl of medium was collected from each reservoir of the chambers, mixed with KCl as to result in a final concentration of 50mM when given back to the chamber and then incubated for 2h before RNA isolation.

Harvesting of synaptic RNAs from microfluidic chambers: SNIDER

In order to parallel cut the PDMS substrate, we designed a machine consisting of a blade-holding arm on a ball-bearing rail, allowing frictionless mobility in one dimension. A screw-driven spring drives the razorblades height position and allows for controlling the penetration depth of the blades into the PDMS. The non-cutting corners of the razorblade were removed with a plunger to only have one accessing point of the blades into the PDMS. Small metal plates were put in between the blades and served as spacers, increasing the inter-blade distance to 900 µm. On the day of harvest cells in the chambers were washed once with PDMS and flipped upside down. Great care was taken to maintain a RNase free environment by prior cleaning of all tools and instruments with RNasezap and 70% EtOH afterwards. To have an endpoint for the long parallel cut we introduced with a scalpel two horizontal cuts between the outer perfusion wells and the upper left respectively upper right well that met at the perfusion stream. Then chambers were aligned by their perfusion stream on a marked line of the device. By close visual inspection the blades were lowered just before entering the PDMS material and blades were brought in parallel to the synaptic compartment. Blades were then lowered 2mm deep into the substrate just before the perfusion outlet and then the metal lever was pulled backwards, moving the blades towards the perfusion wells until the parallel cut met the V-shaped cut induced by scalpel earlier. With a pair of

tweezers, the synaptic compartment was taken out and put into cell lysis buffer solution of GenElute Sigma kit, whereupon we followed the manufactures protocol under 1C to isolate total RNA, including small RNAs.

RNA sequencing

The synaptosomal RNA samples were split into halves; one was further processed to obtain total RNA libraries using the Illumina Truseq total RNA kit, the other half was used for small RNA sequencing using the NEBNext Small RNA Library Prep Kit as described before (Benito *et al*, 2015).

For total RNA sequencing of RNA from microfluid chambers, we always pooled two samples and libraries were created with Takara's SMARTer Stranded Total RNA-Seq Kit v2 - Pico Input Mammalian. small RNA libraries were generated using Takara's SMARTer smRNA-Seq Kit for Illumina. To verify the library and sequencing procedure we added spike-in RNAs from the QIAseq miRNA Library QC kit prior to library creation.

Bioinformatic analysis

Sequencing data was processed using a customized in-house software pipeline. Illumina's conversion software bcl2fastq (v2.20.2) was used for adapter trimming and converting the base calls in the per-cycle BCL files to the per-read FASTQ format from raw images. Quality control of raw sequencing data was performed by using FastQC (v0.11.5). Trimming of 3' adapters for smallRNaseq data was done using cutadapt (v1.11.0). The mouse genome version mm10 was used for alignment and annotation of coding and non-coding genes.

Small RNAs were annotated using miRBase (Griffiths-Jones, 2006) for miRNAs and snOPY (Yoshihama *et al*, 2013) for snoRNAs. For totalRNaseq reads were aligned using the STAR aligner (v2.5.2b) (Dobin *et al*, 2013) and read counts were generated using featureCounts (v1.5.1) (Liao *et al*, 2014). For smallRNaseq reads were aligned using the mapper.pl script from mirdeep2 (v2.0.1.2) (Friedländer *et al*, 2012) which uses bowtie (v1.1.2) (Langmead & Salzberg, 2012) and read counts were generated with the quantifier.pl script from mirdeep2. All read counts were normalized according to library size to transcript per million (TPM).

We used a TPM cutoff of 1000 reads for smallRNAs to make sure that these smallRNAs were considerably detected up to an average raw count of 10 reads. To account for differences in sequencing depth between synaptosomal mRNAs (average of 6mio unique reads per lane) and mRNAs from microfluidic chambers (average of 20mio unique reads per lane) we applied a cutoff of 50 and 100 normalized reads, respectively.

Differential expression analysis was performed with the DESeq2 (v1.26.0) R (v3.6.3) package (Love *et al*, 2014), here unwanted variance was removed using RUVSeq (v1.20.0) (Risso *et al*, 2014). Networks were build using Cytoscape (v3.7.2) (Shannon *et al*, 2003) based on automatically created lists of pairwise interactors.

We used in-house Python scripts to detect interactions between expressed non-coding RNAs (miRNAs, lncRNAs, or snoRNAs) and coding genes; interaction information was collected from six different databases: NPInter (Teng *et al*, 2020), RegNetwork (Liu *et al*, 2015), Rise (El Fatimy *et al*, 2018), STRING (Szklarczyk *et al*, 2019), TarBase (Karagkouni *et al*, 2018), and TransmiR (Tong *et al*, 2019). All interactions classified as weak (if available) were excluded. The lists of pairwise interactors were loaded into Cytoscape and all nodes connected by only one edge were removed to build the final network, respectively.

Imaging

Cells were fixed in 4% PFA in PBS plus 1 μ M MgCl₂, 0.1 μ M CaCl₂ and 120mM Sucrose. Our imaging setup consists of a Leica DMI8 microscope that is equipped with a STEDYcon. Phase contrast images were obtained using the Leica in its normal mode, with the Leica DMI8 software. All other fluorescent images were taken with the STEDYcon in either confocal or STED mode. Antibodies: PSD95 (Merck - MABN 68) and Synaptophysin 1 (Synaptic Systems 101 004), both diluted to 1:400. Secondary antibodies were StarRED (Abberior, STRED-1001-500UG) and Alexa Fluor 633 Anti-Guinea Pig (Invitrogen, A21105) both diluted to 1:400. DAPI was applied for 1min for counterstaining.

Availability of data

All sequencing data are available via GEO database. GSE159248:

<https://www.ncbi.nlm.nih.gov/geo/query/acc.cgi?acc=GSE159248>

Supplemental Tables can be accessed here:

<https://www.biorxiv.org/content/10.1101/2020.11.27.401901v1.supplementary-material>

Code availability

Not applicable

Conflict of interest

The authors declare no conflict of interest

Funding

This work was supported by the following third-party funds to AF: the ERC consolidator grant DEPICODE (648898), funds from the SFB1286 (B06), the DFG under Germany's Excellence Strategy - EXC 2067/1 390729940 the and funds from the German Center for Neurodegenerative Diseases (DZNE).

Author contribution

RE conducted cell culture and RNA-sequencing experiments, build microfluidic chambers and analyzed data. DMK performed bioinformatic analysis, TB isolated synaptosomes, GB and SK helped with the generation of microfluidic chambers, RI performed total RNA-sequencing from hippocampal neuronal cultures in normal culture dishes and curated the disease-related list of microRNAs, AF supervised the project and wrote the manuscript.

Literature

- Ainsley JA, Drane L, Jacobs J, Kittelberger KA, Reijmers LG (2014) Functionally diverse dendritic mRNAs rapidly associate with ribosomes following a novel experience. *Nature communications* 5: 4510
- Ansari A, Maffioletti, E., Milanesi, E., Marizzoni, M., Frisoni, G. B., Blin, O., Richardson, J. C., Bordet, R., Forloni, G., Gennarelli, M., Bocchio-Chiavetto, L., & PharmaCog Consortium (2019) miR-146a and miR-181a are involved in the progression of mild cognitive impairment to Alzheimer's disease. *Neurobiology of Aging* 82: 102-109
- Banzhaf-Strathmann J, Benito E, May S, Arzberger T, Tahirovic S, Kretzschmar H, Fischer A, Edbauer D (2014) MicroRNA-125b induces tau hyperphosphorylation and cognitive deficits in Alzheimer's disease. *EMBO J* 33: 1667-1680
- Benito E, Urbanke E, Barth J, Halder R, Capece V, Jain G, Burkhardt S, Navarro M, Schutz AL, Bonn S *et al* (2015) Reinstating transcriptome plasticity and memory function in mouse models for cognitive decline. *J Clin Invest* 125: 3572-3584
- Bernard D, Prasanth KV, Tripathi V, Colasse S, Nakamura T, Xuan Z, Zhang MQ, Sedel F, Jourdain L, Couplier F *et al* (2010) A long nuclear-retained non-coding RNA regulates synaptogenesis by modulating gene expression. *The EMBO journal* 29: 3082–3093
- Biever A, Glock, C., Tushev, G., Ciirdaeva, E., Dalmay, T., Langer, J. D., & Schuman, E. M. (2020). Monosomes actively translate synaptic mRNAs in neuronal processes. *Science (New York, N.Y.)*, 367(6477), eaay4991. (2020) Monosomes actively translate synaptic mRNAs in neuronal processes. *Science* 3677.
- Boyken J, Grønborg M, Riedel D, Urlaub H, Jahn R, Chua JJ (2013) Molecular profiling of synaptic vesicle docking sites reveals novel proteins but few differences between glutamatergic and GABAergic synapses. *Neuron* 78: 285-297
- Bratkovič T, Božič J, Rogelj B (2020) Functional diversity of small nucleolar RNAs. *Nucleic acids research. Nucleic acids research* 48: 1627-1651
- Cajigas IJ, Tushev G, Will TJ, tom Dieck S, Fuerst N, Schuman EM (2012) The local transcriptome in the synaptic neuropil revealed by deep sequencing and high-resolution imaging. *Neuron* 74: 453–466
- Cavaillé J (2017) ox C/D small nucleolar RNA genes and the Prader-Willi syndrome: a complex interplay. *Wiley interdisciplinary reviews RNA* 8: <https://doi.org/10.1002/wrna.1417>
- Chen BJ, Ueberham U, Mills JD, Kirazov L, Kirazov E, Knobloch M, Bochmann J, Jendrek R, Takenaka K, Bliim N *et al* (2017) RNA sequencing reveals pronounced changes in the noncoding transcriptome of aging synaptosomes. *Neurobiology of aging* 56: 67–77
- Derkow K, Rössling R, Schipke C, Krüger C, Bauer J, Föhling M, Stroux A, Schott E, Ruprecht K, Peters O *et al* (2018) Distinct expression of the neurotoxic microRNA family let-7 in the cerebrospinal fluid of patients with Alzheimer's disease. *PLoS one* 13: e0200602
- Dobin A, Davis CA, Schlesinger F, Drenkow J, Zaleski C, Jha S, Batut P, Chaisson M, Gingeras TR (2013) STAR: ultrafast universal RNA-seq aligner. *Bioinformatics* 13: 673-691
- Doyle M, Kiebler MA (2011) Mechanisms of dendritic mRNA transport and its role in synaptic tagging. *EMBO J* 30: 3540-3552
- El Fatimy R, Li S, Chen Z, Mushannen T, Gongala S, Wei Z, Balu DT, Rabinovsky R, Cantlon A, El Khal A *et al* (2018) MicroRNA-132 provides neuroprotection for tauopathies via multiple signaling pathways. *Acta Neuropathol* 136: 537-555
- Farris S, Ward JM, Carstens KE, Samadi M, Wang, Y., Dudek SM (2019) Hippocampal Subregions Express Distinct Dendritic Transcriptomes that Reveal Differences in Mitochondrial Function in CA2. *Cell reports* 29: 522–539

- Fonkeu Y, Krainyukova N, Hafner AS, Kochen L, Sartori F, Schuman EM, Tchumatchenko T (2019) How mRNA Localization and Protein Synthesis Sites Influence Dendritic Protein Distribution and Dynamics. *Neuron* 103: 1109-1122
- Friedländer MR, Mackowiak SD, Li N, Chen W, Rajewsky N (2012) miRDeep2 accurately identifies known and hundreds of novel microRNA genes in seven animal clades. *Nucleic acids research* 40: 37-52
- Garner CC, Tucker RP, Matus A (1988) Selective localization of messenger RNA for cytoskeletal protein MAP2 in dendrites. *Nature biotechnology*, 336: :674–677
- Griffiths-Jones S (2006) miRBase: the microRNA sequence database. *Methods in molecular biology*: 129-138
- Gurtan AM, Sharp PA (2013) The Role of miRNAs in Regulating Gene Expression Networks. *J Mol Biol* pii: Epub ahead of print
- Hafner AS, Donlin-Asp, P. G., Leitch, B., Herzog, E., & Schuman, E. M. (2019). Local protein synthesis is a ubiquitous feature of neuronal pre- and postsynaptic compartments. *Science* (New York, N.Y.), 364(6441), eaau3644. (2019) Local protein synthesis is a ubiquitous feature of neuronal pre- and postsynaptic compartments. . *Science* 364: eaau3644
- Hefter D, Ludewig S, Draguhn A, Korte M (2020) Amyloid, APP, and Electrical Activity of the Brain. *The Neuroscientist* 26: 231-251
- Holt CE, Martin KC, Schuman EM *tinva*fNsmB, 26(7), 557–566. (2019) *Nature structural & molecular biology* 26: 557–566.
- Jain G, Stuendl A, Rao P, Berulava T, Pena Centeno T, Kaurani L, Burkhardt S, Delalle I, Kornhuber J, Hüll M *et al* (2019) A combined miRNA-piRNA signature to detect Alzheimer's disease. . *Translational Psychiatry* 9: 250
- Jose AM (2015) Movement of regulatory RNA between animal cells. *Genesis* 53: 395-416
- Jovičić A, Roshan R, Moiso N, Pradervand S, Moser R, Pillai B, Luthi-Carter R (2013) Comprehensive expression analyses of neural cell-type-specific miRNAs identify new determinants of the specification and maintenance of neuronal phenotypes. *J Neurosci* 33: 5127-5137
- Karagkouni D, Paraskevopoulou MD, Chatzopoulos S, Vlachos IS, Tastsoglou S, Kanellos I, Papadimitriou D, Kavakiotis I, Maniou S, Skoufos G *et al* (2018) DIANA-TarBase v8: a decade-long collection of experimentally supported miRNA-gene interactions. . *Nucleic acids research* 46: D239–D245
- Kosik KS (2016) Low Copy Number: How Dendrites Manage with So Few mRNAs. *Neuron* 92: 1168–1180
- Kye MJ, Liu T, Levy SF, Xu NL, Groves BB, Bonneau R, Lao K, Kosik KS (2007) Somatodendritic microRNAs identified by laser capture and multiplex RT-PCR. *RNA* 13: 1224–1234
- Langmead B, Salzberg SL (2012) Fast gapped-read alignment with Bowtie 2. *Nat Methods* 9: 357-359
- Liao Y, Smyth GK, Shi W (2014) featureCounts: an efficient general purpose program for assigning sequence reads to genomic features. *Bioinformatics* 30: 923-930
- Liu Y, Zhang Y, Liu P, Bai H, Li X, Xiao J, Yuan Q, Geng S, Yin H, Zhang H *et al* (2019) MicroRNA-128 knockout inhibits the development of Alzheimer's disease by targeting PPAR γ in mouse models. *European journal of pharmacology* 843: 132-144
- Liu ZP, Wu C, Miao H, Wu H (2015) RegNetwork: an integrated database of transcriptional and post-transcriptional regulatory networks in human and mouse. *Database : the journal of biological databases and curatio* bav095
- Love MI, Huber W, Anders S (2014) Moderated estimation of fold change and dispersion for RNA-seq data with DESeq2. *Genome Biol* 15: 550
- Lugli G, Torvik VI, Larson J, Smalheiser NR (2008) Expression of microRNAs and their precursors in synaptic fractions of adult mouse forebrain. *J Neurochem* 106: 650-661

- Most D, Ferguson L, Blednov Y, Mayfield RD, Harris RA (2015) The synaptoneurosome transcriptome: a model for profiling the emolecular effects of alcohol. *The pharmacogenomics journal* 15: 177-188
- Plog BA, Nedergaard M (2018) The glymphatic system in CNS health and disease: past, present and future. *Annu Rev Pathol* 24: 379-394
- Prada I, Gabrielli M, Turola E, Iorio A, D'Arrigo G, Parolisi R, De Luca M, Pacifici M, Bastoni M, Lombardi M *et al* (2018) Glia-to-neuron transfer of miRNAs via extracellular vesicles: a new mechanism underlying inflammation-induced synaptic alterations. *Acta neuropathologica*, 135: 529-550
- Rajman M, Schratt G (2017) MicroRNAs in neural development: from master regulators to fine-tuners. *Development* 44: 2310-2322
- Rao P, Benito E, Fischer A (2013) MicroRNAs as biomarkers for CNS disease. *Front Mol Neurosci* 26: eCollection 2013
- Risso D, Ngai J, Speed TP, Dudoit S (2014) Normalization of RNA-seq data using factor analysis of control genes or samples. *Nature biotechnology* 32: 896
- Rupaimoole R, Slack F, J. (2017) MicroRNA therapeutics: towards a new era for the management of cancer and other diseases. . *Nat Rev Drug Discov* 16: 203-222
- Sambandan S, Akbalik G, Kochen L, Rinne J, Kahlstatt J, Glock C, Tushev G, Alvarez-Castelao B, Heckel A, Schuman EM (2017) Activity-dependent spatially localized miRNA maturation in neuronal dendrites. *Science* 355: 634-637
- Shannon P, Markiel A, Ozier O, Baliga NS, Wang JT, Ramage D, Amin N, Schwikowski B, Ideker T (2003) Cytoscape: a software environment for integrated models of biomolecular interaction networks. *Genome research* 13: 2498.2504
- Smalheiser NR (2014) The RNA-centred view of the synapse: non-coding RNAs and synaptic plasticity. *Philos Trans R Soc Lond B Biol Sci* 369: pii: 20130504
- Smalheiser NR, Lugli G, Zhang H, Rizavi H, Cook EH, Dwivedi Y (2014) Expression of microRNAs and other small RNAs in prefrontal cortex in schizophrenia, bipolar disorder and depressed subjects. *PLoS One* 9: e86469
- Smythies J, Edelstein L (2013) Transsynaptic modality codes in the brain: possible involvement of synchronized spike timing, microRNAs, exosomes and epigenetic processes. *Frontiers in integrative neuroscience* 6: <https://doi.org/10.3389/fnint.2012.00126>
- Sotelo JR, Canclini L, Kun A, Sotelo-Silveira JR, Calliari A, Cal K, Bresque M, Dipaolo A, Farias J, Mercer JA (2014) Glia to axon RNA transfer. . *Developmental neurobiology* 73: 292-302
- Stepniak B, Kästner A, Poggi G, Mitjans M, Begemann M, Hartmann A, Van der Auwera S, Sananbenesi F, Krueger-Burg D, Matuszko G *et al* (2015) Accumulated common variants in the broader fragile X gene family modulate autistic phenotypes. *EMBO Mol Med* 7: 1565-1579
- Szklarczyk D, Gable AL, Lyon D, Junge A, Wyder S, Huerta-Cepas J, Simonovic M, Doncheva NT, Morris JH, Bork P *et al* (2019) STRING v11: protein-protein association networks with increased coverage, supporting functional discovery in genome-wide experimental datasets. *Nucleic Acids Res* 47: D607-D613
- Taylor AM, Dieterich DC, Ito HT, Kim SA, Schuman EM (2010) Microfluidic local perfusion chambers for the visualization and manipulation of synapses. *Neuron*, 66(1), 57-68 66: 57-68
- Teng X, Chen X, Xue H, Tang Y, Zhang P, Kang Q, Hao Y, Chen R, Zhao Y, He S (2020) NPInter v4.0: an integrated database of ncRNA interactions. *Nucleic acids research* 48: 160-165

- Tong Z, Cui Q, Wang J, Zhou Y (2019) TransmiR v2.0: an updated transcription factor-microRNA regulation database. *Nucleic acids research* 47: D253–D258
- Valadi H EK, Bossios A, Sjöstrand M, Lee JJ, Lötvall JO. (2007) Exosome-mediated transfer of mRNAs and microRNAs is a novel mechanism of genetic exchange between cells. *Nat Cell Biol* 9: 654-659
- Weiss K, Antoniou A, Schratt G (2015) Non-coding mechanisms of local mRNA translation in neuronal dendrites. *European journal of cell biology* 94: 363-367
- Xu J, Chen Q, Zen K, Zhang C, Zhang Q (2013) Synaptosomes secrete and uptake functionally active microRNAs via exocytosis and endocytosis pathways. *J Neurochem* 124: 15-25
- Yoshihama M, Nakao A, Kenmochi N (2013) snOPY:a small nucleolar RNA orthological gene database. *BMC research notes* 6

Supplementary Figures

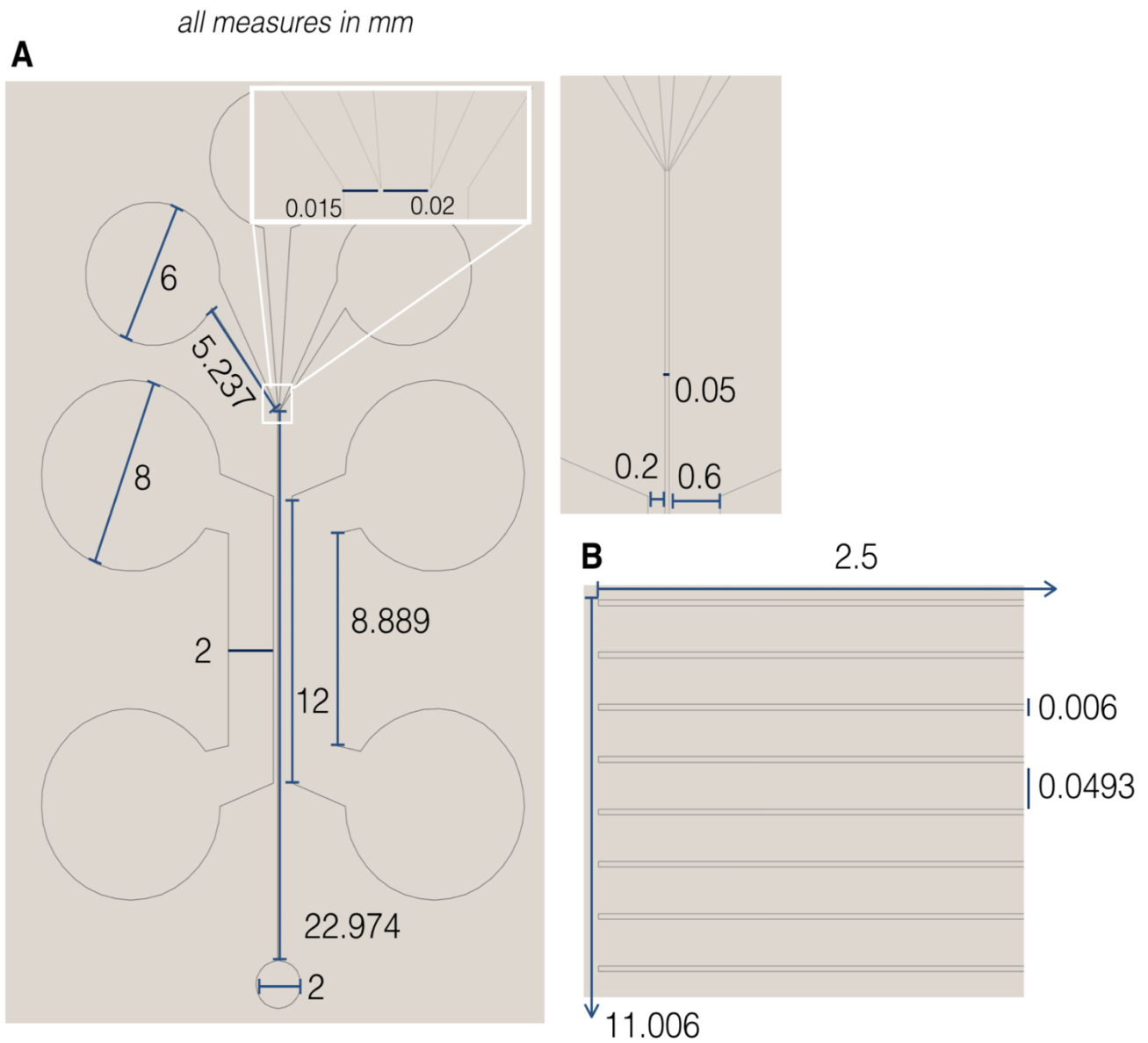


Fig S1: Design of the photolithography masks. **A.** Layout is based on (Taylor 2010). Changes have been introduced in many dimensions to increase the overall yield when cutting the synaptic compartment. The image shows the Mask containing the reservoirs as well as the perfusion channel, for second exposure. Height of the photoresist (SU-8-2050) for this step is 160 μ m. **B.** Mask containing the microgrooves, used for first exposure. Height of the photoresist (SU-8-2025) for this step is 20 μ m.

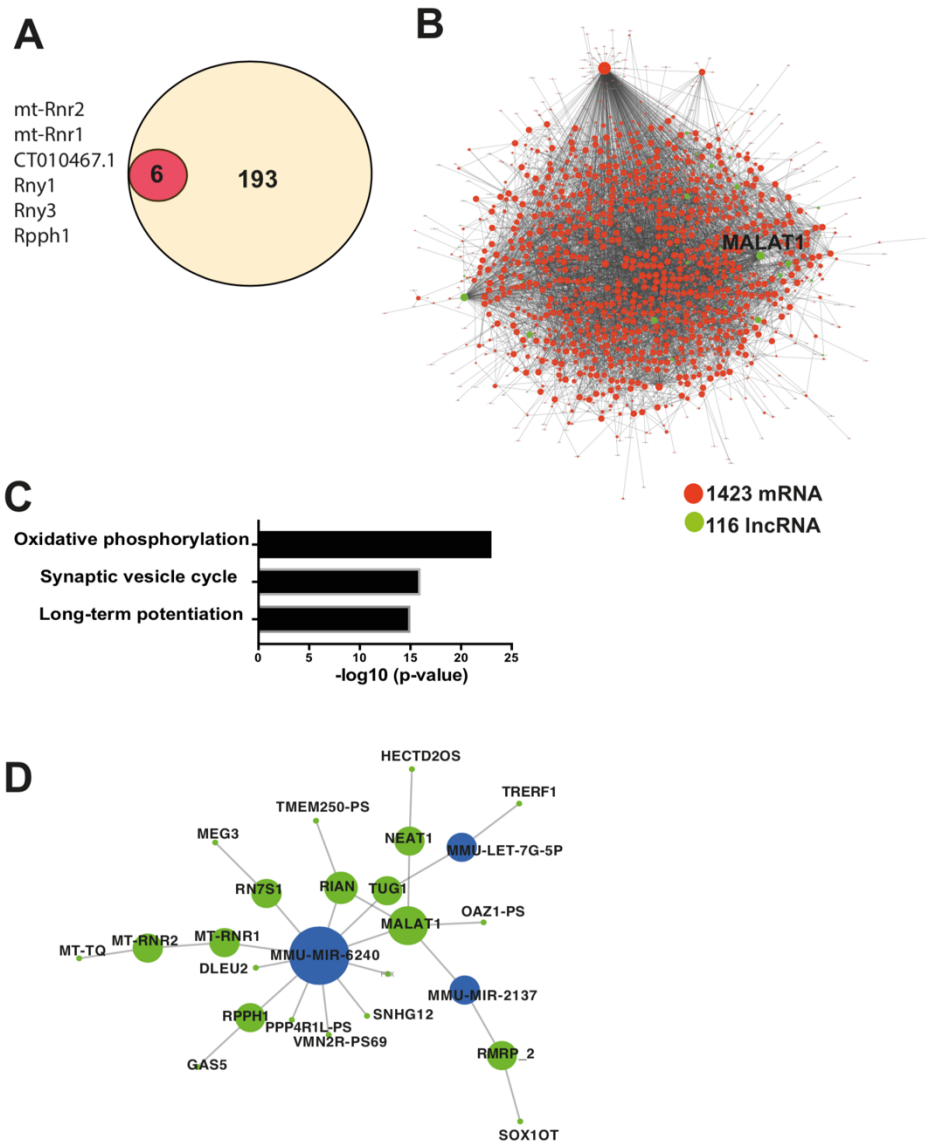


Fig S2: Network analysis of synaptic lncRNAs. **A.** Venn diagram showing that the 6 annotated lncRNA detected in synaptosomes (red circle) are part of the 199 lncRNA detected in the microfluidic chambers. The 6 common lncRNAs are listed in the left panel. **B.** Out of 1460 mRNA detected in microfluidic chambers, 1423 could be fit into a network that also contains 116 of the 199 annotated lncRNA. Specifically Malat 1 appears as a hub lncRNA. **C.** Three main pathways represented by the synaptic mRNAs potentially controlled by the 116 lncRNAs. **D.** Network showing the interactions of synaptic lncRNA (green) and microRNA (blue) detected in microfluidic chambers. Note that the two well-studied lncRNAs Malat1 and Neat 1 are part of a network that controls microRNA-6240, let-7G-5p and microRNA-2137. Please note that panels B and D are available as searchable high resolution PDF files as additional supplemental data.

Addendum (not part of the manuscript)

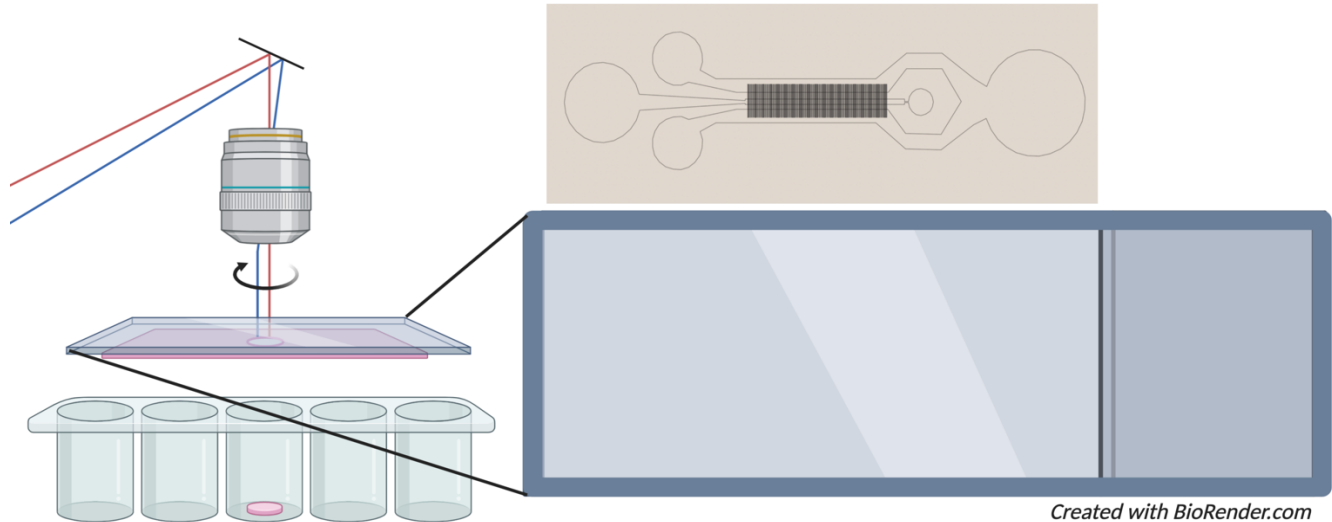


Fig A1: Alternative approach to harvest isolated neurites. Laser microdissection precisely cuts at freely defined areas of a thin membrane. In the top I show a design that maintains the microgrooves and perfusion channel described before, yet fits on the microdissection slides.

Before devising SNIDER, I tried different approaches to achieve the isolation of neurite RNAs.

It is possible to not covalently bind the chamber on PDMS, thus the chamber can be removed after seeding and two weeks of culturing. In doing so, I tried to isolate neurite-RNAs via laser microdissection. To this end I designed a chamber with a similar underlying logic as the SNIDER chamber, only narrower. Instead of three perfusion wells, just one remains; the other two are used to seed cells. Furthermore, both neuronal pools are connected (Fig A1). At DIV14 the chamber can be slowly removed, and the laser cuts the membrane where the microgrooves have been.

This method actually led to successful isolation of neurites, but was found to be too time-consuming. Moreover, due to the non-covalent binding, leakage often occurred and neurons sometimes grew underneath the chamber.

I also tried to cut PDMS chambers with a vibratome, however the blades would not get a good grip of the material, thereby failing to penetrate the PDMS.

When I developed SNIDER, a lot of culturing parameters had to be tested to minimize PDMS toxicity and maximize cell survival (Tab A1). The main issue was the leakage of uncured oligomers into the medium over time (Regehr et al., 2009). My solution were the washing steps as well as the two overnight incubations (once for coating, once with medium before seeding); when replacing both overnight solutions, most uncured oligomers were removed and cells could be cultured for over a month.

Table A1: Tested and optimized parameters for culturing neurons in microfluidic chambers. Entries in bold indicate high cell survival.

Bottom Parts	Coating Molecule	Media	Bonding	Washing	Misc
<i>Glass</i>	PDL (in borate buffer)	Normal Neurobasal	Plasma Cleaner	Water	Wash after coating with very low volume
Plastic	PLO (+ LAM)	enhanced Medium (NB+)	Tesla Coil	MetOH	Papain dissociation
PDMS: 1:10	LAM	Brainphys	Reversible attaching	H2O + EtOH	cell concentration
PDMS: 1:20	PEI (+ LAM)	no medium change		autoclaving	
Agarose, Agarose/PDMS		exchange		ultrasonication	

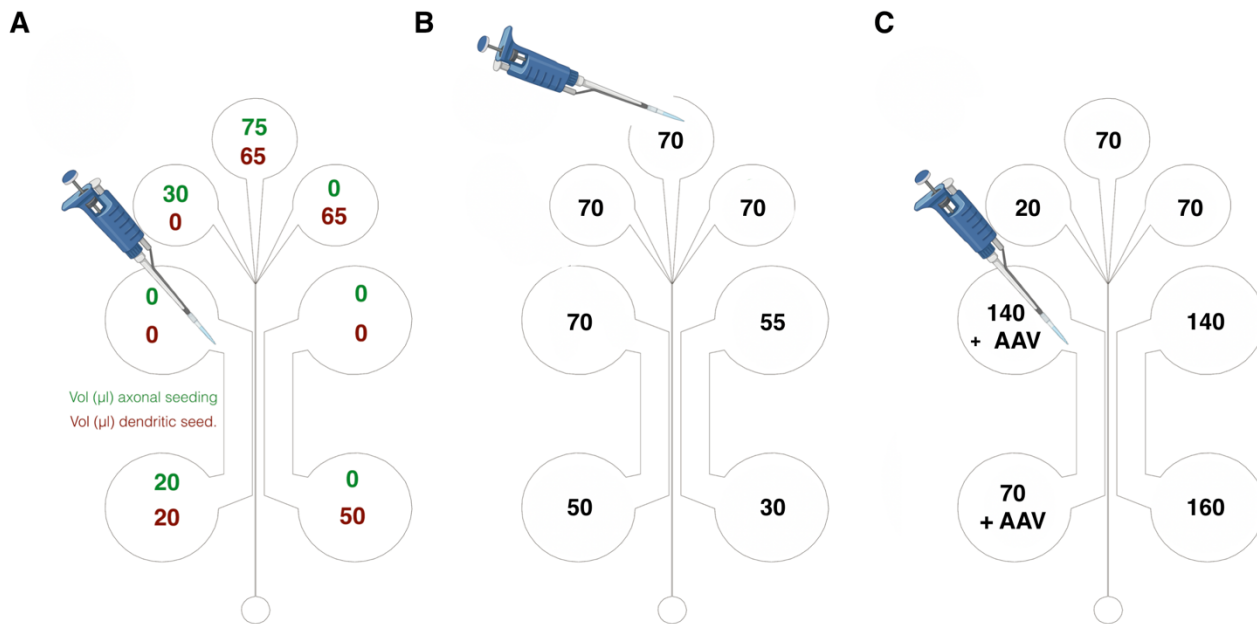


Fig A2: Pipetting schemes. **A)** Protocol for seeding neurons as close to the microgrooves as possible. Prior to seeding, fluid pressure has to be built up by filling each reservoir with medium in the given volumes. Numbers in green indicate the necessary volumes when seeding axonal neurons (the side of the chamber with longer microgrooves before reaching the perfusion channel), numbers in red are for the dendritic side. Seeding is done as described in the manuscript. Axonal side should be seeded first, followed by the dendritic one. **B)** Pipetting scheme for the slow perfusion of synapses with an agent added in the middle perfusion well. Reservoirs should be filled going from the lowest to the highest volume. The middle reservoir of the perfusion channel (indicated by the pipette) should be filled last. **C)** Pipetting scheme for transduction of only dendritic cells. When viral transduction of only one neuronal pool is desired, reservoirs have to be filled as indicated.

The architecture of the microfluidic chambers allows the prolonged sustainability of fluid pressures. As a result, different ways of filling allow for differential direction of liquid flow, while minimizing diffusion from occurring over the microgrooves (Taylor et al., 2010). Thereby, flow from one side of the chamber to the other can be stopped for about 20h (Park et al., 2006). After that time a renewal of the voluminal is necessary.

Another feature of microfluidic systems is laminar flow. Particles of a laminar flow do not mix laterally with another flow. I therefore developed pipetting schemes to achieve different goals. By using the hydrostatic pressure, one can bring cells very close to microgrooves, while preventing any debris or smaller cells to enter (Fig A2A), perfusing only the synapses along the perfusion channel for several hours (Fig A2B) or transducing only one neuronal pool in the chamber (Fig A2C).

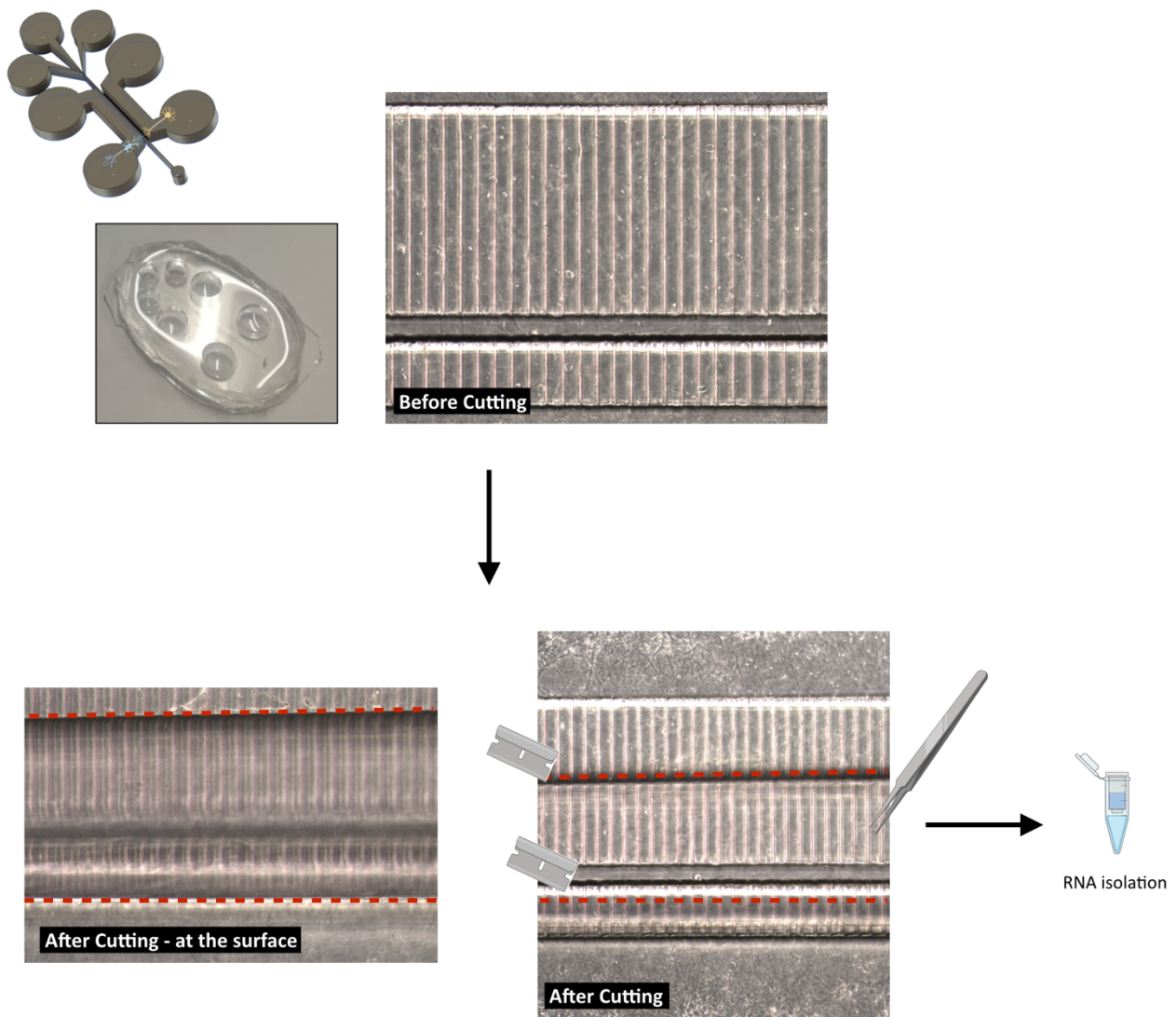


Fig A3: Cutting does not affect the somata of neurons. Top: model of the chamber with indicated growth of neurites into the microgrooves. Photo of a chamber made from PDMS, plasma-bonded to a thin PDMS bottom part. On the right is a phase contrast image of hippocampal neurites inside the microgrooves. Bottom: Images of chamber after being cut with SNIDER. The cut is extremely precise: it runs parallel and does not affect the somata of cells neighboring the microgrooves. Note that the chamber is still attached to the PDMS substrate after cutting.

When I tested if SNIDER would compromise the integrity of the cell bodies closest to the microgrooves, I found them unaffected – thus all isolated RNA stems from neurites in the microgrooves alone and not from nearby, burst or damaged cells (Fig A3).

Chapter 2 - Studying the effects of locally inhibiting a miRNA

Introduction

During our work on the description of the hippocampal synaptic RNAome, we first obtained the synaptosomal miRs. The second highest abundant miR in this dataset was miR-9-5p, which is already known to affect dendrite length and intersections (Giusti et al., 2014), and is speculated to be important during cortical development (Topol et al., 2016).

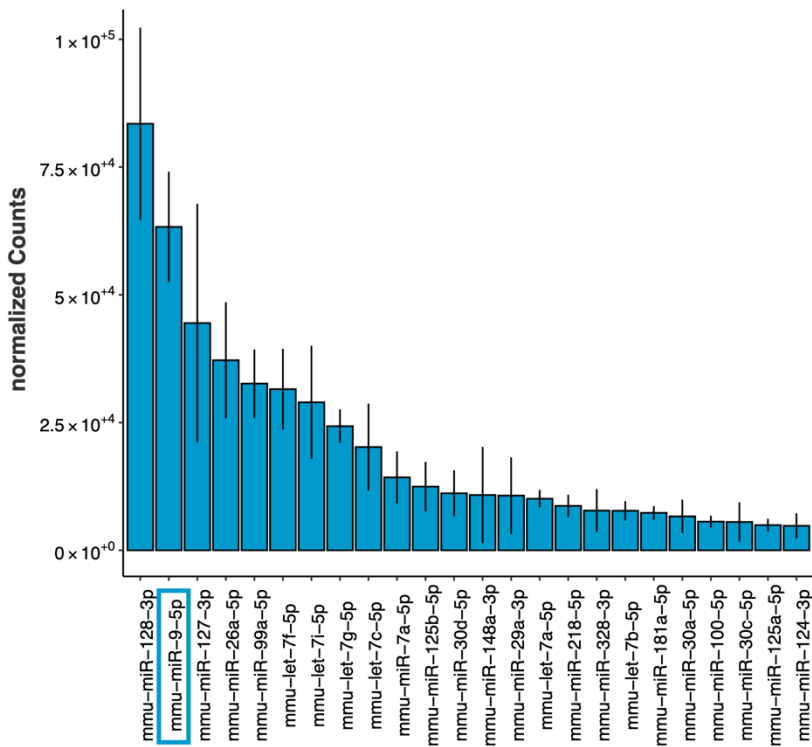


Fig 1: Most abundant miRNAs found in synaptosomes as described in Chapter 1. The second most abundant miR-9-5p serves interesting roles in neurons.

To further investigate the role of this miR on the local RNAome, I decided to specifically inhibit it at the synapses of microfluidic chambers. A Targetscan analysis revealed that of the 1460 mRNAs that we find at synapses (Chapter 1), 98 of them are predicted to be a target of miR-9-5p, implying an important role for this miR in regulating local translation.

Material and Methods

Cell Culture

Primary cell cultures were prepared from the hippocampi of CD1 mice embryos from E16-17 as described in Chapter 1. Cell suspension was seeded in 0.5mg/ml coated 24 well plates for RNA harvesting, on coverslips in 0.5mg/ml coated 24 well plates for imaging or in microfluidic chambers (as detailed in Chapter 1).

Production of lipid nanoparticles

Inhibitor of miR-9-5p (YI04100538-DDB (339131/5FAM)) as well as the control (YI00199006-DDB (339136/5FAM)) were ordered as stable locked nucleic acid (LNA) versions, with a 5'-6FAM reporter signal from Qiagen (miRCURY LNA miRNA inhibitors). Lipid nano particles (LNP) were prepared following the instructions of Precisions Nanosystems Spark, either filled with either miR-9-5p inhibitor or control and stored at 4° until usage; for storage longer than 7 days, LNPs were diluted 1:10 in neurobasal medium Plus (NB+) (A3653401, Gibco).

Application of LNPs to culture

LNPs were added to hippocampal neurons cultured in 24-well plates at DIV14 at 1µg per ml and 10 µl of ApoE4 stock solution as per kit's suggestion. After 24h cells were fixed.

At treatment day, chambers' reservoirs were filled according to a pipetting scheme, allowing long lasting perfusion of synapses (Fig A2C) with minimal diffusion into the somatic compartments. 66.5µl of NB+ were mixed with 2µl of LNPs and 1.5µl of ApoE4 stock solution (from Precisions Nanosystems Spark kit) and then used to fill the middle perfusion well. After 24h neurite synapses were cut out using SNIDER.

Imaging

Prior to fixation, cells were washed once with warm PBS. Fixation was achieved in 4% PFA for 20min. Stainings were performed according to the manufacturer's protocol (Abcam). Antibodies used were as follows: Camkk2: primary (ab96531, Abcam), secondary (STRED-1002-500UG, Abberior) and Synaptophysin: primary (ab8049, Abcam), secondary (ST580-1001-500UG, Abberior). Images were taken on a STEDYcon attached to a Leica DMI8 in confocal mode. During image acquisition each channel's settings were kept for all samples. LNPs could be imaged directly, due to the 6FAM label attached to the oligo cargo, for phase contrast images Leica DMI8 microscope was used with default Leica software (Leica Application Suite X).

LNP measurement

Immediately after isolation, 30µl EVs were diluted to 1:20 with 570µl PBS and measured with Nanosight LM14C (NanoSight Ltd.) at 22°, averaging three measurements of 60sec at different locations of the observational area (NTA 2.3 Analytical Software), with a detection threshold of 15 and a camera level of 15. EVs were applied to cultures directly after measuring.

qPCR

First, RNA was reverse transcribed using miScript II RT Kit (218161, Qiagen), with the HiSpec buffer. qPCR was subsequently done with the miScript SYBR Green PCR Kit (218073, Qiagen). Primers used were the miScript universal primer with either the provided U6 probe as the reference or the MIMAT0000142 primer (Qiagen) for miR-9-5p with the sequence: 5'-UCUUUGGUUAUCUAGCUGUAUGA

To perform the qPCR, duplicates of each sample were measured together in a 96-well on a LightCycler480II. The integrated software was used for calculating the ratio of target to reference crossing point.

Analysis

Per condition (miR-9 inhibition or control) 6 images were taken with 4-6 representative cells per image. Overall, per condition 32 cells were analyzed. Identification and measurement of punctae intensity was done via Cellprofiler, following a recent protocol (Lazzara, 2020).

Results

To validate the miR-9-5p inhibitor we measured the mean expression intensity of Camkk2, a known target of miR-9-5p (Chang et al., 2014). Indeed, inhibition of miR-9-5p increased Camkk2 translation, as indicated by higher average intensity (Fig 2A-C). Moreover, I validated the decline of miR-9-5p levels caused by the inhibitor by qPCR (Fig 2D).

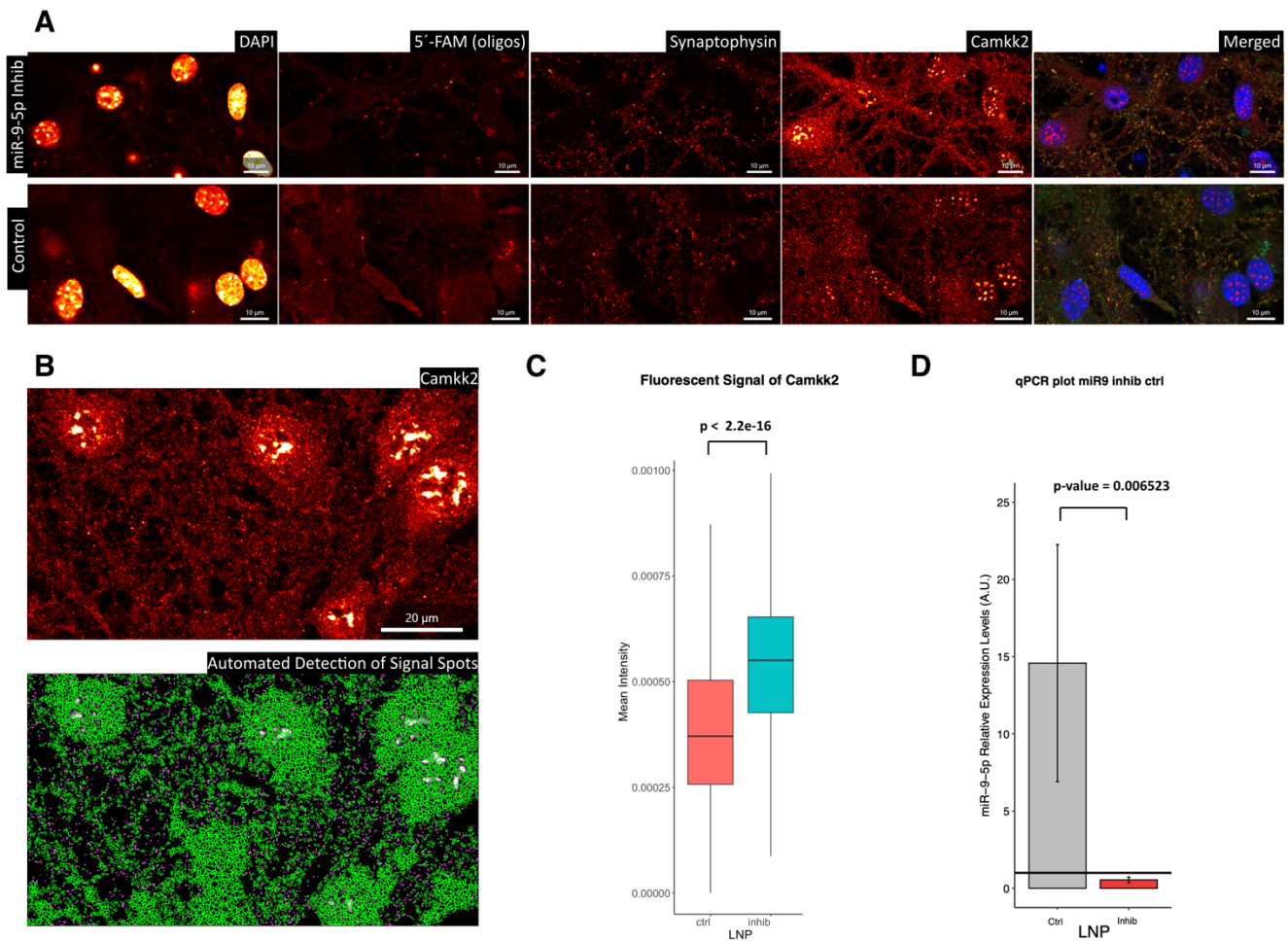


Fig 2: Validation of miR9-5p inhibition. **A)** Staining of fixed primary neuronal cultures after 24h incubation with LNA miRCURY inhibitors against miR9-5p, containing a 5'-6FAM fluorescent label. **B)** CellProfiler was used to identify Camk2 punctae. **C)** Inhibition of miR-9-5p led to higher Camk2 protein levels. Mean intensities of detected punctae were compared. P-value obtained through Welch t-test. $n = 25,302$. **D)** RT-qPCR of LNP-treated neurons confirms the immense downregulation of miR-9-5p. P-value obtained through Welch t-test. $n=6$ (3 samples per group, measured in duplicates).

LNPs have a quite uniform size distribution, as indicated by nanoparticle tracking analysis (Fig 3A), and the 5'-6FAM reporter of the packed inhibitor itself (Fig 3B). This ensured endocytosis of LNPs into nearly all cells (Fig 3C). Under closer inspection, the uptake happened across the entire cell body, including neuronal processes (Fig 3D). Since I could observe LNP uptake also at neurites, I wanted to investigate the effects of miR-9-5p inhibition directly at the synapse. To this end, I wanted to make use of another feature of the microfluidic chambers; the possibility to perfuse synapses without affecting somata (Fig A2B).

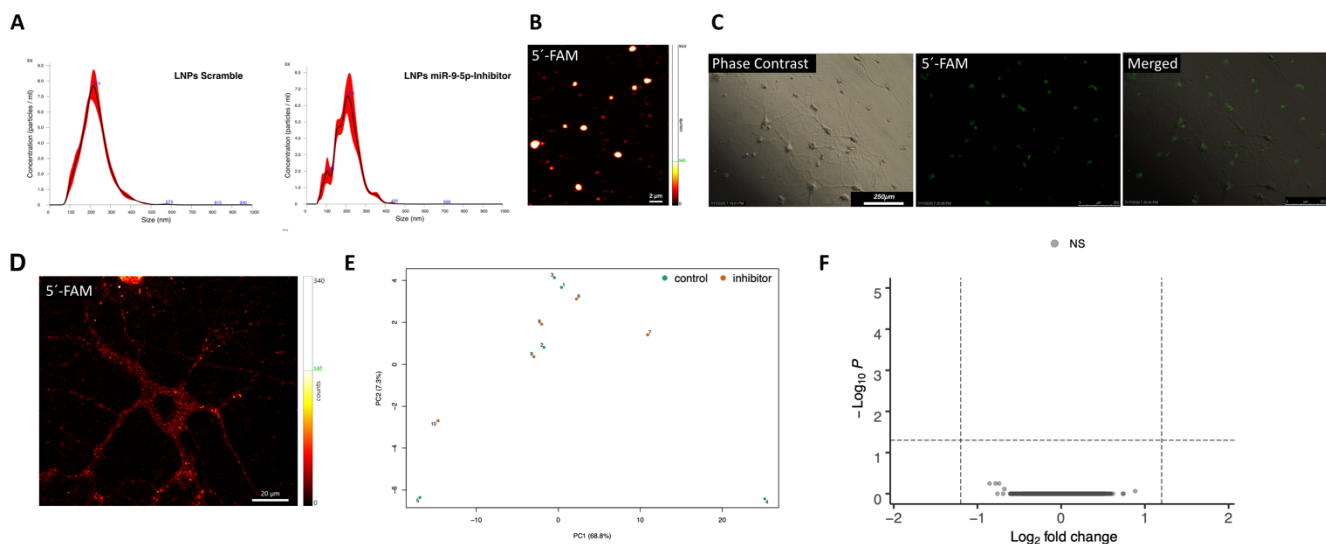


Fig 3: Inhibition of miR9-5p in microfluidic chambers. **A)** Size distribution of LNPs; nanoparticles have diameters around 50-400nm, with a sharp peak at 200nm. **B)** Image of highly concentrated LNPs show uniform size. **C)** Inhibitors inside a neuron. At DIV19 hippocampal neurons were treated with LNPs and imaged after 24h. Most of the nanoparticles were endocytosed across the whole cell body. **D)** Similar to C); yet images were obtained with the Leica software instead. **E)** Principal component analysis after chambers were treated with LNPs shows no clustering of treatment and control groups respectively. **F)** Differential gene expression analysis of synaptic RNA from chambers treated with LNPs reveals no changes in synaptic RNAome after inhibition of miR-9-5p.

At DIV14 LNPs with inhibitor or control sequence were filled into the middle perfusion reservoir of microfluidic chambers (Fig A2B). 24h later, synaptic RNAs were obtained using SNIDER (see Chapter 1), sequenced and compared. Samples did not cluster according to their treatment (Fig 3E).

Surprisingly, the transcriptome did not change at all, regardless of miR9 inhibition (Fig 3F). Subsequently, I sequenced the synaptic small RNAome of the chambers by using SNIDER and discovered that in the pure neuronal synapses miR-9-5p is not present.

Discussion

Here I could show that even though miR-9-5p is the second most abundant miR in synaptosomes, its inhibition does not influence the synaptic RNAome in pure neuronal synapses.

This finding is quite remarkable, since the qPCR and the staining experiment confirmed the presence of miR-9-5p in neurons (as indicated by synaptophysin signal) as well as an observable effect of its inhibition. However, any inhibition at neurites in microgrooves did not result in transcriptome changes.

In fact, as I discovered during the remaining acquisition of data for Chapter 1, miR-9-5p was absent from synapses in microfluidic chambers.

Since we saw miR-9-5p so highly expressed in synaptosomes, the different methods of synaptic RNA isolation might be responsible for this stark difference. Synaptosomes are obtained from tissue, where many different cell types reside among the axon terminal that is purified.

However, in microfluidic chambers any influence from cells other than neurons can be excluded. Diffusion from neuronal pools into the microgrooves was shown to be virtually nonexistent (Taylor et al., 2010). Hence it follows that all molecules in the synaptic compartment of the chambers are transported there actively by neurons.

As we have shown in Chapter 1, other researchers could previously prove that miR-9-5p is cargo of astrocytic exosomes (Jovičić and Gitler, 2017). Taken together, this suggests that synaptic miR-9-5p stems exclusively from astrocytes, and was not present in the chambers due to extremely slow diffusion of astrocytic exosomes into the grooves.

In synaptosomes the close proximity of glia cells, therefore, seems to enable a continuous transfer of exosomes from astrocytes to neurons. With the findings described, the question arises what other RNAs might be transported from astrocytes to neurons.

Chapter 2.1 Intercellular RNA transport

RNA transfer among cells is a widely spread phenomenon in nature; most ancient prokaryotes use horizontal transfer of beneficial genes, especially with regards to conferring immunities. This is mainly achieved by pili, tunnel-like structures forming between the donating organisms and the recipient cell. In animals a plethora of mechanisms have been described to achieve similar feats.

Initiated by findings in the squid axon, researchers have hypothesized RNA transport to occur from glia to neurons already for some time (Giuditta et al., 2002, 2008; Sotelo et al., 2014).

Cell-cell connections via gap junctions can be found in the intestine tissue, in the heart, as well as in the peripheral nervous system (Müller et al., 2018), where fused parts of the membrane have been shown to allow RNA and even ribosomal shuttling between cells. For microRNA, gap junctions have been shown to mediate cell-to-cell transfer (Peng et al., 2019).

Additionally, tube-like structures, termed transient nano tunnels, have been found to connect cells in neuronal cultures. With a highly parallelized, cytoskeleton-based transport system, extending over many micrometers, they have been reported to transfer proteins and even organelles (Ariazi et al., 2017; Haimovich et al., 2017; Wang et al., 2012).

Among those mechanisms, the extracellular vesicle-mediated process for RNA transfer has gained the most popularity in recent years (Gharbi et al., 2020; Ramachandran and Palanisamy, 2012; Valadi et al., 2007).

Transport of RNAs from other cells would have multiple advantages for neurons; intraneuronal transport can be quite slow - potentially resulting in mRNA decay during transport (Fonkeu et al., 2019). Thus, it would be quite costly for neurons to sustain their translational hotspots regularly with mRNAs, even when just maintaining stock. By the same token, protein amount can be improved locally by having certain mRNAs directly at the synapse – avoiding degradation and diffusion that could happen during transport. Also new protein can be produced much quicker upon an activation signal i.e., after theta bursts (Hanus and Schuman, 2013). This is especially important as several synaptic proteins have rather short half-lives; 27 proteins found in synaptosomes even have half-lives below 8h (Fornasiero et al., 2018).

When we look at the anatomy of many excitatory synapses, it becomes clear, why such transfer could happen so much faster than intercellular transport: in tripartite synapses, pre- and post-synaptic membranes are engulfed by astrocytic endfeet, where astrocytes can influence synaptic activity through many different mechanisms (Araque et al., 1999; Perea et al., 2009).

In case more translational hotspots are required - due to an overall increase of input frequency and location – nearby cells would be faster in supplying the neuron with necessary RNAs. Vice versa, if local translation should be stopped, intercellular miR transfer could accomplish rapid inhibition.

Unfortunately, certain hurdles have impeded the observation of large-scale intercellular RNA transport so far; labelling of many RNAs is difficult, considering all candidate RNAs would have to be provided in a modified way to possess aptamer (Autour et al., 2018) or MS2 loops (Wu et al., 2016), enabling those secondary structures to bind fluorescent reporters. Besides, there are often so few RNA molecules at individual synapses, that signal strength would be insufficient for direct imaging (Kosik, 2016).

Instead of investigating RNA transport with imaging tools, it is more efficient to turn to purification techniques to obtain all molecules of interest at once.

Chapter 3 - Astrocytes transfer RNAs to neurons for translation

Detailed Author contribution of Robert Epple (R.E.):

Conceptual work

- Concept development and vector design
- Method establishment of InSUREns, together with Patricia Schikorra
- Designing ADEV experiments

Experimental work

- Cell culture; labelling and RNA isolation, together with Patricia Schikorra
- RNA Sequencing, together with Patricia Schikorra
- Imaging

Data analysis

- GO term analyses
- ncRNA Analyses
- Comparison to genomic average
- Overlaps of datasets
- Differential expression analysis, together with Tonatiuh Pena

Data presentation

- All figures, except Supplemental Figures S2 and S3
- All writing, with editing from Prof. Dr. Andre Fischer

Manuscript is ready for submission.

Astrocytes transfer RNAs to neurons for translation

Robert Eppel¹, Patricia Schikorra², Dennis Krüger¹, Tonatiuh Pena¹, Christine Vogelaar³, Andre Fischer^{1,4,5}

¹Department for Systems Medicine and Epigenetics, German Center for Neurodegenerative Diseases (DZNE), Von Siebold Str. 3a, 37075, Göttingen, Germany

²Institute of Reconstructive Neurobiology, LIFE & BRAIN Center, University of Bonn Venusberg-Campus 1, Bonn, Germany

³Department of Neurology, Focus Program Translational Neuroscience (FTN) and Immunotherapy (FZI), University Medical Center of the Johannes Gutenberg University Mainz, 55131, Mainz, Germany

⁴Cluster of Excellence "Multiscale Bioimaging: from Molecular Machines to Networks of Excitable Cells" (MBExC), University of Göttingen, Germany

⁵Department of Psychiatry and Psychotherapy, University Medical Center Göttingen, Germany

*corresponding author: andre.fischer@dzne.de (ORCID: [0000-0001-8546-1161](https://orcid.org/0000-0001-8546-1161))

Abstract

Neurons have intricate, far-reaching morphologies, and a long sought-after question concerns their ability to supply themselves with enough proteins to not only sustain their current state but also to be in a position to react to plasticity events on a short time scale. Here we looked at astrocytes as a potential RNA source for neurons to translate proteins locally at synapses. We present InSUREns (Intercellularly Shipped and Uptaken RNAs Ensnared), a novel method to identify all RNAs that are transcribed in one cell-type, but transported to another cell-type for translation. It uses a double immunoprecipitation strategy, where first neuronal ribosomes are purified and then astrocytically produced RNAs are subsequently purified from the first immunoprecipitation. The most abundantly shipped RNAs encoded processes involved in synapse structuring and neurite development. Genes that were enriched in InSUREns RNAs when compared to inputs, were linked to translational regulation, indicating a possible involvement in the synaptic tagging and capturing process. Imaging experiments confirmed astrocyte-derived extracellular vesicle (ADEV) uptake by neurons at their somata, as well as along their neurites. ADEVs contained many InSUREns genes, suggesting that astrocytes supply neurons with RNAs via EVs and could contribute significantly to the pool of locally translated mRNAs and its translational regulation.

Keywords: mRNA, lncRNA, extracellular vesicles, astrocytes, neurons, intercellular RNA transfer, local translation, gene-expression, RNA-sequencing, synaptic tagging, InSUREns

Introduction

Specialization of cell-types allowed the development of complex organs like the brain. Neurons stop dividing and outsource many of their tasks to surrounding cells. For example, oligodendrocytes sheath their long axons to enhance signal conductivity, microglia trim superfluous synapses and perforate the extracellular matrix to make space for synaptic changes and pericytes shield neurons from toxic molecules and pathogens in the blood vessels (Kandel, 2013). An important interplay also happens between astrocytes and neurons; astrocytes fuel up neurons with glucose in times of high demand, they partake in rapidly changing extracellular ion concentrations, as well as glutamate levels and they can release their own gliotransmitters to modulate neuronal activity. Since neurons have intricate, far-reaching morphologies, a long sought-after question concerns their ability to supply themselves with enough proteins to not only sustain their current state but also being in a position to react on a short time scale to plasticity events. Learning is the adaptation of synapses to novel inputs and requires a timely synthesis of specific proteins. To overcome logistic challenges parts of the protein synthesis are outsourced to neurites and synapses; a process known as local translation (Wang et al., 2010). Local translation necessitates certain mRNAs at the synapse (Rangaraju et al., 2017), otherwise plasticity changes are only short-lived (Bosch et al., 2014; Kang and Schuman, 1996). Here we looked at astrocytes as a potential RNA source for neurons to translate proteins locally at synapses.

To establish and ensure long term potentiation (LTP), somatic proteins and RNAs have to arrive after a few hours to the synapse. According to the synaptic tagging and capturing hypothesis (Frey and Morris, 1997), there ought to be a signal marking the potentiated synapse in order to capture somatic molecules. As our data indicates, intercellularly transferred RNAs could provide a synaptic tagging mechanism.

Here we present InSUREns (**I**ntercellularly **S**hipped and **U**ptaken **R**NAs **E**nsnared), a novel method to identify systematically all RNAs that were transcribed in one cell-type, but transported to another cell-type for translation. This requires a double immunoprecipitation strategy, where first neuronal ribosome-bound RNAs are isolated and then - subsequently - astrocytically-produced RNAs are purified therefrom.

We observed thousands of mRNAs that were shipped from astrocytes to neurons. The most abundantly shipped RNAs encoded processes involved in synapse structuring and neurite development. Genes that were significantly enriched among the InSUREns dealt with translational regulation, indicating a possible involvement in the synaptic tagging and capturing process. Further experiments provide evidence, that ADEVs are the most likely route for RNA transfer.

Results

Establishment of InSUREns

To show intercellular RNA transfer, we marked astrocytic RNAs and neuronal ribosomes in a cortical cocultures (**Fig 1A**). In order to label ribosomes, we used an AAV1/2-vector, where under the human synapsin promoter RPL22 is expressed, carrying three hemagglutinin tags and an eGFP reporter after its fourth exon (**Supplementary material S1**), enabling a HA-Antibody-based pulldown. This labeling method, termed Ribotag, was first introduced via transgenic mice (Sanz et al., 2009) and works in a very similar fashion to TRAP (Doyle et al., 2008), however it uses RPL22 (instead of RPL10a) and multiple epitopes, allowing for high signal-to-noise immunopurifications (Lesiak et al., 2015).

RNA labeling was achieved by another AAV1/2-vector, where we combined the *Toxoplasma gondii* version of Uracil phosphoribosyltransferase (UPRT) under the astrocyte-specific GFAP promoter and with the mKate2 reporter protein fused to the C-terminus of the protein (**Supplementary material S2**). UPRT is also expressed in mammals, however only the enzyme from *T. gondii* can incorporate 4-Thiouracil (4TU) - a thiol-modified uracil base - seamlessly into RNAs, which renders those RNAs able for biotinylation and subsequent streptavidin purification (Cleary et al., 2005; Gay et al., 2013; Miller et al., 2009).

TU tagging labels all RNA types, regardless of cellular location, or translational state. Additionally, it allows for temporal control, as it is only enabled of when 4TU is supplied.

First, we established both purification methods. Cell-type-specificity was confirmed for each virus separately; morphology shows clearly that only neurons express the ribotag construct and only astrocytes express UPRT (**Fig 1B**). Upon infecting a co-culture with both viruses, no overlap of the reporter signal was observed (**Fig 1C**).

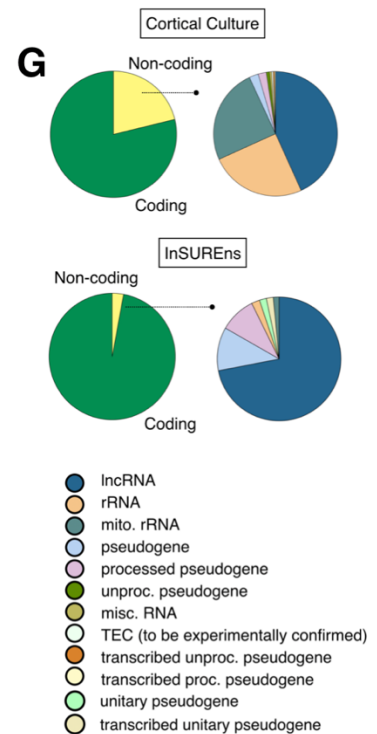
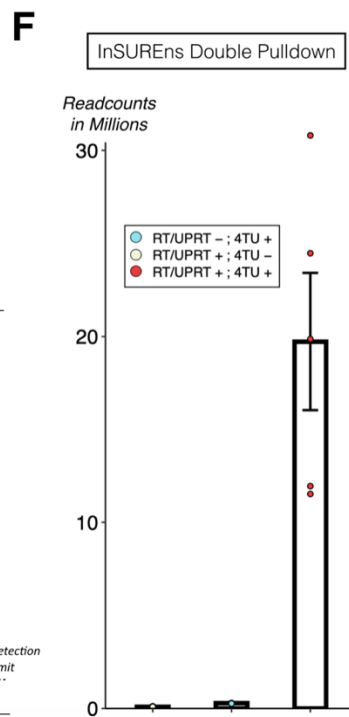
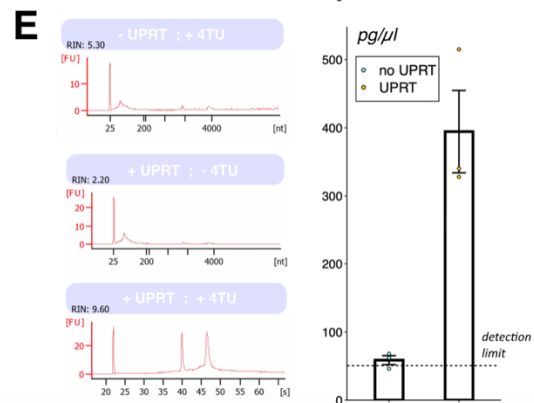
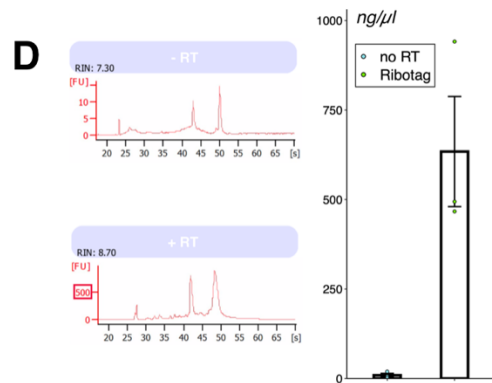
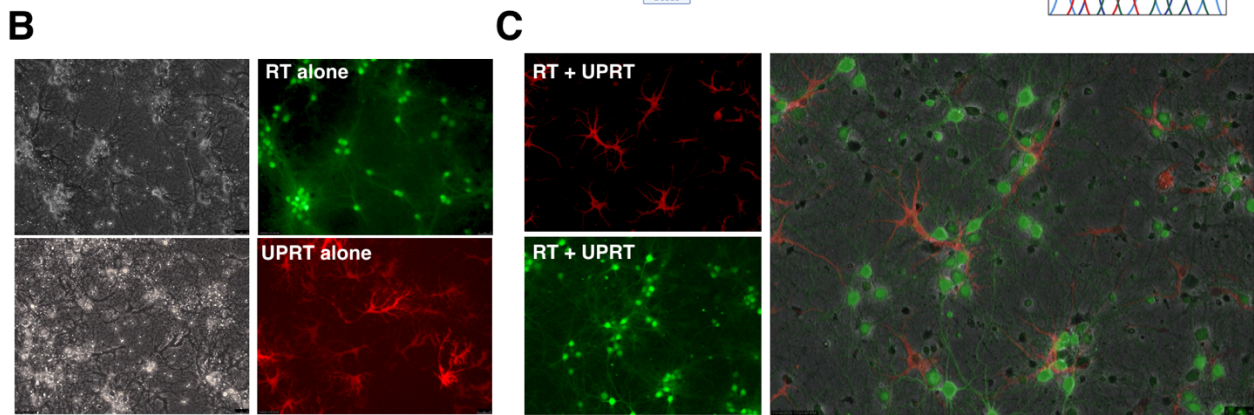
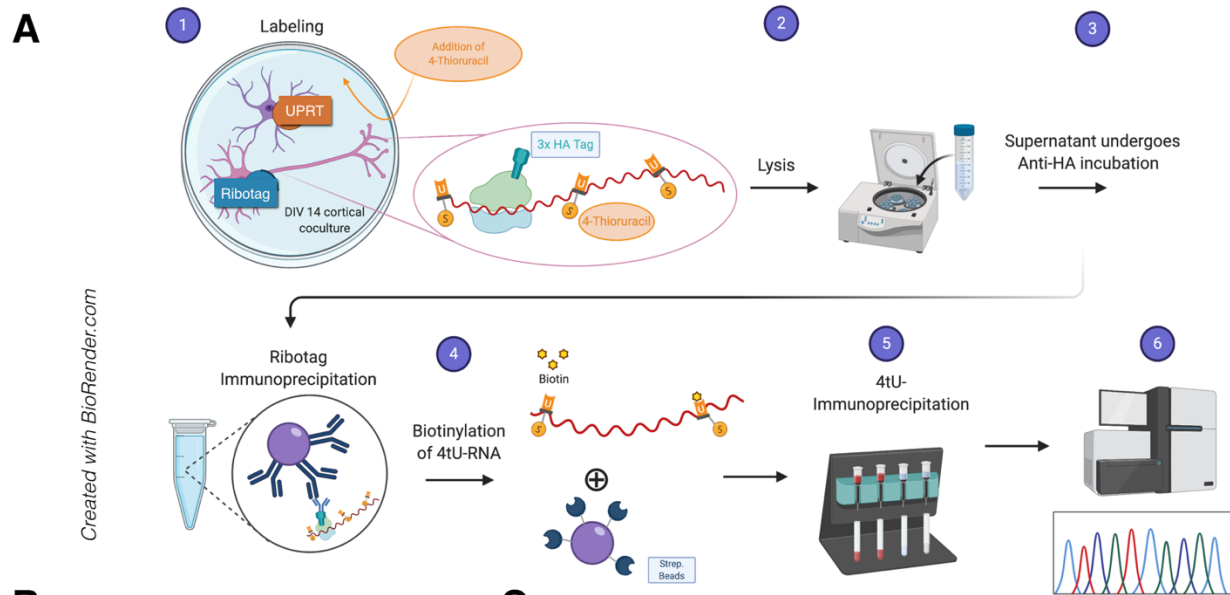
Ribotag pulldown was confirmed by bioanalyzer assay. The HA-pulldown of tagged ribosomes yielded on average 634ng/ μ l, compared to only 9 ng/ μ l of the unlabeled control (**Fig 1D**). Small electropherograms depict a vast difference for pulldowns without the ribotag construct.

For the 4TU pulldown, samples with the UPRT construct yielded 394pg/ μ l RNA on average -without the enzyme only 59pg/ μ l (**Fig 1E**). Levels of background in 4TU samples were similarly scarce when either the enzyme or the labeled uracil were omitted (**Fig 1E**, small inlets).

Controls for the InSUREns double pulldown consisted both of non-transduced cultures that received 4TU and of transduced cultures receiving vehicle instead of 4TU. Both types of controls equally resulted in virtually no reads after sequencing. A mere $0.16 * E^6$ exon read counts were amassed on average for control samples, while the labeled samples had an average of $19.72 * E^6$ exon read counts (**Fig 1F**).

Control readcounts consisted mainly of random noise and did not form clusters (**Fig S1**). As we purified ribosomes, we mainly detected coding transcripts and among the non-coding transcripts were mostly pseudogenes and long-non-coding RNAs (lncRNAs), RNAs that were likely interacting with a ribosome-bound mRNA at the time of pulldown (**Fig 1G**). The low amount of ncRNAs and the absence of rRNAs further indicates a high-quality pulldown.

Figure 1 (on next page): Ribotag-4TU Double Pulldown. **A**) Scheme of Experiment. In a mixed primary cortical culture two different AAVs transduce neurons with the ribotag tag construct, and astrocytes with the UPRT construct. Starting on DIV13 4TU is introduced to allow astrocytes the incorporation of this labeled base into their RNAs. After two more additions of 4TU, cells are lysed on DIV14. First the labeled ribotags are isolated via a HA-antibody. Then 4TU gets biotinylated, rendering all labeled RNAs precipitable via streptavidin beads on μ Macs columns. Any RNA remaining after the double pulldown has been produced by astrocytes and then transported onto neuronal ribosomes. Resulting RNAs undergo library preparation and are sequenced. **B**) Fluorescent images showing the cell-type-specificity of both constructs. Morphologies of the fluorescent signals show only neurons expressing ribotag and only astrocytes expressing UPRT. **C**) Similar to B), but both constructs were applied simultaneously, showing restriction of expression to one cell-type. **D**) Left: Bioanalyzer plots showing a huge reduction in RNA yield when no ribotag is expressed, indicated by the vast differences in fluorescence units. Right: bar plot depicting the differences in RNA concentration when ribotag was applied versus background precipitation. $n=3$. **E**) Left: Bioanalyzer plots showing that the 4TU pulldown fails if either enzyme or 4TU is missing. Right: bar plot depicting the differences in RNA concentration when UPRT was applied versus background precipitation. $n=3$. **F**) Resulting exon readcounts of the libraries after the double pulldown. $n=5$ (samples), $n = 3$ (control: RT/UPRT + ; 4TU -), $n = 2$ (control: RT/UPRT - ; 4TU +). **G**) Coding and non-coding reads. Pie charts show the average readcounts for the displayed RNA category. Primary cortical cultures (upper panel) contain more non-coding transcripts than InSUREns samples (lower panel). However, among the non-coding transcripts of transferred RNAs, lncRNAs and pseudogenes are strongly overrepresented, whereas mitochondrial and rRNA are underrepresented. Only those ncRNA types are depicted, where the accumulated average readcount for all RNAs of that specific ncRNA category combined was above 10,000.



Analysis of most enriched transferred genes

InSUREns samples represent a subset of the inputs; thus, around two thirds of all genes present in cortical cultures were found in InSUREns samples, too (**Fig 2A**). When we performed a principal component analysis (PCA), both groups clustered together and separately from one another (**Fig 2B**).

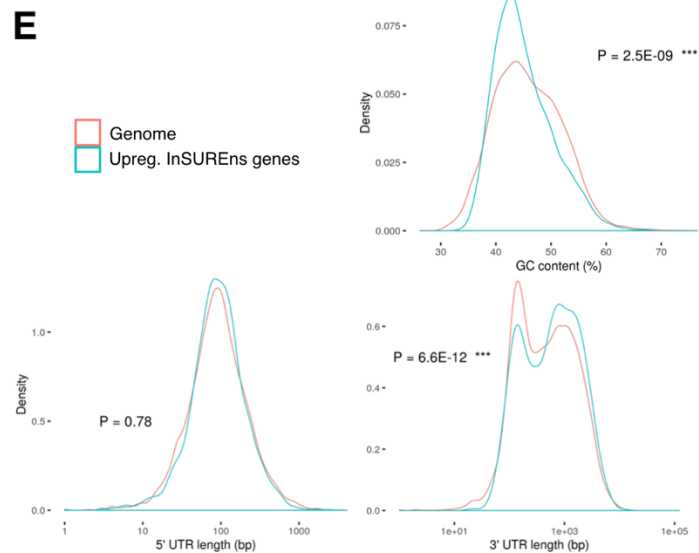
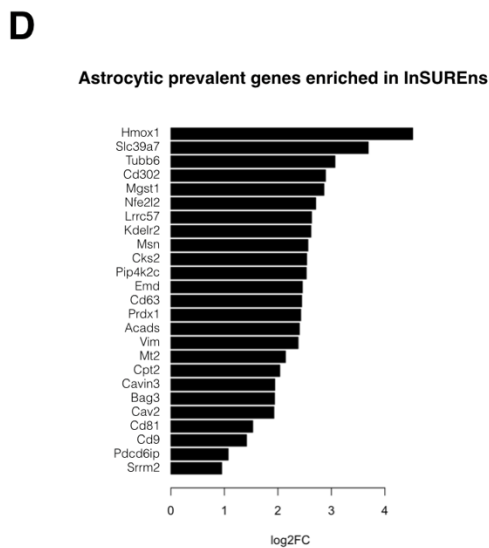
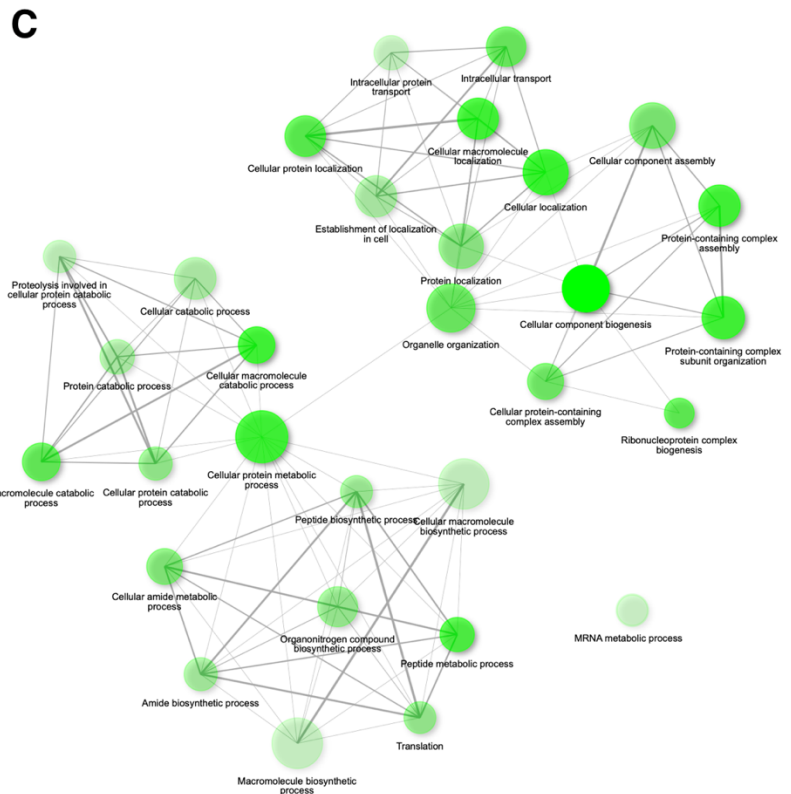
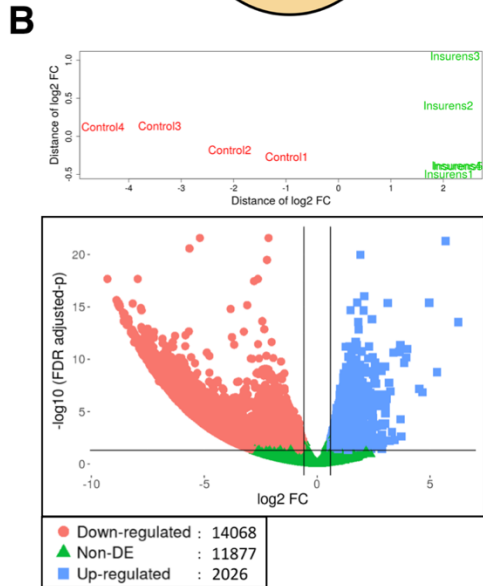
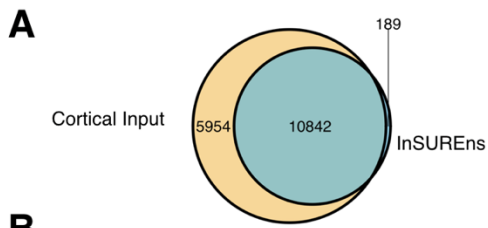
To see which genes are enriched in InSUREns sample, we performed a DESEQ2 analysis and found 2026 genes were upregulated (**Fig 2B**). The majority of genes was downregulated, expected due to the pulldown nature of the method.

Upregulated genes formed two big, interconnected hubs of physiological functions; metabolic processes and localization, with mRNA metabolic processes being a proximate yet unconnected term (**Fig 2C**).

Interestingly, among the most enriched genes were several genes (**Fig 2D**) that are significantly more abundant in astrocytes than in neurons (Zhang et al., 2014), further substantiating RNA transfer from astrocytes to neurons. What is more, four ADEV markers - CD9, CD63, CD81 and Pdc6ip (Kowal et al., 2016; You et al., 2020) - were highly enriched as well, hinting at EVs as a means of transferred mRNAs.

Upregulated InSUREns genes' guanine-cytosine (GC) content was significantly lower than the genomic average, a sign of more accessible transcripts. Moreover their 3' untranslated regions (UTRs) were longer when compared to the genome (**Fig 2E**), a feature typically seen in synaptic genes.

Figure 2 (on next page): Differential Expression Analysis between InSUREns and cortical inputs. **A)** Around two thirds of all transcripts of cortical inputs were transferred **B)** Summary of DESeq2 results; PCA shows a clear separation between the inputs and InSUREns samples. The Volcano plot depicts more genes being downregulated than non-differentially expressed. 2026 genes are significantly enriched in InSUREns samples. **C)** Network analysis of all upregulated genes shows two big hubs of functions; metabolic processes and localization. **D)** Examples of genes that are upregulated in InSUREns and more prevalent in astrocytes than in neurons. **E)** GC content of upregulated InSUREns genes is significantly lower than a random set of 2026 genes from the genome would be, also their 3' - UTRs, but not their 5'-UTRs are longer compared to the genome.



Analysis of most abundant transferred genes

Several differentially expressed InSUREns genes were enriched compared to the input, yet still only moderately expressed. To further investigate the role of transferred transcripts we also looked at the highest quartile of InSUREns genes (2758) and performed a pathway analysis. Many pathways revolved around the organization of synapses and vesicle-mediated transport therein, with other pathways belonging to ribosome and ribonucleoprotein biogenesis as well as mRNA handling and splicing (**Fig 3A**).

Interestingly, among the top transferred genes were many genes that are also highly expressed in cortical inputs; the hyper-geometric test used to this end revealed strong correlation between the ranks of few hundred genes, which then leveled off; RRHO red pixels highlight a greater number of common genes than expected for that specific bin, whereas blue pixels color a lower-than-expected number (**Fig 3B**). Apart from RNAs being specifically shipped for a reason, this implies also a supportive role of astrocytes towards the general neuronal transcriptome.

The most abundant transferred genes also had a significantly lower GC content than a random set of the same number of genes from the genome would have had (**Fig 3C**). Additionally, the top quartile of transferred genes carried significantly longer 5'- and 3'- UTRs (**Fig 3C**).

Notably, BDNF, Homer1 and Arc, which have been suggested as synaptic tags (Okuda et al., 2020), are amid the most highly abundant InSUREns genes. Likewise, we found four genes known to contribute to synaptic tagging and capturing in the top quartile of InSUREns genes; NCAM1, PKA and Camk2a and TrkB (Okuda et al., 2020).

Next, we looked at the overlaps between the top quartile and the upregulated InSUREns genes. Roughly half of the enriched InSUREns genes were also in the top quartile of genes, thus highly abundant, and some of the upregulated InSUREns genes were only moderately expressed. Our initial hypothesis stated the advantages astrocytic RNA transfer could have directly at the synapse, therefore we also looked how many InSUREns genes are of synaptic localization. Recently we obtained a pure neuronal synaptic transcriptome by utilization of microfluidic chambers (Epple et al., 2020). That dataset only contains neurites grown into very narrow channels, preventing diffusion from any nearby glia cell EVs and hence represents only RNAs that neurons themselves can provide to their synapses.

Half of the top quarter InSUREns genes and a sixth from enriched InSUREns genes overlapped with our synaptic genelist (**Fig 3D**), indicating astrocytic horizontal RNA transfer at the synapse. We then wanted to compare the GO term analysis for biological processes between the upregulated and top expressed InSUREns genes. Both sets have significant enrichment for ribosome and ribonucleoprotein biogenesis as well as for mRNA handling and splicing (**Fig 3E**), suggesting transferred genes could influence and orchestrate RNA translation at the synapse.

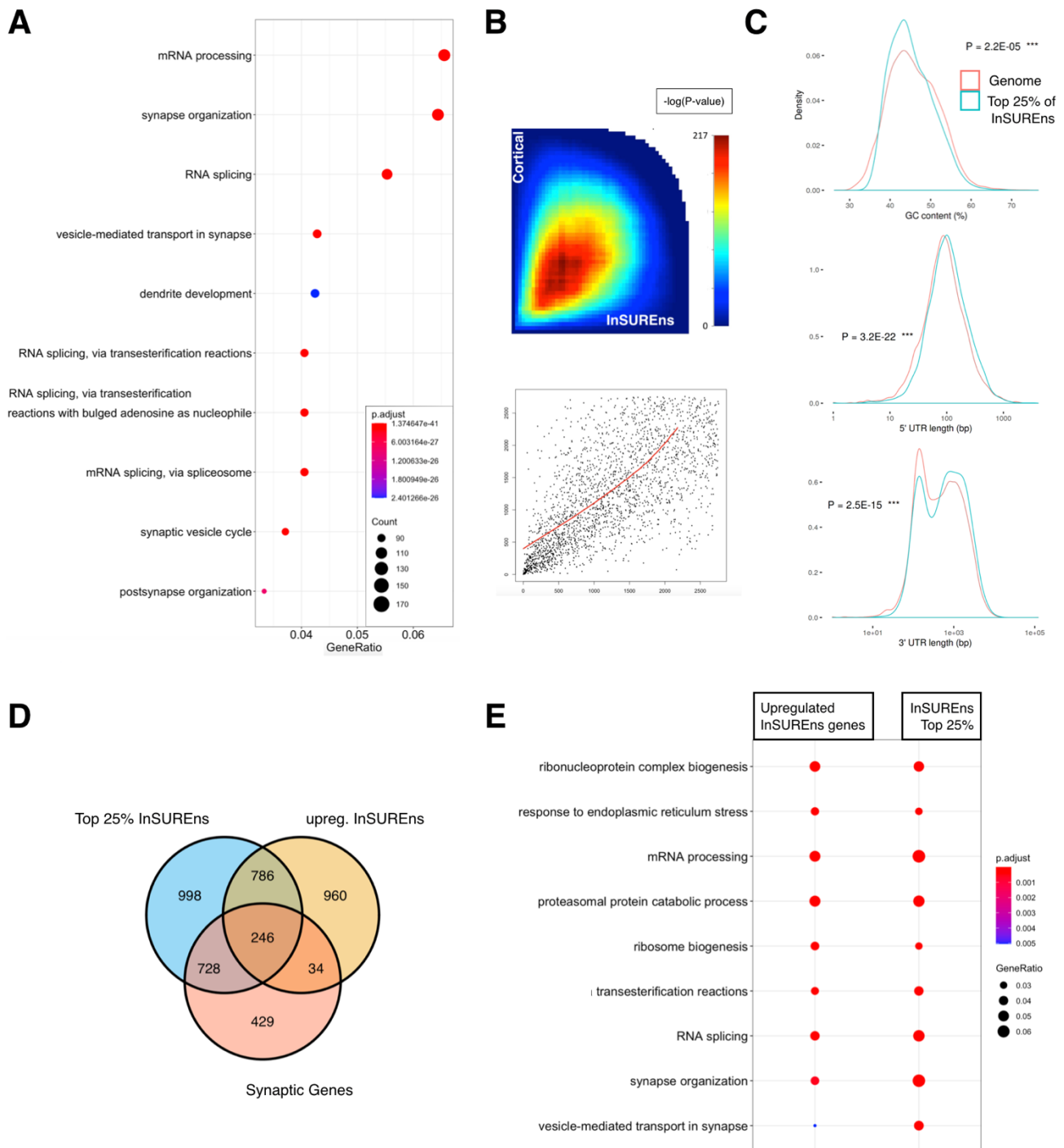


Figure 3: Analysis of the top 25% expressed InSUREns genes. **A)** GO Term analysis for biological processes, cellular component and molecular function for the top quartile of InSUREns genes reveals many pathways for synaptic mechanism as well as RNA processing. **B)** Rank-rank hypergeometric analysis between the top 2758 genes and the top 2758 cortical input shows that a group of highly abundant input transcripts is transferred to a big extent. **C)** GC content of top InSUREns genes is significantly lower than a random set of 2758 genes from the genome would be. Moreover their 5' and 3' UTRs are longer compared to the genomic average. **D)** Comparison of gene-lists. Half of the upregulated InSUREns genes are also in the top quartile of InSUREns genes, indicating a high abundance level of enriched genes.

(Figure 3, continued) Around 1000 neuronal synaptic genes are present in both InSUREns sets combined, 246 genes are found in all 3 lists. **E**) Comparison of GO term analysis for biological processes between the upregulated and top expressed InSUREns genes. Both sets have significant enrichment for ribosome and ribonucleoprotein biogenesis as well as for mRNA handling and splicing.

Interaction networks of InSUREns RNAs

Although less abundant than in cortical cultures, a certain number of lncRNAs were robustly present in InSUREns samples. We analyzed the interactions of these lncRNAs with our recently obtained dataset of synaptic mRNAs (Epple et al., 2020). 357 of the transferred lncRNAs have experimentally validated interactions with our list of 1460 synaptic mRNA, forming a dense and intricate network (**Fig S2**).

Recently, a dataset of astrocytic miRs in exosomes was published (Jovičić and Gitler, 2017); strikingly many of the 145 miRs in astrocytic exosomes are known to target the top quartile of transferred genes, showing a complex regulatory network (**Fig S3**).

Culture supernatant enables ribosome- and likely RNA transfer

Next, we wanted to elucidate the route of RNA transfer from astrocytes to neurons. In an initial experiment, we observed that primary neuronal cultures secrete RNA into medium over time, whereas medium itself barely contained RNAs (**Fig 4A**). It is important to note that we did not filter the medium, thus it still contained all EVs. Strikingly, many of those secreted RNAs share the most prominent pathways of highly abundant InSUREns genes (**Fig 4B**).

We then tested if RNA transfer happens via secretion into medium; to this end we used stellate astrocytic cultures from the transgenic mouse line Ribotracker x GFAP-Cre, which expresses RPL4-RFP after the Tamoxifen-induced Cre cuts out the exon-stop (**Fig 4C**).

We found tagged astrocytic ribosomes along the entire neuronal cell body, including neurites and often closely located to synapses, as indicated by the synaptophysin signal (**Fig 4D**).

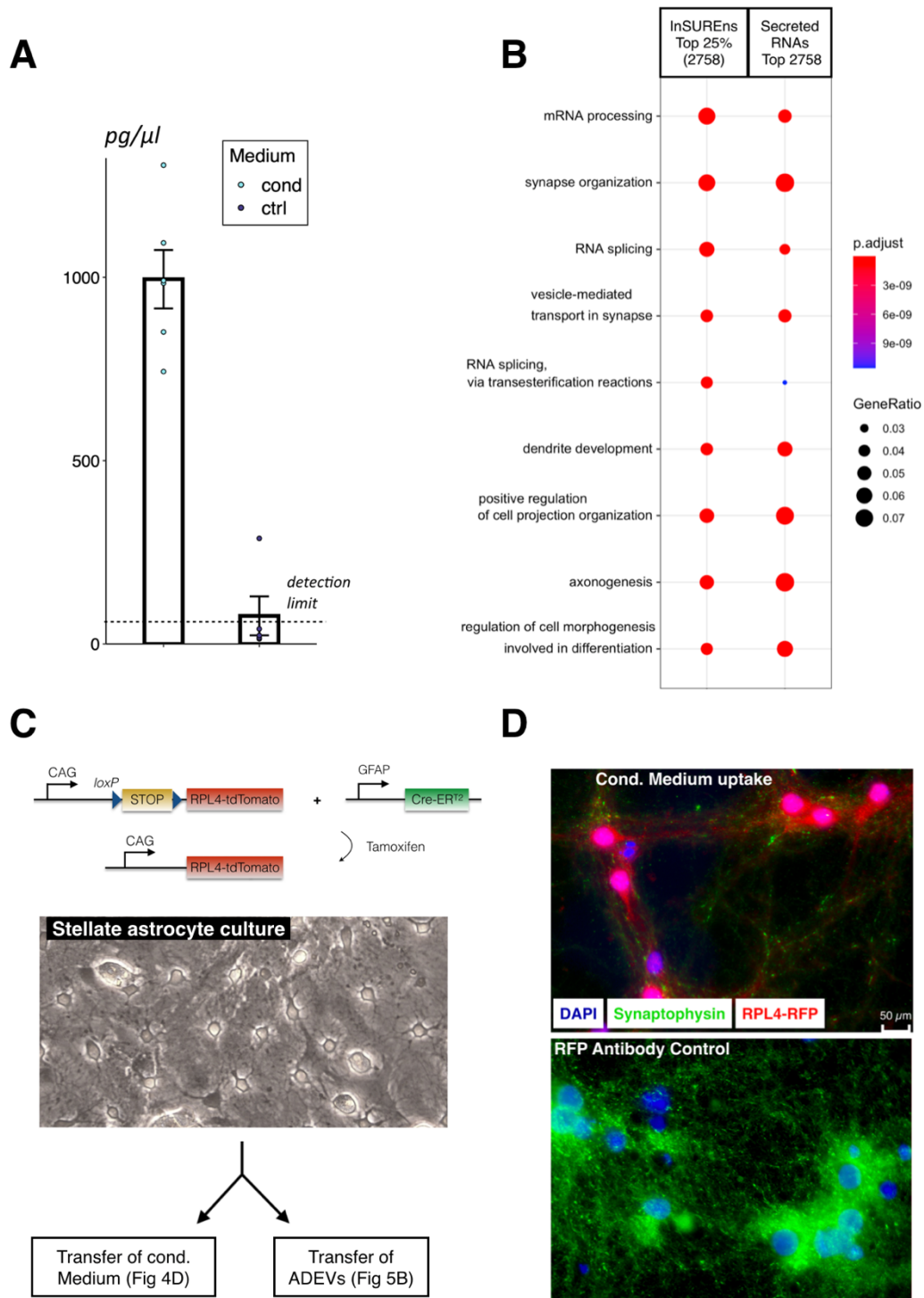


Figure 4: Secretion of RNAs. Ribosomes are transferred via EVs. **A)** RNA concentration in conditioned medium of a hippocampal culture at DIV14, after isolation. **B)** Comparison of GO term analysis for biological processes between the secreted and top expressed InSUREns genes. Both sets have significant enrichment for synaptic terms for development as well as for terms surrounding mRNA handling and splicing.

(Figure 4, continued) **C)** Experimental scheme to observe uptake of astrocytic material by neurons. Stellate astrocytes were cultured from Ribotracker X GFAP-Cre mice. Under tamoxifen Cre allows the expression of RPL4-tdTomato which labels astrocytic ribosomes in conditioned medium and ADEVs.

D) Astrocytic ribosomes in conditioned medium are internalized by neurons across their soma and neurites. RFP signal had to be enhanced by RFP-antibody staining to be visible. The antibody control shows no unspecific labeling in untreated cultures.

Astrocytic derived extracellular vesicles transport RNAs into neurons

Based on recent literature we reasoned this transfer would happen primarily over EVs, thus we isolated ADEVs from ribotracker AWESAM cultures. Importantly, two days prior to ADEV isolation, we replaced the medium with serum-free medium, which was free from exogenous EVs (**Fig 5A**). Nanosight analysis also confirmed a sharper, more defined peak at 100nm for the size of ADEVs when isolation was performed with Amicon centrifugation filters (Merck-Website) rather than an ultracentrifugation protocol (**Fig 5A**). Hence all subsequent ADEV isolations were done via Amicon filters.

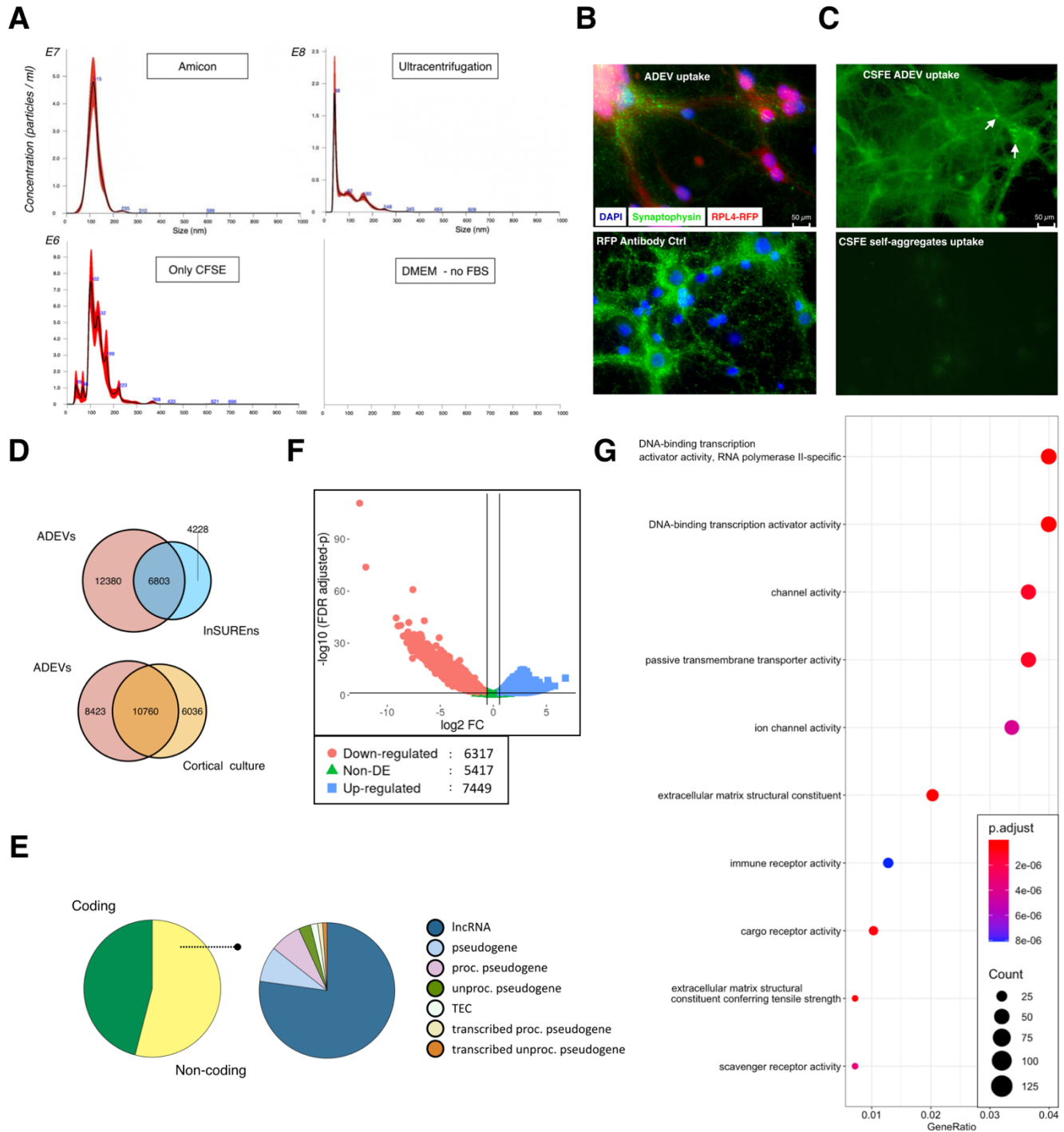
ADEVs were applied to wildtype cultures, at a concentration of around 10.000 EVs per recipient cell. Recipient neurons internalized astrocytic ribosomes into their cytosol and neurites, with a similar pattern as the uptake of ribosomes from conditioned medium (**Fig 5B**).

This result was confirmed by another tracking method that labels EVs directly instead of their cargo; the fluorophor Carboxyfluorescein succinimidyl ester (CFSE) covalently binds lysine residues as well as amine sources on the inside of membranes, without changing EV volume and only forming few self-aggregates (Morales-Kastresana et al., 2017), therefore making it superior to lipid dyes. ADEVs from wild-type cultures were collected, stained with CFSE and applied in the same manner as ribotracker ADEVs. Again, we observed internalization across the whole cell body, including neurites. Additionally, ADEVs were also clustering close to the nucleus, potentially resembling late endosomes (**Fig 5C**, white arrows). From the staining experiments we concluded ADEVs could constitute a major mechanism for RNA transfer; with some RNAs potentially already loaded onto ribosomes.

Next, we wanted to know what total RNA is contained in ADEVs and isolated their RNA. We measured an average RNA content of 73ng in ADEVs per million astrocytes and sequenced it in the same way as InSUREns RNAs. Strikingly, more than 19,000 genes were found in ADEVs, including most of the InSUREns transcripts and even more of the inputs' transcripts (**Fig 5D**).

The majority of ADEV RNAs was non-coding, containing primarily lncRNAs and pseudogenes, thereby featuring a ncRNA composition more similar to InSUREns samples than to cortical inputs (**Fig 5E**).

We then tested, which transcripts are enriched in ADEVs compared to cortical cultures, and saw 7449 upregulated genes compared to 6317 downregulated transcripts (**Fig 5F**). A GO term analysis for molecular functions of all upregulated genes revealed that genes for extracellular matrix, transcription and receptor related pathways were significantly overrepresented in ADEVs (**Fig 5G**).



(legend on next page)

Figure 5: RNA content of ADEVs. **A)** Nanoparticle tracking analysis to measure sizes of EVs. Upper panels show a sharp peak around 100nm for ADEVs isolated with Amicon centrifugation filters, whereas ultracentrifugation resulted in several minor peaks and a maximum at 38nm. Lower panels depict that self-aggregated CFSE particles have a peak around 100nm, yet their profile is less clear and overall their concentration is one order of magnitude below ADEV purification with Amicon. Medium without serum contains no measurable particles after the Amicon isolation protocol. **B)** ADEVs containing RPL4-RFP display the same pattern of uptake across the soma and neurites as the RPL4-RFP containing supernatant, indicating that ribosome transfer happens via EVs. Also, here the antibody does not cause unspecific staining. **C)** ADEVs stained by CFSE show higher uptake at neurites than the labeled astrocytic ribosomes. Accumulations of stained ADEVs are visible along neurites and mainly around the nucleus, most likely indicating late endosomes and lysosomes (white arrows). CFSE self-aggregates are rarely being uptaken. **D)** Overlaps between ADEVs and cortical cultures as well as with the InSUREns genes. Transcriptomes differ to an extent, which might be due to ADEVs stemming from monocultures and different media used. Nonetheless the majority of InSUREns genes was found to be present in ADEVs. **E)** Most ADEV transcripts are non-coding, with a similar composition of ncRNA types as the InSUREns samples. **F)** Volcano plot depicting differential expression analysis between the cortical culture inputs (the same as used for the InSUREns comparison) and ADEV's total RNAs. ADEVs are strongly depleted in over 6000 genes, and have over 7000 enriched genes. **G)** Molecular function GO term analysis of the 7449 upregulated ADEV genes reveals extracellular matrix, transcription and receptor related pathways as significantly overrepresented groups.

Discussion

We introduced a novel method to track RNAs that are being transported from one cell-type to another. While in principle this method could work with any two cell-types, we focused on the transport of astrocytic RNAs into neurons, and wanted to know in particular to what extent synaptic genes are being transferred. Several control experiments were done to confirm the purity of both pulldowns, and protocols were optimized based on former publications, protocols and personal communication with the authors.

Over the last years a wide variety of pulldown methods for cell-type-specific RNAs has been developed; TRAP captures all RNAs bound to ribosomes (Doyle et al., 2008), miRAP isolates microRNAs (miRs) via cell-type-specific, promoter driven expression of tagged-AGO2 (He et al., 2012) and INTACT gets ahold of the desired cell-types' nuclei (Deal and Henikoff, 2011). Although to date there is no methodology that allows to differentiate the origin and destination of transcripts.

By combining two labeling methods we make use of their synergy: first, the ribosome-bound nature of the isolated RNAs proved that InSUREns RNAs are being transferred for translation in the recipient.

Second, the sequential purification was only possible, due to the isolated RNA from the first step being labeled itself – thereby allowing further purification; whereas the above-mentioned methods always work by a single pulldown of RNA-binding proteins.

Purity of Pulldowns

Even though a small background persisted after the ribotag purification, 4TU purification generates barely any background, thus effectively eliminating the background of the first pulldown through the second pulldown. Additionally, to our control experiments, other works have found virtually no background signal in cortical neurons when given 4TU without the UPRT enzyme (Chatzi et al., 2016), neither was any background visible in the original work (Cleary et al., 2005) nor in primary fibroblasts (Rinn et al., 2008). Only in one zebrafish study did researchers find very small amounts of background (Erickson and Nicolson, 2015), even though Erickson and colleagues utilized hair cells and it was previously reported that virtually all background labeling arises from non-CNS tissue (Miller et al., 2009). Rinn and colleagues also proved that biotinylation introduces no background (Rinn et al., 2008).

Moreover, the RNA profile changed dramatically after the 4TU purification (Fig 2B), with barely any detectable signal beyond 100 nucleotides, whereas the noise introduced by the ribotag purification seems to represent a more general unspecific pulldown, incorporating RNAs of all length.

Recent work has further demonstrated that two sequential pulldowns strongly remove noise; Gregory and colleagues did two consecutive pulldowns of ribosomes tagged with different tags, and reported no detectable cross-contamination (Gregory et al., 2020).

Considering that in InSUREns both pulldowns happen consecutively and result in quite minute amounts of RNA, we reckoned background signal as negligible.

Indeed, when we looked at the few genes present across controls and comparing their readcounts ratio to InSUREns RNA, we only needed to exclude a few dozen genes. Based on those observations we decided that immunoprecipitation versus input analysis would be sufficiently done by comparing the final reads of the InSUREns genes to the transcriptome of cortical culture inputs, functioning as the overall input. Accounting for both input types, i.e., having inputs for both immunoprecipiations would severely complicate the matter and be less intuitive to interpret.

We have not verified the cell-types of InSUREns transduced cultures by separate marker stainings, nevertheless we could not detect any mKate2 signal in neurons nor any eGFP signal in astrocytes. Moreover, our chosen neuronal promoter is known to confer pristine neuronal specificity (Kügler et al., 2003); similarly the short astrocytic GFAP promoter is very specific (Lee et al., 2008).

We can exclude that unspecific binding of labeled RNAs to ribosomes happened during lysis, as in such case we would not find the very similar abundances of InSUREns genes across samples. Furthermore, the InSUREns samples are very similar to one another (Fig S1).

Amount and type of discovered InSUREns transcripts

Remarkably, we found a vast number of shipped genes, albeit around 1,000 less than the 12,000 genes described by another ribotag study (Furlanis et al., 2019). What is more, Furlanis and colleagues did not find astrocyte markers, or only detected them at low levels, whereas we saw genes enriched on neuronal ribosomes after the InSUREns protocol that are typically more abundant in astrocytes, arguing for the astrocytic origin of InSUREns genes.

Only very few ncRNAs were found among the InSUREns transcripts, implying a high-grade pulldown in which only ribosome-bound RNAs (and RNAs attached to those) are purified. Most InSUREns ncRNAs are lncRNAs. Especially interesting here is that of all known lncRNA over a third is exclusively transcribed in the brain, tightly controlled by physiological states (Briggs et al., 2015) and in turn also regulating mRNA translation (Statello et al., 2020).

Extracellular vesicle characterization

In choosing AWESAM cultured astrocytes, we were able to create pure stellate astrocytic cultures that are relatively close to *in vivo* cells (Wolfes et al., 2017), as they e.g. possess spontaneous calcium signaling (Wolfes and Dean, 2018), expecting to thereby create ADEVs correspondingly close to *in vivo* ADEVs.

Even though we did not confirm the exact type of EVs by utilizing markers, we see a sharp and big peak of EV size at 100nm, indicative of exosomes (Tancini et al., 2019). Likewise, there is almost no rRNA present in our ADEV preparation, which would be expected in case of other EVs, such as apoptotic vesicles in similar contexts (György et al., 2011; Osteikoetxea et al., 2015). Nonetheless multivesicular bodies and apoptotic bodies cannot be ruled out completely at this point, though their widely ranged size profile, ranging from 100-1000nm (György et al., 2011; Osteikoetxea et al., 2015), would be visible in Nanosight.

TU-Tagging time hints towards EVs as main RNA ferry

Interesting is also the labeling time it took before we could see signal from the 4TU-pulldown. Groups working with 4TU-tagging report an ideal labeling time of 1-8h, with most studies doing 4h pulse chase harvesting (Cleary et al., 2005; Gay et al., 2013, 2014; Rädle et al., 2013). Furthermore, it is stated by Gay and colleagues that harvesting tissue more than 12h after labeling yields significant less RNA (Gay et al., 2014).

In contrast, while establishing the method we found we needed to label thrice, with around 10h in between to yield enough labeled RNA. In light of the hypothesis that EVs are the main means of shipped RNA transport, that makes sense insofar as it would require some time for 4-Thiouracil to reach the nucleus, be incorporated into RNA, packed into EVs, secreted and then internalized by neurons. Several studies are stating that exosome uptake *in vitro* takes many hours up to a full day to reach its highest reporter signal and are showing that exosomal uptake reaches after 12h (Mutschelknaus et al., 2016; Zanotti et al., 2018).

ADEV transcripts

We detected a vast number of genes consistently present in ADEVs, containing two thirds of the transcriptome of cortical cultures, hinting at the possibility that horizontal RNA transfers cover most of a neuron's mRNA needs with regard to variety. The earliest wide-scope study describing the RNA content of EVs from MC/9 cells found 1300 mRNAs via microarrays and proved their functionality: by using an *in vitro* translation kit of exosomal RNAs and downstream protein isolation Valadi and colleagues could prove that EVs mRNAs are translatable (Valadi et al., 2007). Furthermore, this study described similar underlying functions of EV-RNA as we do here, i.e., protein synthesis and RNA modifications. Another study reported 27,000 transcripts in glioblastoma cells' microvesicles, also with microarrays (Skog et al., 2008).

By utilizing Next-generation-sequencing Wei and colleagues investigated the RNAome of glioblastoma exosomes, in which over 17.200 mRNAs were found in microvesicles and over 11.500 mRNAs in exosomes (Wei et al., 2017).

The overlap of InSUREns RNAs with ADEVs was only partial; this might be due to differences of astrocytic transcriptomes when cultured alone or in mixed primary cultures. Also, AWESAM cultures were supplied serum-free DMEM two days prior to medium extraction, which likely skewed the observed ADEV transcriptome. The composition of ncRNAs we observed in ADEVs however, shares a lot of resemblance with the InSUREns RNAs; they mainly contain long-ncRNAs and pseudogenes, and much less rRNA or mitochondrial rRNAs compared to the cortical culture, indicative of InSUREns transcripts being transported via ADEVs.

For the first time, we also describe here total RNA from stellate ADEVs, and find most of the top intercellularly shipped RNAs to be cargo of ADEVs. ADEVs' GO terms encompassed receptor activity and extracellular matrix, both being important for synaptic plasticity, substantiating our claim of RNA transfer for local translation.

Two other prominent terms were about DNA transcription - implying that ADEV RNA affects gene expression in the recipient cells.

Given the stark difference between both types of GO terms, we suggest different EVs could be released by astrocytes, depending on the immediate vicinity; astrocytic membrane patches closer to the neuronal cytosol might secrete ADEVs that carry primarily transcripts regulating DNA transcription, whereas astrocytic endfeet would secrete ADEVs with transcripts for RNA processing and splicing genes – a concept that we develop below. In fact, it was shown by different studies before that different types of EVs contain different sets of RNAs (Lässer et al., 2018). However, we might have not been able to isolate all such specialized vesicles, since astrocytes were cultured by themselves, lacking neuronal stimuli.

We did not perform small ncRNA sequencing, yet the tight regulation we observed between the top expressed InSUREns genes and ADEV miRs (Fig S3) points towards co-transportation, where astrocytic miRs are bound to mRNAs, possibly to prevent premature translation.

With more than half of all transcripts inside ADEVs being lncRNAs, and the enriched pathways of InSUREns genes revolving around RNA processing and translational regulation, we suggest that lncRNAs are being shuttled in parallel with mRNAs to achieve tightly controlled translation of the transferred coding transcripts as well as of the recipient's RNAome. Many roles have been described for lncRNAs; most notably here is their function as endogenous competitive binding molecules. lncRNAs are known to sponge transcriptional factors or other ncRNAs - such as miRNAs (Paraskevopoulou and Hatzigeorgiou, 2016) – in order to prevent their interactions with mRNAs or DNAs, thus leading to differences in the lifetime and transcript abundance of mRNAs (Carrieri et al., 2012; Gong and Maquat, 2011; Kretz et al., 2013; Yoon et al., 2012). Those changes can go either way; by interacting with Staufen1 some lncRNAs are known to degrade or enhance the stability of certain coding transcripts (Batista and Chang, 2013). Interestingly, Staufen1 is widely known for transportation of mRNAs along dendrites (Balasanyan and Arnold, 2014; Falley et al., 2009). Further proof of the complementary nature of both types of transcripts comes from the low GC content of the most abundant InSUREns genes; GC-low sequences form less stable secondary structures (Chan et al., 2009) and low GC regions are found to be less likely bound by ribosomes (Martens et al., 2015). Transferred genes might therefore have less stable secondary structures and are less likely to be bound by ribosomes, making them more available to miR and ncRNA binding. Consequently, we propose a complex, multi-layered transcriptional regulation network of transferred RNAs, which would be of special importance at the synapse to guarantee timesensitive translation during plasticity events.

Implications of RNA transfer for tripartite synapses

The tripartite synapse describes the arrangement of a presynapse and a postsynapse being engulfed by an astrocytic process. Astrocytes release EVs at their endfeet (Venturini et al., 2019), which can increase the frequency of the recipient neurons' miniature excitatory postsynaptic potential (Antonucci et al., 2012).

In addition, ADEVs stimulate dendritic branching and promote neuronal survival (Datta Chaudhuri et al., 2020) and have been linked to neuronal plasticity, when they are loaded with specific miRs (Lafourcade et al., 2016). Interestingly, EVs can stay bound to a specific patch of membrane via tetherin before secretion (Edgar et al., 2016). Such linking proteins might be reactive to surrounding firing synapses and could then release stockpiled ADEVs to deliver mRNAs directly to the spines and axonal terminals in order to provide transcripts required for LTP induction.

Indeed, for oligodendrocytes this has already been demonstrated; they release exosomes when neurons are chemically stimulated and those neurons subsequently internalize the exosomes at axons and dendrites (Frühbeis et al., 2013). Astrocytes release intracellularly calcium upon nearby synaptic glutamate secretion (Kim et al., 1994) and react to voltage changes with K^+ conducting channels (Olsen et al., 2015) or Na^+ conducting channels (Sontheimer et al., 1996). Calcium influences a multitude of intracellular processes and it is conceivable that tetherin-bound ADEVs at tripartite synapses are released under glutamate influence.

Subcellular accumulation of mRNAs in astrocytic endfeet at synapses has been shown recently (Sakers et al., 2017). LTP induction causes nearby astrocytes to extend more endfeet to associate with synaptic clefts and those contacts are closer to the synaptic membranes than before LTP induction (Wenzel et al., 1991). Additionally, close and sustained contact of astrocytic endfeet to dendrites is important for dendritic stabilization and maturation (Nishida and Okabe, 2007), which could imply that astrocytes decrease the distance to synaptic membranes to enhance ADEV specificity and increase successful transport.

Finally, the protein Sortin Nexin 4, which processes exosomes, was found at very high levels in neurons at the synapse and its knock-down led to high deregulation of proteins of synaptic pathways such as neurotransmission and synapse assembly (Vazquez-Sanchez et al., 2020).

ADEV-RNAs as candidates for synaptic tagging

For LTP to be sustainable, three things are necessary;

first, short-lived local events like the integration of more AMPA-receptors into the postsynaptic membrane; second, somatic protein supply for the synapse-to-be-changed has to be transported into neurites and third, an indicator where exactly those somatic proteins should be employed has to be generated and maintain at their location. To this day, the search for a definitive tag or a set of tags remains elusive – but so far, research was primarily focused on proteins. The resupply of a synapse undergoing LTP takes several hours and one main problem is the diffusion away of any candidate away from the tagged synapse.

As laid out above, a more precise spatial tagging could be achieved with ADEVs being internalized directly at changing synapses. Instead of the tag already present when the plasticity event is occurring, we propose that they are only translated upon the change itself.

Moreover, the tight interplay of ncRNAs and coding transcripts inside of ADEVs and those already present at synapses (Epple et al., 2020) would allow the changing synapse to further modify translation of the tag and either produce it continuously or delay translation to minimize diffusion until somatic proteins arrive. In line with this, we found many transferred lncRNAs to interact and regulate this synaptic mRNA set (Fig S2).

Strikingly, among the most abundant transferred RNAs we found BDNF, Homer1 and Arc - all are discussed in literature as candidates for synaptic tags. On the same note NCAM1, PKA and Camk2a and TrkB are known to be involved in the tagging and capturing process and were in the top quartile of InSUREns genes, too.

Our proposition allows also for vice versa regulation:

Many of the mRNAs from neuronal somata that are sent into neurites are packed tightly in stress granules and surrounded by RNA binding proteins as well as other regulatory ncRNAs. Inter-cellularly shipped ncRNAs, especially lncRNA, could potentially break up the stress granules by competitive binding, as laid out above. They would thereby loosen up somatic mRNAs' secondary structure, rendering them available for translation at the synapse-to-be-changed.

Materials and Methods

Vector design and virus production

Vectors were designed according to the sequences of previously published works, with very minor modifications (see supplementary materials S1 and S2). Production of vectors was done by VectorBuilder. Chosen serotype was AAV1/2 as this chimeric vector transduces neurons and astrocytes equally well. Virus production was done using HEK293T cells for transfection, according to a recent protocol (McClure et al., 2011), with minor modifications: virus harvesting was performed for 30min at 37° in a shaking incubator, 195mg NaCl was added (in 10ml reaction volume). Afterwards, solutions were placed for 30min in a water bath at 56°C, before being frozen at -80° overnight. On the next day, virus was thawed at 37° and then centrifuged for 30min at 4000g, keeping the supernatant. Furthermore, rAAVs were purified via an Iodixanol gradient rather than heparin columns. To this end, we carefully layered different Iodixanol (D1556, Sigma-Aldrich) concentrations in the following order from top to bottom into Oak ridge tubes (Thermo Scientific 314348): 3.5ml of 15%, 4ml of 25%, 3ml of 40% and 3ml of 54%.

The supernatant was carefully layered on top, before centrifuging for 1.5h at 365.000g in a fixed angle rotor (Sorvall T-865, Thermo Fisher). With a 20G canula we collected the 40% phase by placing the Canula's tip at the 40%/54% interphase. Collected virus solution was filled up to 10ml with 1x PBS-MK (PBS + 10mM MgCl₂ + 25mM KCl). Washing and concentration was done with 100k Amicon filters (UFC910024, Merck); filters were first prewetted with PBS-MK, then virus solution was added and centrifuged at 2000g to around 500µl. Flowthrough was removed, then filter tube was filled up to 10ml again with PBS-MK before repeating the centrifugation. After performing this step two more times, concentrated virus was collected with a 20G canula and sterile filtered through a 0.22µm filter. The syringe-driven filter was flushed with 100µl PBS-MK to collect any residual particles. Titration was done according to McClure and colleagues (McClure et al., 2011), subsequently virus was aliquoted and stored at -80° for long-term or at 4° for short-term usage.

Cell culture and viral transduction

All flasks and petri dishes were coated with 0.5 mg/ml PDL (P7886, Sigma-Aldrich). All experiments were performed according to the protocols approved by local ethics committee.

Primary cultures were made from E17 embryos of CD1 mice (Janvier). After cervical dislocation under isoflurane anesthesia, embryos were taken out and their brains quickly removed in cold PBS. Cortices were obtained by first removing meninges, cutting away the hippocampus and bulbus olfactorius, then cutting the cortices loose from the midbrain. Collected cortices were put in 0.25% Trypsin in PBS, and placed in a water bath at 37° for 13min. Thereafter the enzymatic reaction was stopped by adding the same volume of prewarmed processing medium (DMEM with 10% fetal bovine serum (FBS) (F9665, Sigma-Aldrich) and 1% Penicillin-Streptomycin (P/S) (P0781, Sigma-Aldrich). To render the cells less sticky, 10µl of DNase was added, the falcon tube was inverted once for mixing and solution was left for 1min. Afterwards cells were washed twice with prewarmed processing medium and triturated with 8x pipetting against the bottom and 8x pipetting the wall.

Cells were then collected by centrifuging at 300g for 5min at 37°, the supernatant removed and the cell pellet resuspended in BrainPhys plating medium (05794, StemCell technologies), supplied with 2% NeuroCult SM1 (05711, StemCell Technologies), 0.5 L-glutamine (both according to manufacturer's protocol), 1% P/S (A8943,0100; Applichem) and 1x GlutaMax (35050061, Gibco).

Then, to prevent cell clumps, suspension was filtered through a 100µm nylon strainer (352350, Falcon). Cells were seeded at 900.000/ml in 10cm and 14.5cm dishes and at 300.000/ml in 24 well plates. According to StemCell Technologies manual, we changed half of the plating medium after 5 days to BrainPhys maturation medium (supplied with 2% NeuroCult SM1 and 1% P/S), and performed third-medium changes every 3 days from then on.

Transduction and cell harvesting

At DIV7 cultures were transduced with the constructs GFAP-UPRT-mKate2 and hsyn-RPL4-3xHA-eGFP. At DIV13 we added 0.5 mM 4TU (440736, Sigma-Aldrich, dissolved in DMSO (276855, Sigma-Aldrich) into the medium, which was repeated twice, leaving 9-12h between each addition. To mitigate cell stress from too much DMSO, a third of medium got replaced right before the second addition of 4TU.

At DIV14 cells were washed once with PBS, collected in ribotag homogenization buffer (HB: 50 mM Tris-HCl, 100 mM KCl, 12 mM MgCl₂, 1% NP-40, 1 mM DTT (10197777001, Roche), protease inhibitor (05892791001, Roche), 100 Units/ml RNase inhibitor (N2515, Promega), 100 µg/ml cycloheximide (C4859, Sigma), 1 mg/ml Heparin (H4784, Sigma)), then centrifuged at 4° C, 10.000g, whereafter the supernatant was collected and samples were frozen at -20° until further processing. 50µl of the supernatant were kept as the input (described here as cortical culture input).

Isolation of secreted RNAs

For measuring RNA secreted into the medium, conditioned medium was filtered through a vacuum pump-driven 0.22µm filter. Afterwards volume was filled up with sterile PBS to 15 ml, then 200 units of RNase inhibitor were added (N2511, Promega) and 150 µg DNase. To concentrate RNAs (a ssRNA of 1000nt has a molecular weight of 320 kDa (ThermoFisher)) we used a 3kDa centrifugation filter (Millipore) at 4000g for 1h in a swinging bucket rotor. Thereafter we added 4x lysis buffer and 3x 100% EtOH and followed the rest of the protocol for the GenElute Single Cell RNA Purification Kit (RNB300, Sigma).

RNA concentration

RNA concentrations were measured with the Bioanalyzer (Agilent Technologies) on RNA 6000 Pico chips.

Astrocyte culture

To obtain stellate astrocyte cultures, we followed the recently published AWESAM protocol (Wolfes et al., 2017). Briefly, this entails normal culturing of mixed primary cells, yet on DIV6 cultures are shaken for 6h, removing all loosened cells, trypsinizing the still bound astrocytes, centrifuging and seeding at 0.6 Million cells /ml in T75 flasks with 10ml Neurobasal+ (A3582901, ThermoFisher), containing 10% fetal bovine serum (FBS), B27+ (A3582801, ThermoFisher), 1 % P/S and 5ng/ml HB-EGF (E4643, Sigma-Aldrich).

To test for the uptake of stellate astrocytic EVs we used the Ribotracker x GFAP-CreER line to create AWESAM cultures. After 10 DIV we applied 5mM Tamoxifen (HY-13757A, MedChemExpress) to allow Cre expression.

Astrocyte Culture for Ribotracker Supernatant

Ten days after Cre induction we took the conditioned medium and applied it to wild-type cortical cultures, replacing half of the medium and incubating the recipients for 10h before washing and fixing. To enhance the weak RFP-signal, we amplified it by antibody staining (Invitrogen 16D7).

Extracellular vesicle isolation

Two days prior to EV isolation, cells were washed once with warm PBS and medium was replaced with 15ml DMEM (+ 1% P/S), without FBS, as serum contains exogenous EVs. Thus, by replacing the medium, all EVs isolated thereafter originated from cultured astrocytes.

We isolated EVs with a recently introduced exosome method by Merck (Merck-Website); first AU-15 Amicon Ultra filter (UFC901024, Merck-Millipore) were pre-wetted by adding 2ml of PBS into the filter and centrifuging in a swinging bucket rotor for 10min at 4000g. PBS was then removed from collection and filtrate tube. Conditioned medium was filtered through a Steriflip unit (SCGP00525, Merck-Millipore) via a vacuum pump and subsequently added to filtration tube, then centrifuged at 4000g for 30min. Afterwards the collection tube was emptied and 14ml of PBS were added into the filter. Using a 1ml, pipette liquid was pipetted softly up and down along the filters to mix well. The second centrifugation was done again at 4000g for 30min, then concentrated EVs were collected from the Amicon filter.

To sequence ADEVs, we isolated their RNA with GenElute™ Single Cell RNA Purification Kit (RNB300, Sigma), after isolation was performed as described above.

Labeling extracellular vesicles

Carboxyfluorescein succinimidyl ester (CFSE) staining was performed with a kit (ThermoFisher, C34554). CFSE stock solution was prepared by adding 18µl of DMSO into a stock vial. Isolated EVs were mixed with 10µM of CFSE and incubated at 37° in a shaking incubator set to 100rpm for 30min in dark. To remove excess dye, EVs were filtered once again through a pre-wetted AU-15 Amicon Ultra filter for 30min at 4000g. To monitor the degree of self-assembled CFSE aggregates, we incubated 10µM of CFSE in PBS alone along with the samples and also carried out the subsequent centrifugation step before measuring them in Nanosight.

Extracellular vesicle measurement

Immediately after isolation, 30µl EVs were diluted to 1:20 with 570µl PBS and measured with Nanosight LM14C (NanoSight Ltd.) at 22°, averaging three measurements of 60sec at different locations of the observational area (NTA 2.3 Analytical Software), with a detection threshold of 15 and a camera level of 15. EVs were applied to cultures directly after measuring.

Ribotag pulldown

All water used was of molecular grade. Steps were performed in dark in case of double-pulldown. HA-based pulldown of labeled ribosomes (RPL22-HA) was carried out mainly as described in a formerly published protocol (Chukrallah et al., 2020), with several changes taken from two other publications (Sanz et al., 2019; Schleif, 2018) as explained below.

Cells harvested in HB buffer, as described above, were used. Pipetting steps with beads were performed by putting the tubes on a magnetic rack, so that beads could form a pellet.

First, protein A/G magnetic beads (88803, Thermo Fisher) were washed with HB thrice for 5min at 4° under rotation. The original volume of bead solution was restored with HB afterwards.

Preclearing was done to minimize unspecific binding to A/G beads: per mililiter sample, 50µl washed beads were added, and incubated for 1h at 4° under rotation. Supernatant was kept and filled into new tubes and beads were discarded.

Mouse-IgG-anti-HA antibody (26183, Invitrogen) was added at 12µl/ml and incubated for 1h at 4° with rotation. Subsequently 200µl of washed beads were added per ml of sample and incubated 2h at 4° rotating. Pellets were washed thrice in high salt buffer (50 mM Tris, 300 mM KCl, 12 mM MgCl₂, 1% NP-40 (74385, Fluka), 1 mM DTT, 100 µg/ml cyclohexamide, 100 Units/ml RNase inhibitor (RNasin, Promega)). Each washing step took 5min. Buffer was removed, resuspension of beads was done in 400µl RLT (+1µl of βME (M6250, Sigma-Aldrich) per ml of RLT). RNA from inputs, which were not undergoing the steps so far laid out in this paragraph, was isolated by adding 350µl of RLT to them. Input RNA and tagged Ribosome-bound RNA was then further isolated via the clean-up section of the RNEasy MinElute Cleanup Kit (74204, Qiagen) and eluted in 14µl. If RNA was also 4TU labeled, 4TU purification was done right away to minimize sample degradation.

4TU pulldown

4TU might crosslink under light, leading to potential blocking of biotin binding sites. Thus, working in the dark is important until RNA is converted to cDNA during the library preparation steps. This should be taken into consideration during the ribotag pulldown as well. Water used was of molecular grade. RNAs were kept on ice during pipetting steps.

This pulldown was based on two protocols (Gay et al., 2014; Rädle et al., 2013) and slightly modified as shown below.

Up to 5µg of RNA (all after Ribotag-pulldown) were used for biotinylation and mixed with 1 mM EDTA (E5134, Sigma-Aldrich), 20mM HEPES (H3375, Sigma-Aldrich), 16.4µM MTSEA-biotin-XX (B-90066-1, Hölzel Biotech, in DMF (227056, Sigma-Aldrich)).

Volume was adjusted with water to 50µl, reaction vials were placed for 30 min in the dark at RT with rotation. Excess biotin was eliminated as follows: first 50µl of water, 100µl of 24:1 Chloroform/Isoamylalcohol (10103971, Fisher Scientific) and 50µl of 1xTE buffer were added and tubes shaken for 15sec, before incubating for 2min at RT. Then samples were centrifuged at 12,000g for 5min at 4°. By using a fine needle and syringe, we collected the aqueous phase. In a new tube, 350µl of RLT buffer from the RNEasy MinElute Cleanup Kit (74204, Qiagen) and 250µl of 100% EtOH were mixed with the aqueous phase. Subsequently, purification of RNA was done via the RNEasy MinElute Cleanup kit, eluting RNAs in a final volume of 50µl water.

Streptavidin pulldown was performed using the µMACS Streptavidin Starting Kit (130-091-287, Miltenyi Biotec). First biotinylated RNA was incubated for 10min at 65°, then placed in ice for 5min. Afterwards 100µl of streptavidin beads were added and incubated for 15min under rotation. Columns were equilibrated with the kit's respective buffer for nucleic acids, and the magnetic rack was assembled with 4 columns on the stand and a big tray to collect flowthrough during washes. Samples containing the beads were applied to columns and washed thrice with 0.9ml of 65° warm washing buffer (100mM Tris pH 7.4, 10mM EDTA, 1M NaCl and 0.1% Tween 20 (P9416, Sigma-Aldrich)). Thereafter columns were washed again thrice with washing buffer of RT. The collecting tray was replaced with fresh tubes containing 700 RLT buffer from RNEasy MinElute Cleanup Kit under each column and labeled RNAs were eluted by twice applying 100µl molecular grade water (+ 5%β-ME). Final purification was done by following the protocol from the RNease MinElute Cleanup kit. RNAs were eluted in 12µl water. In case of a single 4TU pulldown, RNA from cell cultures was directly isolated via the Rneasy Mini kit (74104, Qiagen).

Library preparation and sequencing

Given that very little RNA is detectable following the two consequent pulldowns, a minimal input library preparation kit is advised. We used SMARTer Stranded Total RNA-Seq Kit v2 - Pico Input Mammalian kit (Takara) and followed manufacturer's instructions. Sequencing was performed on a HiSeq2000 machine from Illumina, using dual indices and the single-end mode.

Analysis

Analyses were done in R with packages or with web tools as indicated below.

We subtracted all genes from further analyses (Fig 3-6) if their average normalized read count in controls was 25% or higher than in labeled samples, thereby removing a total of 29 genes from analysis. This was done for both types of controls separately. The same was done for non-coding (nc) RNAs, where 31 transcripts were removed.

Barplots and pie charts were produced with ggplot2 package (Wickham, 2016). GC, 5' and 3' analysis, as well as networks, were done with ShinyGO (Ge et al., 2020), Rank-Rank Hypergeometric test with the RRHO package (Rosenblatt and Stein, 2014) and Venn diagrams with the VennDiagram package (Chan, 2018). GO term analyses were done with ClusterProfiler (Yu, 2012) with the following settings: p-adjustment according to Benjamini-Hochberg, with a 0.01 p-Value cutoff, a 0.05 q-Value cutoff and ontologies as indicated for each graph.

Differential expression analysis was performed with DESEQ2 (Love et al., 2014) as follows: raw counts were used, yet only genes with a count per million (CPM) of 1 in at least 2 samples were considered. Genes were classified as differentially expressed with FDR adjusted p-value lower than or equal to 0.05 and a minimum fold change of 1.5. Since we observed a high background for ADEV RNAs, we proceeded only with ADEV genes whose transcripts per million (TPM) were equal or above 10 – in case of the DESeq2 analysis between ADEV and cortical inputs we used the raw counts after that filtering step.

RNA-Network analysis was done based on all RNA interactions that were listed as experimentally validated in several databases; STRING (Szklarczyk et al., 2019), RegNetwork (Liu et al., 2015), TransmiR (Tong et al., 2019), Rise (Gong et al., 2018), NPInter (Teng et al., 2020) and TarBase (Karagkouni et al., 2018). Interactions classified as weak were filtered out.

All interactions were compiled and matched with transcript lists using in-house Python scripts.

Matched lists were then used in Cytoscape (v3.7.2) to create the networks.

Imaging

Cells on coverslips were fixed in 4% PFA in PBS plus 1 μ M MgCl₂, 0.1 μ M CaCl₂ and 120mM Sucrose. Stainings were done according to Abcam's protocol (Abcam).

For samples that received ADEV or conditioned supernatant treatment, fixation was done 8-12h after the treatment. RFP signal was amplified by an antibody against it.

Antibodies used were: Synaptophysin (ab8049, Abcam) with the secondary antibody Alexa Fluor 488 (goat anti-mouse, A-21121, Invitrogen) and Anti-RFP (600-401-379, Rockland) with the secondary antibody Alexa Fluor 555 (anti rabbit, A27039, Invitrogen). Primary antibodies were diluted to 1:300, secondary antibodies 1:400. Coverslips were mounted using Fluoromount-G (00-4958-02, Invitrogen).

Our imaging setup consisted of a Leica DMI8 microscope with default Leica software (Leica Application Suite X). Settings were kept between groups of the same experiment. Background was removed from all images using the default setting from ImageJ.

Availability of data

Depending on journals' publishing policies, read count tables will be made available here:
<https://data.goettingen-research-online.de>

Compliance with Ethical Standards

The authors declare no conflict of interest. This work includes experiments with mice. All described experiments approved by the local animal care committee.

Conflict of interest

The authors declare no conflict of interest.

Acknowledgments

RE is a member of the international Max Planck Research School (IMPRS) for Neuroscience, Göttingen. This work was supported by the following third-party funds to AF: the ERC consolidator grant DEPICODE (648898), funds from the SFB1286 (B06), the DFG under Germany's Excellence Strategy - EXC 2067/1 390729940 the and funds from the German Center for Neurodegenerative Diseases (DZNE).

Author contribution

RE designed experiments, conducted cell culture and RNA-sequencing experiments, analyzed data and wrote the manuscript. PS conducted cell culture and RNA-sequencing experiments and helped establishing the method. DK performed network analyses. TP provided bioinformatic support. CV provided Ribotracker x GFAP-CreER mice and helped designing ADEV experiments. AF supervised the project.

References

Abcam Immunocytochemistry and immunofluorescence staining protocol:

<https://www.abcam.com/protocols/immunocytochemistry-immunofluorescence-protocol>

- Antonucci, F., Turola, E., Riganti, L., Caleo, M., Gabrielli, M., Perrotta, C., Novellino, L., Clementi, E., Giussani, P., Viani, P., et al. (2012). Microvesicles released from microglia stimulate synaptic activity via enhanced sphingolipid metabolism: Microglial MVs increase sphingolipid metabolism in neurons. *The EMBO Journal* *31*, 1231–1240.
- Balasanyan, V., and Arnold, D.B. (2014). Actin and Myosin-Dependent Localization of mRNA to Dendrites. *PLoS ONE* *9*, e92349.
- Batista, P.J., and Chang, H.Y. (2013). Long Noncoding RNAs: Cellular Address Codes in Development and Disease. *Cell* *152*, 1298–1307.
- Bosch, M., Castro, J., Saneyoshi, T., Matsuno, H., Sur, M., and Hayashi, Y. (2014). Structural and Molecular Remodeling of Dendritic Spine Substructures during Long-Term Potentiation. *Neuron* *82*, 444–459.
- Briggs, J.A., Wolvetang, E.J., Mattick, J.S., Rinn, J.L., and Barry, G. (2015). Mechanisms of Long Non-coding RNAs in Mammalian Nervous System Development, Plasticity, Disease, and Evolution. *Neuron* *88*, 861–877.
- Carrieri, C., Cimatti, L., Biagioli, M., Beugnet, A., Zucchelli, S., Fedele, S., Pesce, E., Ferrer, I., Collavin, L., Santoro, C., et al. (2012). Long non-coding antisense RNA controls Uchl1 translation through an embedded SINEB2 repeat. *Nature* *491*, 454–457.
- Chan, H. (2018). VennDiagram: Generate High-Resolution Venn and Euler Plots. R package version 1.6.20. <https://CRAN.R-project.org/package=VennDiagram>.
- Chan, C., Carmack, C.S., Long, D.D., Maliyekkel, A., Shao, Y., Roninson, I.B., and Ding, Y. (2009). A structural interpretation of the effect of GC-content on efficiency of RNA interference. *BMC Bioinformatics* *10*, S33.
- Chatzi, C., Zhang, Y., Shen, R., Westbrook, G.L., and Goodman, R.H. (2016). Transcriptional Profiling of Newly Generated Dentate Granule Cells Using TU Tagging Reveals Pattern Shifts in Gene Expression during Circuit Integration. *ENeuro* *3*, ENEURO.0024-16.2016.
- Chukrallah, L.G., Seltzer, K., and Snyder, E.M. (2020). RiboTag Immunoprecipitation in the Germ Cells of the Male Mouse. *JoVE* 60927.
- Cleary, M.D., Meiering, C.D., Jan, E., Guymon, R., and Boothroyd, J.C. (2005). Biosynthetic labeling of RNA with uracil phosphoribosyltransferase allows cell-specific microarray analysis of mRNA synthesis and decay. *Nature Biotechnology* *23*, 232–237.
- Datta Chaudhuri, A., Dasgheyb, R.M., DeVine, L.R., Bi, H., Cole, R.N., and Haughey, N.J. (2020). Stimulus-dependent modifications in astrocyte-derived extracellular vesicle cargo regulate neuronal excitability. *Glia* *68*, 128–144.
- Deal, R.B., and Henikoff, S. (2011). The INTACT method for cell type-specific gene expression and chromatin profiling in *Arabidopsis thaliana*. *Nat Protoc* *6*, 56–68.
- Doyle, J.P., Dougherty, J.D., Heiman, M., Schmidt, E.F., Stevens, T.R., Ma, G., Bupp, S., Shrestha, P., Shah, R.D., Doughty, M.L., et al. (2008). Application of a Translational Profiling Approach for the Comparative Analysis of CNS Cell Types. *Cell* *135*, 749–762.

- Edgar, J.R., Manna, P.T., Nishimura, S., Banting, G., and Robinson, M.S. (2016). Tetherin is an exosomal tether. *ELife* 5, e17180.
- Epple, R., Krüger, D., Berulava, T., Brehm, G., Islam, R., Köster, S., and Fischer, A. (2020). The Coding And Small-Non-Coding Hippocampal Synaptic RNAome (Neuroscience). *BioRxiv*: 10.1101/2020.11.27.401901
<https://www.biorxiv.org/content/10.1101/2020.11.27.401901v1.full>
- Erickson, T., and Nicolson, T. (2015). Identification of sensory hair-cell transcripts by thiouracil-tagging in zebrafish. *BMC Genomics* 16, 842.
- Falley, K., Schütt, J., Iglauer, P., Menke, K., Maas, C., Kneussel, M., Kindler, S., Wouters, F.S., Richter, D., and Kreienkamp, H.-J. (2009). Shank1 mRNA: Dendritic Transport by Kinesin and Translational Control by the 5' Untranslated Region. *Traffic* 10, 844–857.
- Frey, U., and Morris, R.G. (1997). Synaptic tagging and long-term potentiation. *Nature* 385, 533–536.
- Frühbeis, C., Fröhlich, D., Kuo, W.P., Amphornrat, J., Thilemann, S., Saab, A.S., Kirchhoff, F., Möbius, W., Goebels, S., Nave, K.-A., et al. (2013). Neurotransmitter-Triggered Transfer of Exosomes Mediates Oligodendrocyte–Neuron Communication. *PLoS Biol* 11, e1001604.
- Furlanis, E., Traunmüller, L., Fucile, G., and Scheiffele, P. (2019). Landscape of ribosome-engaged transcript isoforms reveals extensive neuronal-cell-class-specific alternative splicing programs. *Nat Neurosci* 22, 1709–1717.
- Gay, L., Miller, M.R., Ventura, P.B., Devasthali, V., Vue, Z., Thompson, H.L., Temple, S., Zong, H., Cleary, M.D., Stankunas, K., et al. (2013). Mouse TU tagging: a chemical/genetic intersectional method for purifying cell type-specific nascent RNA. *Genes Dev* 27, 98–115.
- Gay, L., Karfilis, K.V., Miller, M.R., Doe, C.Q., and Stankunas, K. (2014). Applying thiouracil tagging to mouse transcriptome analysis. *Nat Protoc* 9, 410–420.
- Ge, S.X., Jung, D., and Yao, R. (2020). ShinyGO: a graphical gene-set enrichment tool for animals and plants. *Bioinformatics* 36, 2628–2629.
- Gong, C., and Maquat, L.E. (2011). lncRNAs transactivate STAU1-mediated mRNA decay by duplexing with 3' UTRs via Alu elements. *Nature* 470, 284–288.
- Gong, J., Shao, D., Xu, K., Lu, Z., Lu, Z.J., Yang, Y.T., and Zhang, Q.C. (2018). RISE: a database of RNA interactome from sequencing experiments. *Nucleic Acids Res* 46, D194–D201.
- Gregory, J.A., Hoelzli, E., Abdelaal, R., Braine, C., Cuevas, M., Halpern, M., Barretto, N., Schrode, N., Akbalik, G., Kang, K., et al. (2020). Cell Type-Specific In Vitro Gene Expression Profiling of Stem Cell-Derived Neural Models. *Cells* 9, 1406.
- György, B., Szabó, T.G., Pásztói, M., Pál, Z., Misják, P., Aradi, B., László, V., Pállinger, É., Pap, E., Kittel, Á., et al. (2011). Membrane vesicles, current state-of-the-art: emerging role of extracellular vesicles. *Cell. Mol. Life Sci.* 68, 2667–2688.
- He, M., Liu, Y., Wang, X., Zhang, M.Q., Hannon, G.J., and Huang, Z.J. (2012). Cell-Type-Based Analysis of MicroRNA Profiles in the Mouse Brain. *Neuron* 73, 35–48.
- Jovičić, A., and Gitler, A.D. (2017). Distinct repertoires of microRNAs present in mouse astrocytes compared to astrocyte-secreted exosomes. *PLoS One* 12, e0171418.
- Kandel, E.R. (2013). *Principles of neural science*, 5th Edition (New York: McGraw-Hill).

- Kang, H., and Schuman, E.M. (1996). A Requirement for Local Protein Synthesis in Neurotrophin-Induced Hippocampal Synaptic Plasticity. *Science* 273, 1402–1406.
- Karagkouni, D., Paraskevopoulou, M.D., Chatzopoulos, S., Vlachos, I.S., Tastsoglou, S., Kanellos, I., Papadimitriou, D., Kavakiotis, I., Maniou, S., Skoufos, G., et al. (2018). DIANA-TarBase v8: a decade-long collection of experimentally supported miRNA-gene interactions. *Nucleic Acids Res* 46, D239–D245.
- Kim, W.T., Rioult, M.G., and Cornell-Bell, A.H. (1994). Glutamate-induced calcium signaling in astrocytes. *Glia* 11, 173–184.
- Kowal, J., Arras, G., Colombo, M., Jouve, M., Morath, J.P., Primdal-Bengtson, B., Dingli, F., Loew, D., Tkach, M., and Théry, C. (2016). Proteomic comparison defines novel markers to characterize heterogeneous populations of extracellular vesicle subtypes. *Proc Natl Acad Sci USA* 113, E968–E977.
- Kretz, M., Siprashvili, Z., Chu, C., Webster, D.E., Zehnder, A., Qu, K., Lee, C.S., Flockhart, R.J., Groff, A.F., Chow, J., et al. (2013). Control of somatic tissue differentiation by the long non-coding RNA TINCR. *Nature* 493, 231–235.
- Kügler, S., Kilic, E., and Bähr, M. (2003). Human synapsin 1 gene promoter confers highly neuron-specific long-term transgene expression from an adenoviral vector in the adult rat brain depending on the transduced area. *Gene Therapy* 10, 337–347.
- Lafourcade, C., Ramírez, J.P., Luarte, A., Fernández, A., and Wyneken, U. (2016). MIRNAS in Astrocyte-Derived Exosomes as Possible Mediators of Neuronal Plasticity: Supplementary Issue: Brain Plasticity and Repair. *J Exp Neurosci* 10s1, JEN.S39916.
- Lässer, C., Jang, S.C., and Lötval, J. (2018). Subpopulations of extracellular vesicles and their therapeutic potential. *Molecular Aspects of Medicine* 60, 1–14.
- Lee, Y., Messing, A., Su, M., and Brenner, M. (2008). *GFAP* promoter elements required for region-specific and astrocyte-specific expression. *Glia* 56, 481–493.
- Lesiak, A.J., Brodsky, M., and Neumaier, J.F. (2015). RiboTag is a flexible tool for measuring the translational state of targeted cells in heterogeneous cell cultures. *BioTechniques* 58.
- Liu, Z.-P., Wu, C., Miao, H., and Wu, H. (2015). RegNetwork: an integrated database of transcriptional and post-transcriptional regulatory networks in human and mouse. *Database (Oxford)* 2015.
- Love, M.I., Huber, W., and Anders, S. (2014). Moderated estimation of fold change and dispersion for RNA-seq data with DESeq2. *Genome Biol* 15, 550.
- Martens, A.T., Taylor, J., and Hilser, V.J. (2015). Ribosome A and P sites revealed by length analysis of ribosome profiling data. *Nucleic Acids Research* 43, 3680–3687.
- McClure, C., Cole, K.L.H., Wulff, P., Klugmann, M., and Murray, A.J. (2011). Production and Titering of Recombinant Adeno-associated Viral Vectors. *JoVE* 3348.
- Merck-Website Extracellular Vesicle Protocol:
- https://www.merckmillipore.com/DE/de/life-science-research/protein-sample-preparation/Extracellular-Vesicle-Preparation/Extracellular-Vesicle-Protocol/Temb.qB.gq8AAAFOWfs1ITD_nav
- Miller, M.R., Robinson, K.J., Cleary, M.D., and Doe, C.Q. (2009). TU-tagging: cell type-specific RNA isolation from intact complex tissues. *Nat Methods* 6, 439–441.

- Morales-Kastresana, A., Telford, B., Musich, T.A., McKinnon, K., Clayborne, C., Braig, Z., Rosner, A., Demberg, T., Watson, D.C., Karpova, T.S., et al. (2017). Labeling Extracellular Vesicles for Nanoscale Flow Cytometry. *Sci Rep* 7, 1878.
- Mutschelknaus, L., Peters, C., Winkler, K., Yentrapalli, R., Heider, T., Atkinson, M.J., and Moertl, S. (2016). Exosomes Derived from Squamous Head and Neck Cancer Promote Cell Survival after Ionizing Radiation. *PLoS ONE* 11, e0152213.
- Nishida, H., and Okabe, S. (2007). Direct Astrocytic Contacts Regulate Local Maturation of Dendritic Spines. *Journal of Neuroscience* 27, 331–340.
- Okuda, K., Højgaard, K., Privitera, L., Bayraktar, G., and Takeuchi, T. (2020). Initial memory consolidation and the synaptic tagging and capture hypothesis. *Eur J Neurosci* ejn.14902.
- Olsen, M.L., Khakh, B.S., Skatchkov, S.N., Zhou, M., Lee, C.J., and Rouach, N. (2015). New Insights on Astrocyte Ion Channels: Critical for Homeostasis and Neuron-Glia Signaling. *Journal of Neuroscience* 35, 13827–13835.
- Osteikoetxea, X., Balogh, A., Szabó-Taylor, K., Németh, A., Szabó, T.G., Pálóczi, K., Sódar, B., Kittel, Á., György, B., Pállinger, É., et al. (2015). Improved Characterization of EV Preparations Based on Protein to Lipid Ratio and Lipid Properties. *PLoS ONE* 10, e0121184.
- Paraskevopoulou, M.D., and Hatzigeorgiou, A.G. (2016). Analyzing MiRNA–LncRNA Interactions. In *Long Non-Coding RNAs*, Y. Feng, and L. Zhang, eds. (New York, NY: Springer New York), pp. 271–286.
- Rädle, B., Rutkowski, A.J., Ruzsics, Z., Friedel, C.C., Koszinowski, U.H., and Dölken, L. (2013). Metabolic Labeling of Newly Transcribed RNA for High Resolution Gene Expression Profiling of RNA Synthesis, Processing and Decay in Cell Culture. *JoVE* 50195.
- Rangaraju, V., Tom Dieck, S., and Schuman, E.M. (2017). Local translation in neuronal compartments: how local is local? *EMBO Rep.* 18, 693–711.
- Rinn, J.L., Wang, J.K., Allen, N., Brugmann, S.A., Mikels, A.J., Liu, H., Ridky, T.W., Stadler, H.S., Nusse, R., Helms, J.A., et al. (2008). A dermal HOX transcriptional program regulates site-specific epidermal fate. *Genes & Development* 22, 303–307.
- Rosenblatt, J., and Stein, J. (2014). RRHO, R package.
- Sakers, K., Lake, A.M., Khazanchi, R., Ouwenga, R., Vasek, M.J., Dani, A., and Dougherty, J.D. (2017). Astrocytes locally translate transcripts in their peripheral processes. *Proc Natl Acad Sci USA* 114, E3830–E3838.
- Sanz, E., Yang, L., Su, T., Morris, D.R., McKnight, G.S., and Amieux, P.S. (2009). Cell-type-specific isolation of ribosome-associated mRNA from complex tissues. *Proc. Natl. Acad. Sci. U.S.A.* 106, 13939–13944.
- Sanz, E., Bean, J.C., Carey, D.P., Quintana, A., and McKnight, G.S. (2019). RiboTag: Ribosomal Tagging Strategy to Analyze Cell-Type-Specific mRNA Expression In Vivo. *Current Protocols in Neuroscience* 88.
- Schleif, M. (2018). Regulation of gene expression in specific mouse brain cells during neurodegenerative prion disease. Dissertation.
- Skog, J., Würdinger, T., van Rijn, S., Meijer, D.H., Gainche, L., Curry, W.T., Carter, B.S., Krichevsky, A.M., and Breakefield, X.O. (2008). Glioblastoma microvesicles transport RNA and proteins that promote tumour growth and provide diagnostic biomarkers. *Nat Cell Biol* 10, 1470–1476.
- Sontheimer, H., Black, J.A., and Waxman, S.G. (1996). Voltage-gated Na⁺ channels in glia: properties and possible functions. *Trends in Neurosciences* 19, 325–331.

Statello, L., Guo, C.-J., Chen, L.-L., and Huarte, M. (2020). Gene regulation by long non-coding RNAs and its biological functions. *Nat Rev Mol Cell Biol*.

Szklarczyk, D., Gable, A.L., Lyon, D., Junge, A., Wyder, S., Huerta-Cepas, J., Simonovic, M., Doncheva, N.T., Morris, J.H., Bork, P., et al. (2019). STRING v11: protein–protein association networks with increased coverage, supporting functional discovery in genome-wide experimental datasets. *Nucleic Acids Research* *47*, D607–D613.

Tancini, B., Buratta, S., Sagini, K., Costanzi, E., Delo, F., Urbanelli, L., and Emiliani, C. (2019). Insight into the Role of Extracellular Vesicles in Lysosomal Storage Disorders. *Genes* *10*, 510.

Teng, X., Chen, X., Xue, H., Tang, Y., Zhang, P., Kang, Q., Hao, Y., Chen, R., Zhao, Y., and He, S. (2020). NPInter v4.0: an integrated database of ncRNA interactions. *Nucleic Acids Res* *48*, D160–D165.

ThermoFisher DNA and RNA Molecular Weights and Conversions:

<https://www.thermofisher.com/de/de/home/references/ambion-tech-support/rna-tools-and-calculators/dna-and-rna-molecular-weights-and-conversions.html>

Tong, Z., Cui, Q., Wang, J., and Zhou, Y. (2019). TransmiR v2.0: an updated transcription factor-microRNA regulation database. *Nucleic Acids Res* *47*, D253–D258.

Valadi, H., Ekström, K., Bossios, A., Sjöstrand, M., Lee, J.J., and Lötvall, J.O. (2007). Exosome-mediated transfer of mRNAs and microRNAs is a novel mechanism of genetic exchange between cells. *Nat Cell Biol* *9*, 654–659.

Vazquez-Sanchez, S., Gonzalez-Lozano, M.A., Walfenzao, A., Li, K.W., and van Weering, J.R.T. (2020). The endosomal protein sorting nexin 4 is a synaptic protein. *Sci Rep* *10*, 18239.

Venturini, A., Passalacqua, M., Pelassa, S., Pastorino, F., Tedesco, M., Cortese, K., Gagliani, M.C., Leo, G., Maura, G., Guidolin, D., et al. (2019). Exosomes From Astrocyte Processes: Signaling to Neurons. *Front. Pharmacol.* *10*, 1452.

Wang, D.O., Martin, K.C., and Zukin, R.S. (2010). Spatially restricting gene expression by local translation at synapses. *Trends in Neurosciences* *33*, 173–182.

Wei, Z., Batagov, A.O., Schinelli, S., Wang, J., Wang, Y., El Fatimy, R., Rabinovsky, R., Balaj, L., Chen, C.C., Hochberg, F., et al. (2017). Coding and noncoding landscape of extracellular RNA released by human glioma stem cells. *Nat Commun* *8*, 1145.

Wenzel, J., Lammert, G., Meyer, U., and Krug, M. (1991). The influence of long-term potentiation on the spatial relationship between astrocyte processes and potentiated synapses in the dentate gyrus neuropil of rat brain. *Brain Research* *560*, 122–131.

Wickham, H. (2016). *ggplot2: Elegant Graphics for Data Analysis*.

Wolfes, A.C., and Dean, C. (2018). Culturing In Vivo-like Murine Astrocytes Using the Fast, Simple, and Inexpensive AWESAM Protocol. *JoVE* 56092.

Wolfes, A.C., Ahmed, S., Awasthi, A., Stahlberg, M.A., Rajput, A., Magruder, D.S., Bonn, S., and Dean, C. (2017). A novel method for culturing stellate astrocytes reveals spatially distinct Ca²⁺ signaling and vesicle recycling in astrocytic processes. *Journal of General Physiology* *149*, 149–170.

Yoon, J.-H., Abdelmohsen, K., Srikantan, S., Yang, X., Martindale, J.L., De, S., Huarte, M., Zhan, M., Becker, K.G., and Gorospe, M. (2012). lincRNA-p21 Suppresses Target mRNA Translation. *Molecular Cell* *47*, 648–655.

You, Y., Borgmann, K., Edara, V.V., Stacy, S., Ghorpade, A., and Ikezu, T. (2020). Activated human astrocyte-derived extracellular vesicles modulate neuronal uptake, differentiation and firing. *Journal of Extracellular Vesicles* *9*, 1706801.

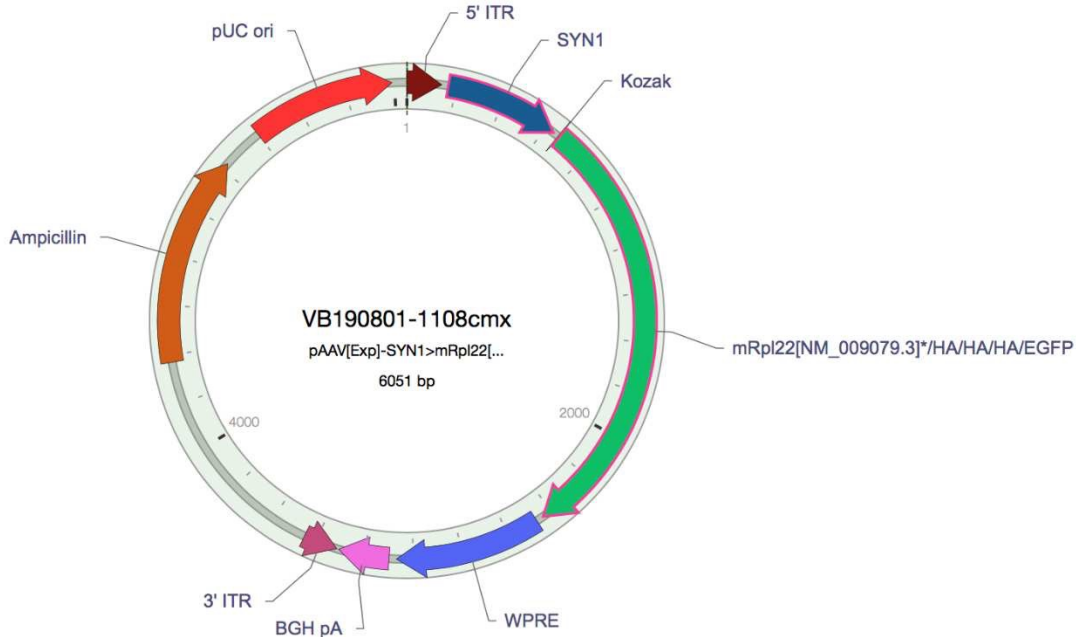
Yu, G. (2012). clusterProfiler: an R package for comparing biological themes among gene clusters.

Zanotti, S., Gibertini, S., Blasevich, F., Bragato, C., Ruggieri, A., Saredi, S., Fabbri, M., Bernasconi, P., Maggi, L., Mantegazza, R., et al. (2018). Exosomes and exosomal miRNAs from muscle-derived fibroblasts promote skeletal muscle fibrosis. *Matrix Biology* 74, 77–100.

Zhang, Y., Chen, K., Sloan, S.A., Bennett, M.L., Scholze, A.R., O’Keeffe, S., Phatnani, H.P., Guarnieri, P., Caneda, C., Ruderisch, N., et al. (2014). An RNA-Sequencing Transcriptome and Splicing Database of Glia, Neurons, and Vascular Cells of the Cerebral Cortex. *Journal of Neuroscience* 34, 11929–11947.

Supplementary Materials

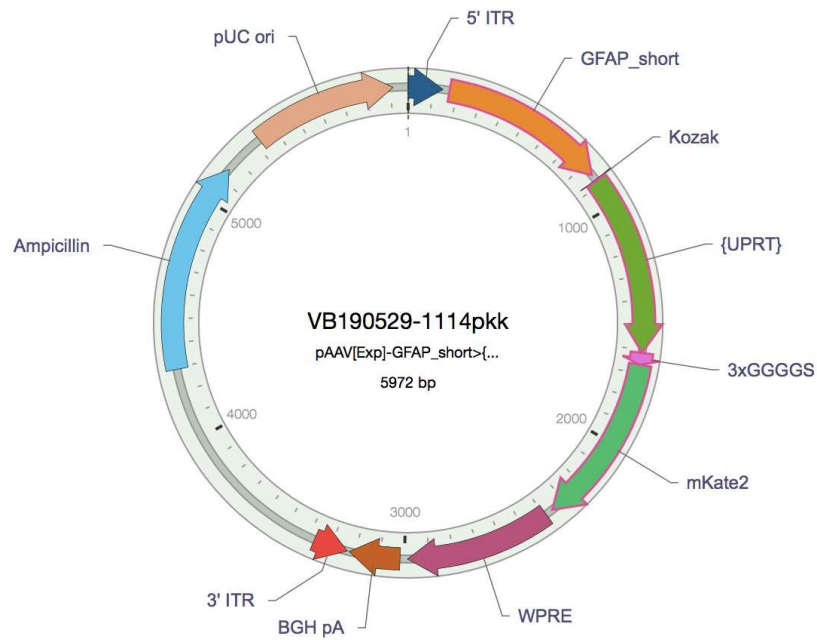
S1) Sequence of hSyn-Rpl22-3xHA-eGFP plasmid



TAGCTGCGCGCTCGCTCGCTCACTGAGGCCGCCCGGGCAAAGCCCGGGCGTCCGGGCGACCTTTGGTCGCCCGCCTCAGTGAGCGAG
CGAGCGCGCAGAGAGGGAGTGCCAACTCCATCACTAGGGGTTCTTGAGTTAATGATTAACCCGCCATGCTACTTATCTACGTAGCC
ATGCTCTAGGTACCAGCGCACAGAGCCTTCTGCGTGGGGAAGCTCCTTGCTGCGTCATGGCTCAGCTATTCTCAGCCTCTCTCCTTTTA
TGGTGCCGGAAGCAGGCAGGCTGCTGCTTCTAGTCAGCGCACAGAGCCTTCTGCGTGGGGAAGCTCCTTGCTGCGTCATGGCTCAGC
TATTCTCAGCCTCTCTCCTTTATGGTGCCGGAAGCAGGCAGGCTGCTGCTTCTAGTCAGCGCACAGAGCCTTCTGCGTGGGGAAGCT
CCTTGCTGCGTCATGGCTCAGCTATTCTCAGCCTCTCTCCTTTATGGTGCCGGAAGCAGGCAGGCTGCTGCTTCTAGTCAGCGCACAGA
GCCTTCTGCGTGGGGAAGCTCCTTGCTGCGTCATGGCTCAGCTATTCTCAGCCTCTCTCCTTTATGGTGCCGGAAGCAGGCAGGCTG
CTGCTTCTAGAGCGCAGCAGAGCACATTAGTCACTCGGGGCTGTGAAGGGGCGGGTCTTGAGGGCACCCACGGGAGGGGAGCGAG
TAGGCGCGGAAGGCGGGCCTGCGGCAGGAGAGGGCGCGGGCGGGCTCTGGCGCGGAGCCTGGGCGCCGCAATGGGAGCCAGG
GCTCCACGAGCTGCCGCCACGGGCCCGCGCAGCATAAATAGCCGCTGGTGGCGGTTTCGGTGCAGAGCTCAAGCGAGTTCTCCCGC
AGCCGAGTCTCTGGGCTCTCTAGCTTACGCGGCGACGAGCCTGCCACACTCGTAAGCTCCTCCGGCACCGCACACCTGCCACTGCC
GCTGCAGCCGCCGGCTCTGCTCCCTTCGGCTTCTGCTCAGAGGAGTTCTTAGCCTGTTTCGGAGCCGACACCGACGACCAGACTAG
TGTCGCCACCATGGTGAGCAAGGGCGAGGAGCTGTTACCGGGGTGGTGCCCATCTGGTCGAGCTGGACGGCGACGTAACGGCCA
CAAGTTCAGCGTGTCCGGCGAGGGCGAGGGCGATGCCACCTACGGCAAGCTGACCCTGAAGTTCATCTGCACCACCGGCAAGCTGCCC
GTGCCCTGGCCACCCTCGTGACCACCCTGACCTACGGCGTGAGTGCTTACGCCGCTACCCCGACCACATGAAGCAGCAGCACTTCTT
CAAGTCCGCCATGCCCCAAGGCTACGTCCAGGAGCGCACCATCTTCTCAAGGACGACGGCAACTACAAGACCCGCGCCGAGGTGAAG
TTCGAGGGCGACACCTGGTGAACCGCATCGAGCTGAAGGGCATCGACTTCAAGGAGGACGGCAACATCTGGGGCACAAGCTGGAG
TAACTACAACAGCCACAACGTCTATATCATGGCCGACAAGCAGAAGAACGGCATCAAGGTGAACCTTCAAGATCCGCCACAACATCG
AGGACGGCAGCGTGACGCTCGCCGACCACTACCAGCAGAACACCCCATCGGGCAGCGCCCGTGTGCTGCCGACAACCACTACCT
GAGCACCCAGTCCGCCCTGAGCAAAGACCCCAACGAGAAGCGCGATCACATGGTCTGCTGGAGTTCGTGACCGCCGCGGGATCACT
CTCGCATGGACGAGCTGTACAAGTAAAGCGGGAATTCGATATCAAGCTTATCGATAATCAACCTCTGGATTACAAAATTTGTGAAAGA

TTGACTGGTATTCTTAACTATGTTGCTCCTTTACGCTATGTGGATACGCTGCTTAAATGCCTTTGTATCATGCTATTGCTTCCCCTATGGC
TTTCATTTTCTCCTCCTGTATAAATCCTGGTTGCTGTCTTTATGAGGAGTTGTGCCCGTTGTCAGGCAACGTGGCGTGGTGTGCACT
GTGTTTGCTGACGCAACCCCACTGGTTGGGGCATTGCCACCACCTGTCAGCTCCTTTCCGGGACTTTTCGCTTTCCCCTCCCTATTGCCA
CGGCGAACTCATCGCCGCTGCCTTGCCGCTGCTGGACAGGGGCTCGGCTGTTGGGCACTGACAATCCGTGGTGTGTCGGGGAA
ATCATCGTCTTTCTTGGCTGCTCGCCTGTGTTGCCACCTGGATTCTGCGCGGGACGTCCTTCTGTACGTCCCTTCGGCCCTCAATCCA
GCGGACCTTCTTCCCGCGGCTGCTGCCGGCTCTGCGCCTCTTCCGCTTTCGCTTCCGCCCTCAGACGAGTCGGATCTCCCTTGG
GCCGCTCCCCGCATCGATACCGTCGACTCGCTGATCAGCCTCGACTGTGCCTTCTAGTTGCCAGCCATCTGTTGTTGCCCTCCCCGT
GCCTTCTTGACCCTGGAAGGTGCCACTCCACTGTCTTCTAATAAAATGAGGAAATTCATCGCATTGTCTGAGTAGGTGTCATTC
TATTCTGGGGGGTGGGGTGGGGCAGGACAGCAAGGGGGAGGATTGGGAAGACAATAGCAGGCATGCTGGGGATGCGGTGGGCTCT
ATGGCTTCTGAGGCGAAAGAACCAGCTGGGGCTCGACTAGAGCATGGCTACGTAGATAAGTAGCATGGCGGGTTAATCATTAACTAC
AAGGAACCCCTAGTGATGGAGTTGGCCACTCCCTCTCTGCGCTCGCTCGCTACTGAGGCCGGGCGACCAAAGGTCGCCGACGCC
CGGCTTTGCCGGGCGCCTCAGTGAGCGAGCGAGCGCAGAGCTTTTTGCAAAGCCTAGGCCTCAAAAAAGCCTCCTCACTAC
TTCTGGAATAGCTCAGAGCCGAGGCGGCTCGCCCTCTGCATAAATAAAAAAATTAGTCAGCCATGGGGCGGAGAATGGGCGGAA
CTGGGCGGAGTTAGGGGCGGGATGGGCGGAGTTAGGGGCGGGACTATGGTTGCTGACTAATTGAGATGCATGCTTGCATACTTCTG
CCTGCTGGGGAGCCTGGGGACTTCCACACCTGGTTGCTGACTAATTGAGATGCATGCTTGCATACTTCTGCTGCTGGGGAGCCTGG
GGACTTCCACACCCTAACTGACACACATTCCACAGCTGCATTAATGAATCGGCCAACGCGCGGGGAGAGGCGTTTTCGCTATTGGGC
GCTTCCGCTTCTCGCTACTGACTCGCTGCGCTCGGTCGTTCCGGCTGCGGCGAGCGGTATCAGCTCACTCAAAGGCGGTAATACGG
TTATCCACAGAATCAGGGGATAACGCAGGAAAGAATGTGAGCAAAGGCCAGCAAAGGCCAGGAACCGTAAAAAGGCCGCGTT
GCTGGCGTTTTTCCATAGGCTCCGCCCCCTGACGAGCATCAAAAAATCGACGCTCAAGTCAGAGGTGGCGAAACCCGACAGGACTA
TAAAGATAACCAGGCGTTTTCCCTGGAAGCTCCCTCGTGCCTCTCTGTTCCGACCTGCCGTTACCGGATACCTGTCCGCTTTCTCC
CTTCGGGAAGCGTGGCGCTTCTCATAGCTCAGCTGTAGGTATCTCAGTTCGGTGTAGGTCGTTCCGCTCCAAGCTGGGCTGTGTGCAC
GAACCCCGTTTCAGCCGACCGCTGCGCCTTATCCGGTAACTATCGTCTTGTAGTCAACCCGGTAAGACACGACTTATCGCCACTGGC
AGCAGCCACTGGTAACAGGATTAGCAGAGCGAGGTATGTAGGCGGTCTACAGAGTCTTGAAGTGGTGGCCTAACTACGGCTACT
AGAAGAACAGTATTTGGTATCTGCGCTGCTGTAAGCCAGTTACCTTCGGAAAAAGAGTTGGTAGCTCTTGATCCGGCAAACAACCCAC
CGCTGGTAGCGGTGGTTTTTTTGTGCAAGCAGCAGATTACGCGCAGAAAAAAGGATCTCAAGAAGATCCTTTGATCTTTTCTACGG
GGTCTGACGCTCAGTGAACGAAAACTCACGTTAAGGGATTTTGGTCATGAGATTATCAAAAAGGATCTTACCTAGATCCTTTAAAT
TAAAAATGAAGTTTTAAATCAATCTAAAGTATATAGATAAACTTGGTCTGACAGTTACCAATGCTTAATCAGTGAGGCACCTATCTCA
GCGATCTGTCTATTTGTTTCATCCATAGTTGCCTGACTCCCCGTCGTGTAGATAACTACGATACGGGAGGGCTTACCATCTGGCCCCAGT
GCTGCAATGATACCGCGAGACCCACGCTACCGGCTCCAGATTTATCAGCAATAAACAGCCAGCCGGAAGGGCCGAGCGCAGAAGT
GGTCTGCAACTTTATCCGCCTCCATCCATTAATTGTTGCCGGAAAGCTAGAGTAAGTAGTTCGCCAGTTAATAGTTTTCGCAACGTTGT
TGCCATTGCTACAGGCATCGTGGTGTACGCTCGTCTGTTGGTATGGCTTCATTAGCTCCGTTCCCAACGATCAAGGCGAGTTACAT
GATCCCCATGTTGTGCAAAAAGCGGTTAGCTCCTTCCGCTCCTCCGATCGTTGTGAGAAGTAAGTTGGCCGAGTGTATCACTCATG
GTTATGGCAGCACTGCATAATTCTTACTGTATGCCATCCGTAAGATGCTTTTCTGTGACTGGTGAAGTACTCAACCAAGTCAATTCTGA
GAATAGTGTATGCGGCGACCGAGTTGCTCTTCCCGGCGTCAATACGGGATAAATACCGCGCCACATAGCAGAAGTTTAAAAGTGCTCA
TCATTGGAACGTTCTTCCGGGCGAAAACTCTCAAGGATCTTACCCTGTTGAGATCCAGTTCGATGTAACCCACTCGTGACCCAACT
GATCTTACGATCTTTTACTTTCACCAGCGTTTCTGGGTGAGCAAAAACAGGAAGGCAAAATGCCGCAAAAAAGGGAATAAGGGCGAC
ACGGAATGTTGAATACTCATACTTCTCTTTTCAATATTATTGAAGCATTATCAGGGTTATTGTCTCATGAGCGGATACATATTTGAA
TGTATTTAGAAAAATAACAAATAGGGGTTCCGCGCACATTTCCCCGAAAAGTGCCACCTGACGTCTAAGAAACCATTTATCATGAC
ATTAACCTATAAAAATAGGCGTATCAGGAGCCCTTTCGTCGCGCTTTCGGTGTGACGGTGAACCTCTGACACATGCAGCTCC
CGGAGACGGTCACAGCTTGTCTGTAAGCGGATGCCGGGAGCAGACAAGCCCGTCAGGGCGGTCAGCGGGTGTGGCGGGTGTCCG
GGCTGGCTTAACTATGCGGCATCAGAGCAGATTGACTGAGAGTGCACCATTGACGCTCTCCCTATGCGACTCCTGCATTAGGAAGC
AGCCAGTAGTAGGTTGAGGCCGTTGAGCACCCGCCGCAAGGAATGGTGCATGCAAGGAGATGGCGCCAACAGTCCCCGGCCA
CGGGGCTGCCACCATACCACGCCGAAACAAGCGCTCATGAGCCGAAGTGGCGAGCCGATCTTCCCATCGGTGATGTCGGCGAT
ATAGGCGCCAGCAACCGCACCTGTGGCGCCGGTGTATGCCGCCACGATGCGTCCGGCGTAGAGGATCTGGCTAGCGATGACCCTGCT
GATTGGTTCCGCTGACCATTTCCGGGTGCGGGACGGCGTTACCAGAACTCAGAAGGTTCTCAACCAAACCGACTCTGACGGCAGTT
TACGAGAGAGATGATAGGGTCTGCTTCAAGTAAAGCCAGATGCTACACAATTAGGCTTGTACATATTGTCGTTAGAACGCGGCTACAATTA
ATACATAACCTTATGTATCATACACATACGATTTAGGTGACACTATAGAATACACGGAATTAATTC

S2) Sequence of GFAP-UPRT-mKate2 plasmid



CCTGCAGGCAGCTGCGCGCTCGCTCGCTCACTGAGGCCGCCCGGGCAAAGCCCGGGCGTTCGGGCGACCTTTGGTCGCCCCGGCCTCAGT
GAGCGAGCGAGCGCGCAGAGAGGGAGTGGCCAACTCCATCACTAGGGGTTCTTCTAGACAACCTTTGTATAGAAAAGTTGAACATATC
CTGGTGTGGAGTAGGGGACGCTGCTCTGACAGAGGCTCGGGGGCCTGAGCTGGCTCTGTGAGCTGGGGAGGAGGCAGACAGCCAGG
CCTTGTCTGCAAGCAGACCTGGCAGCATTGGGCTGGCCGCCCCAGGGCCTCCTTTCATGCCAGTGAATGACTCACCTTGGCACAG
ACACAATGTTGCGGGTGGGCACAGTGCCTGCTTCCCGCCGACCCAGCCCCCTCAAATGCCTCCGAGAAGCCCATTGAGCAGGGG
GCTTGCATTGCACCCAGCCTGACAGCCTGGCATCTTGGGATAAAAGCAGCACAGCCCCCTAGGGGCTGCCCTTGTGTGGCGCCAC
CGGCGGTGGAGAACAAGGCTCTATTCAGCCTGTGCCAGGAAAGGGGATCAGGGGATGCCAGGCATGGACAGTGGGTGGCAGGGG
GGGAGAGGAGGGCTGTCTGCTTCCAGAAGTCCAAGGACACAAATGGGTGAGGGGAGAGCTTCCCATAGCTGGGCTGCGGCCCAA
CCCCCCCCCTCAGGCTATGCCAGGGGGTGTGGCAGGGGCACCCGGGCATCGCCAGTCTAGCCCACTCCTTCATAAAGCCCTCGCATC
CCAGGAGCGAGCAGAGCCAGAGCAGGTTGGAGAGGAGACGCATCACCTCCGCTGCTCGCCAAGTTTGTACAAAAAAGCAGGCTGCCA
CCATGGCGCAGGTCCCAGCGAGCGGAAAGCTCCTTGTGATCCCCGATATTGACAAACGACCAGGAAGAAAGCATTCTCCAGGACAT
CATCACGAGGTTTCCCAATGTGGTGCTCATGAAGCAGACGGCTCAGCTTCGAGCGATGATGACCATCATTCGTGATAAAGAAACCCG
AAGGAAGAATTCGTCTTACGCCGACCGCTGATTGCTCCTCATCGAAGAAGCTTTGAACGAACTGCCGTTGAAAAGAAGGAAGT
GACAACCCCTCTGGATGTGTACATACCATGGAGTTTCTTCTATTCCAAGATCTGTGGCGTCTCGATTGTGAGAGCTGGCGAGTCGATGG
AAAGCGGCTTGGCGGCAGTTTGGCGGGCTGCCGATCGGGAAAATCCTCATCCAGAGAGACGAAACAACCTGCGGAGCCTAAGCTGA
TCTACGAGAAGCTGCCTGCCGACATTAGAGATCGCTGGGTGATGCTGCTAGATCCGATGTGCGCGACGGCGGGCAGTGTGTGCAAAG
CGATCGAGGTCCTCCTGAGGCTCGGCGTGAAGGAAGAGAGAATCATTTTCGTCAACATTTTGGCTGCTCCCCAAGGCATTGAACGTGT
TTCAAGGAATACCCGAAAGTCCGCATGGTCACTGCTGCTGTTGACATCTGCCTGAACTCGAGGTAACATCGTCCCCGGCATTGGTGA
TTTCGGTGACCGGTAATTTGGAACCATGTTGTCTGGTGGCGGAGGCTCGGGCGGAGGTGGGTGCGGTGGCGGGCGGATCAATGGTGA
CGAGCTGATTAAGGAGAACATGCACATGAAGCTGTACATGGAGGGCACCGTGAACAACCACTTCAAGTGCACATCCGAGGGCGA
AGGCAAGCCCTACGAGGGCACCCAGACCATGAGAATCAAGGCGGTGAGGGGCGGCCCTCCTCCCTTCGCTTCGACATCCTGGCTACC
AGCTTCATGTACGGCAGCAAAACCTTCATCAACCACACCCAGGGCATCCCCGACTTCTTTAAGCAGTCTTCCCCGAGGGCTTCACATGG
GAGAGAGTACCCACATACGAAGACGGGGCGTGTGACCGCTACCCAGGACACCAGCCTCCAGGACGGCTGCCTCATCTACAACGTCA
AGATCAGAGGGGTGAACTTCCCATCCAACGGCCCTGTGATGCAGAAGAAAACACTCGGCTGGGAGGCCTCCACCGAGACCCTGTACCC
CGCTGACGGCGGCCTGGAAGGCAGAGCCGACATGGCCCTGAAGCTCGTGGGCGGGGGCCACCTGATCTGCAACTGAAGACCACATA
CAGATCCAAGAAACCCGTAAGAACCTCAAGATGCCCCGGCTACTATGTGGACAGAAGACTGGAAAGAATCAAGGAGGCCGACAA
AGAGACCTACGTCGAGCAGCAGAGGTGGCTGTGGAGTGGGAATTTACGCTATGTATAAATCCTGGTTGCTGTCTTTATGAGGAGT
TGTGGCCCGTTGTGAGCAACGTGGCGTGGTGTGACTGTGTTTGTGACGCAACCCCACTGGTTGGGGCATTGCCACCACCTGTCAG
CTCCTTCCGGGACTTTCGCTTCCCTCCTATTGCCACGGCGGAACATCGCCGCTGCCTTCCCGCTGCTGGACAGGGGCTCGG

CTGTTGGGCACTGACAATCCGTGGTGTGTCGGGGAAGCTGACGTCCTTTCCATGGCTGCTCGCCTGTGTTGCCACCTGGATTCTGCG
CGGACGTCCTTCTGCTACGTCCCTTCGGCCCTCAATCCAGCGGACCTTCTTCCCGCGCCTGCTGCCGGCTCTGCGGCCTTCCGCG
TCTTCGCCTTCGCCCTCAGACGAGTCGGATCTCCCTTTGGGCCGCTCCCCGCATCGGGAATTCCTAGAGCTCGTGATCAGCCTCGACT
GTGCCCTTCTAGTTGCCAGCCATCTGTTGTTTCCCCCTCCCCGTGCCTTCTTGACCCTGGAAGGTGCCACTCCCCTGTCTTTCTAAT
AAAATGAGGAAATTGCATCGCATTGTCTGAGTAGGTGTCTATTCTATTCTGGGGGGTGGGGTGGGGCAGGACAGCAAGGGGGAGGATT
GGGAAGAGAATAGCAGGCATGCTGGGGAGGGCCGAGGAACCCCTAGTGATGGAGTTGGCCACTCCCTCTCTGCGCGCTCGCTCGCT
CACTGAGGCCGGGGCGACCAAAGGTGCCCCGACGCCGGGCTTTGCCCGGGCGGCCTCAGTGAGCGAGCGAGCGCGCAGCTGCCTGCA
GGGGCGCCAGATACTGCGACCTCCCTAGCAAACCTGGGGCACAGATGAACCCAGCTTCTTGTAACAACCGATAATCAACCTCTGGATTA
CAAAATTTGTGAAAGATTGACTGGTATTCTTAACTATGTTGCTCCTTTGGATACGCTGCTTAAATGCCTTTGTATCATGCTATTGCTCCC
GTATGGCTTTCATTTTCTCCTCCTTGATTTTCTCCTTACGCATCTGTGCGGTATTTACACCGCATACGTCAAAGCAACCATAGTAAGCG
GCGCATTAAAGCGCGGGCGGGGTGGTGGTTACGCGCAGCGTGACCGCTACACTTGCCCGCCGCTCCTTTCGCTTCTTCCCTTCTTTCT
CGCCACGTTCCCGGCTTCCCCGCTCTGATGCGGTGCGCCCTGTAGCGCCTAGAAGCTCTAAATCGGGGGCTCCCTTAGGGTTC
GATTTAGTGCTTACGGCACCTCGACCCAAAAAACTTGATTTGGGTGATGGTTCACGTAGTGGGCCATCGCCCTGATAGACGGTTTTTC
GCCCTTGACGTTGGAGTCCACGTTCTTAACTAGTGGACTCTTGTCCAAACTGGAACAACACTCAACTCTATCTCGGGCTATTCTTTGA
TTTATAAGGGATTTTCCGATTTCCGGTCTATTGGTTAAAAAATGAGCTGATTTAACAAAAATTTAACCGGAATTTTAAACAAATATTAAC
GTTTACAATTTTATGGTGCCTCTCAGTACAATCTGCTCTGATGCCGCATAGTTAAGCCAGCCCCGACACCCGCCAGTGACCGTCTGCCT
CGTGATAATGTGCGGAATGCTTCAATAATATTGAAAAGGAAGAGTATGAGTATTCAACATTTCCGTGTCGCCCTTATCCCTTTTTTG
CGGCATTTTGCCTTCTGTTTTGCTCACCCAGAAACGCTGGTAAAAGTAAAAGATGCTGAAGATCAGTTGGGTGCACGAGTGGGTAC
ATCGAACTGGATCTCAACAGCGGTAAGATCCTTGAGAGTTTTCGCCCCGAAGAACGTTTTCCAATGATGAGCACTTTTAAAGTTCTGCTA
TGTGGCGCGGTATTATCCCGTATTGACGCCGGGCAAGAGCAACTCGGTGCGCCGATACACTATTCTCAGAATGACTTGGTTGAGTACTC
ACCAGTCACAGAAAAGCATCTTACGGATGGCATGACAGTAAGAGAATTATGCAGTGCTGCCATAACCATGAGTGATAACACTGCGGCC
AACTTACTTCTGACAACGATCGGAGGACCGAAGGAGCTAACCCTTTTTTGCACAACATGGGGGATCATGACACCCGCTGACGCGCCCT
GACGGGCTTGTCTGCTCCCGCATCCGCTTACAGACAAGCTCCGGGAGCTGCATGTGTGAGAGTTTTACCGTCATCACCAGAACGCG
CGAGACGAAAGGACGCTATTTTTATAGGTTAATGTATGATAATAATGGTTTCTTAGACGTCAGGTGGCACTTTTCGGGGAGAACCCC
TATTTGTTATTTTTCTAAATACATTCAAATATGTATCCGCTCATGAGACAATAACCCTGATATAACTCGCCTTGATCGTTGGGAACCGGA
GCTGAATGAAGCCATACCAAACGACGAGCGTGACACCACGATGCCTGTAGCAATGGCAACAACGTTGCGCAAACCTATTAAGTGGCGAA
CTACTTACTCTAGCTTCCCGCAACAATTAATAGACTGGATGGAGGCGGATAAAGTTGCAGGACCACTTCTGCGCTCGGCCCTCCGGC
TGGCTGGTTTATTGCTGATAAATCTGGAGCCGTGAGCGTGGAAGCCGCGGTATCATTGCAGCACTGGGGCCAGATGGTAAGCCCTCC
CGTATCGTAGTTATCTACACGACGGGGAGTCAGGCAACTATGGATGAACGAAATAGACAGATCGCTGAGATAGGTGCCTCACTGATTA
AGCATTGGTAACTGTCAGACCAAGTTTACTCATATATACTTTAGATTGATTTAAAACCTCATTTTTAAATTTAAAAGGATCTAGGTGAAGAT
CCTTTTTGATAATCTCATGACCAAATCCCTAACGTGAGTTTTGTTCCACTGAGCGTCAGACCCCGTAGAAAAGATCAAAGGATCTTC
TTGAGATCCTTTTTTCTGCGCGTAATCTGCTGCTTGCAAAACAAAAAACACCGCTACCAGCGGTGGTTTGTGGCCGATCAAGAGCT
ACCAACTCTTTTTCCGAAGGTAAGTGGCTTACGACAGAGCGCAGATACCAAATACTGTTCTTCTAGTGTAGCCGTAGTTAGGCCACCACTT
CAAGAACTCTGTAGCACCGCCTACATACTCGCTCTGTAATCCTGTTACCAGTGGCTGCTGCCAGTGGCGATAAGTCGTGCTTACCGG
GTTGGACTCAAGACGATAGTTACCGGATAAGGCGCAGCGTCCGGCTGAACGGGGGGTTCGTGCACACAGCCAGCTTGGAGCGAAC
GACCTACACCGAACTGAGATACCTACAGCGTGAGCTATGAGAAAGCGCCACGCTTCCGAAGGGAGAAAGGCGGACAGGTATCCGGT
AAGCGGCAGGGTCGGAACAGGAGAGCGCACGAGGGAGCTTCCAGGGGAAACGCCTGGTATCTTTATAGTCTGTGCGGTTTCGCCA
CCTCTGACTTGAGCGTCGATTTTTGTGATGCTCGTCAGGGGGCGGAGCCTATGGAAAAACGCCAGCAACGCGGCCTTTTTACGGTTCC
TGGCCTTTTGTGCTGCCTTTTGTCTCACATGT

Supplementary Figures

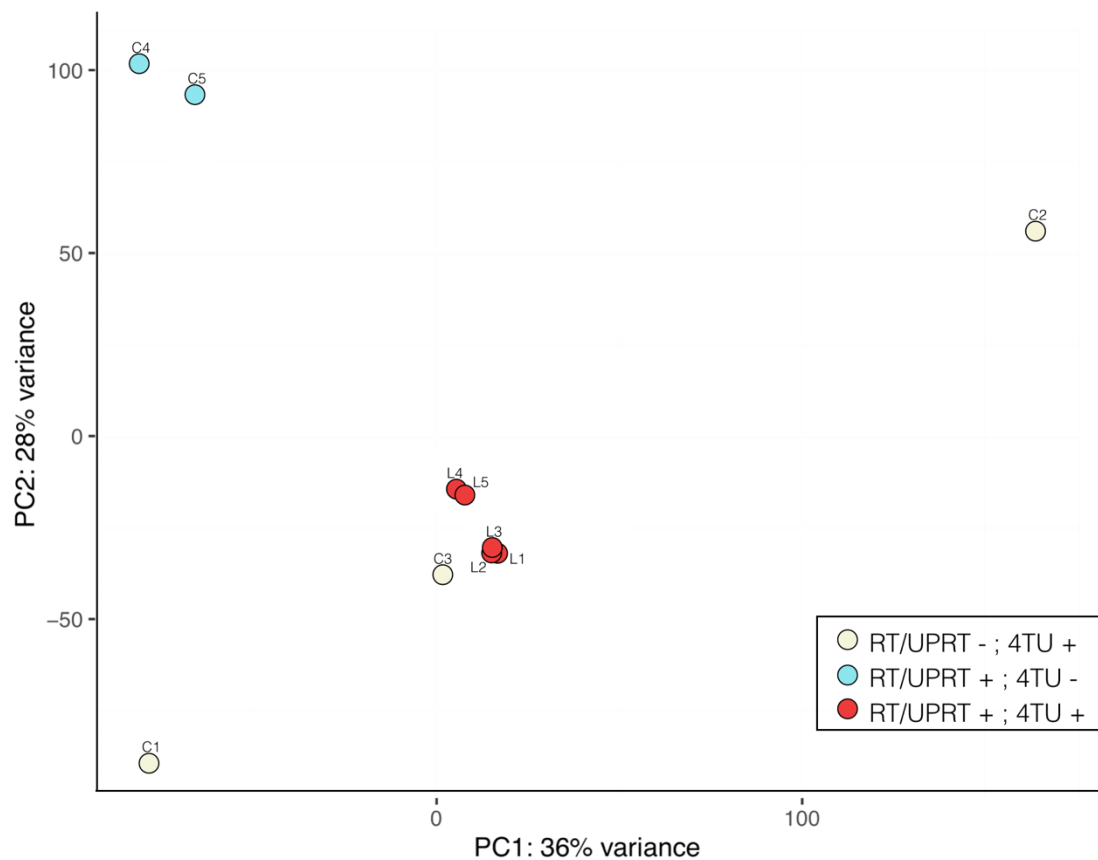


Fig S1: Unspecific genes after pulldowns are noisy in nature Principal component analysis displaying strong clustering of all double-precipitated RNAs, whereas controls are widely spread, indicating a highly random background. n=5 (samples), n = 4 (inputs).

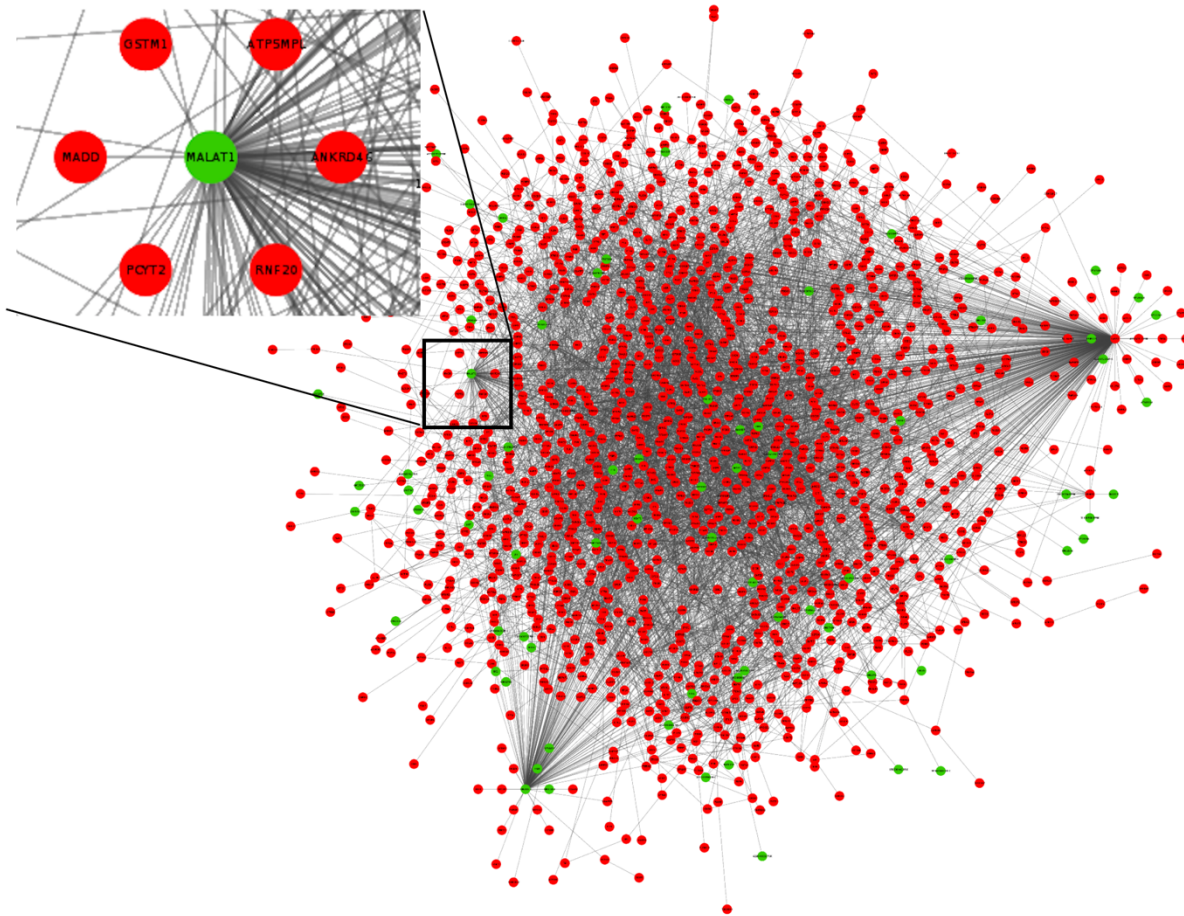


Fig S2: Interactions between transferred lncRNAs and the synaptic RNAome. 357 lncRNAs (green) that are transferred from astrocytes to neurons interact in a multitude of ways with 1460 synaptic mRNAs (red). The zoomed part depicts the prominent lncRNA MALAT1 with its many connections.

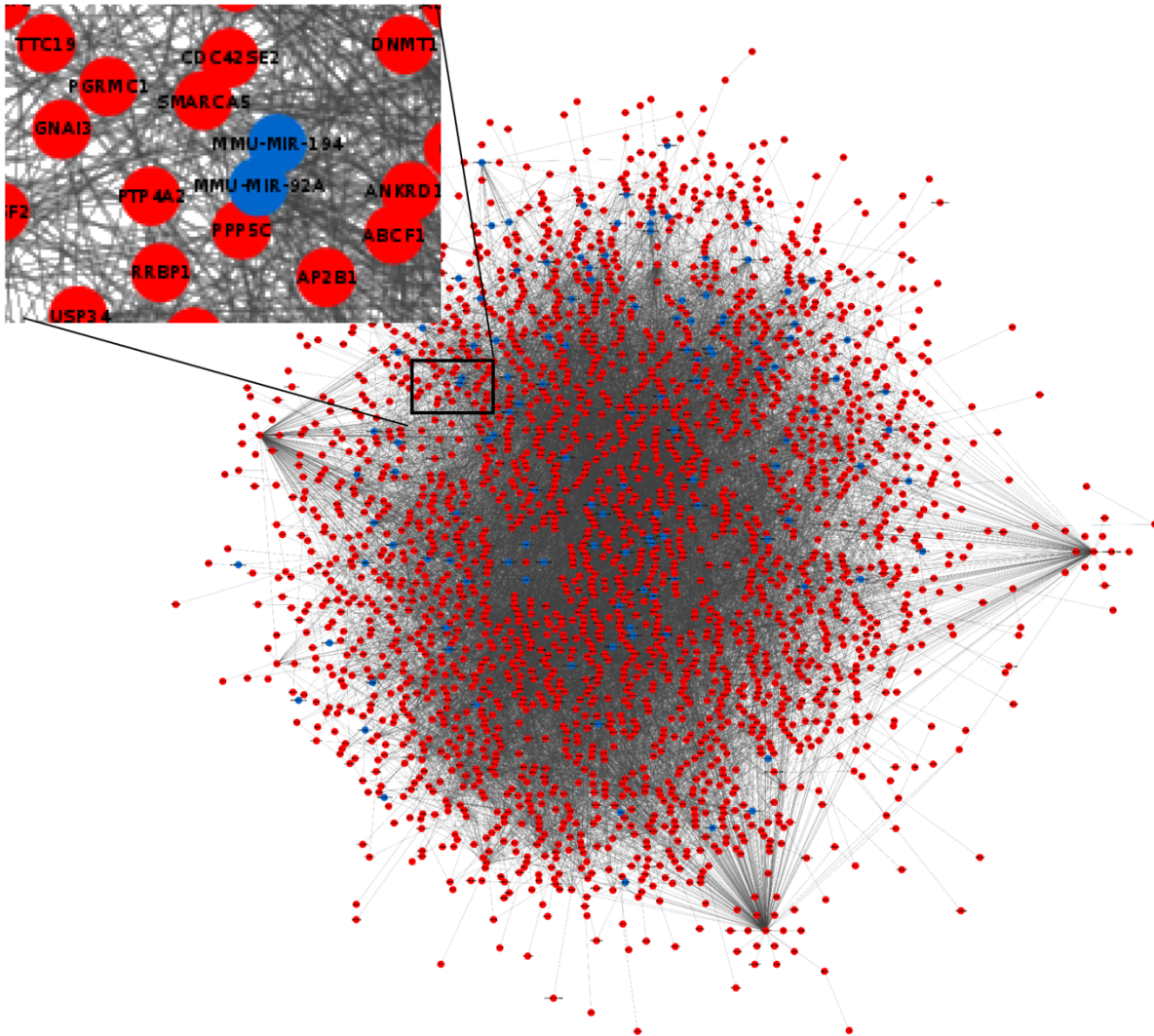


Fig S3: Interactions between astrocytic exosomal miRNAs and the top 25% InsUREns genes. 145 miRNAs that were published to be found in astrocytic exosomes, regulate a huge amount of the most frequently transferred mRNAs. The zoomed part depicts two exemplary astrocytic exosome miRNAs with their targets.

Discussion

Importance of local translation in diseases

Local translation is at the center of plasticity. Without it, changes in synaptic weight that are made to reflect novelty in our lives would not be durable. We have seen how logistical problems of a neuron are solved by its decentralized protein synthesis and we have seen how many different transcripts are located inside neurites to allow this process to be spatially precise.

Defective local translation is increasingly linked to the etiology and symptoms of diseases. In an ALS mouse model that uses FUS mutation, local translation in axons was decreased (López-Erauskin et al., 2018). When neurons are exposed to A β 1-42, they transport an increased amount of the ATF4-mRNA into their axons, where it is translated and retrogradely brought to the nucleus, inducing cell death (Baleriola et al., 2014).

Htt protein was shown to support localization of dendritic RNAs. If Htt however contains an irregular polyglutamine extension - as presented in Huntington's disease - it is suggested to disturb the transport of granules containing RNAs towards post-synapses, effectively causing symptoms of Huntington's disease (Savas et al., 2010).

Synaptopathies are neurological diseases that develop due to abnormalities at synapses. Recently, diseases and disorders with unclear origination were considered to have a synaptopathologic etiology, including schizophrenia (Hayashi-Takagi, 2017) and autism spectrum disorder (Wang et al., 2018). Similarly in Alzheimer's, a devastating neurodegenerative disease, the synapse degeneration starts in the early phase and precedes neuronal death (Arendt, 2009; Kerrigan and Randall, 2013). Deeper understanding of local translation will therefore help us to elucidate the molecular basis of synaptopathologies.

Identification of synaptic RNAs

We have seen the variety of synaptic RNAs and how many interactions they can have with one another. To gain access to pure neuronal synapses, without influences of other cell types, I presented a novel tool, with which we discovered many mRNAs and lncRNAs that were undetectable in synaptosomes.

This was achieved by cutting whole neurites instead of isolating mere synaptic terminals. In addition, we found a lot more lncRNAs than in synaptosomes. Both findings are indicative of a preference of certain transcripts to local translation hotspots in neurites - rather than to individual synapses.

In chapter 1 we accomplished the first analysis of the combined total and small mouse hippocampal synaptic RNAome. The hippocampus is a key area for forming memories (Lisman et al., 2017), hence the findings presented here are of particular interest for the underlying local transcriptome of memory formation.

Identifying key players and their interaction partners will allow to develop hypotheses about specific RNA candidates and their roles during LTP and LTD events.

The composition of the local transcriptome depends on the isolation technique applied and on the brain area sampled; nonetheless there seems to be a consistent pool of RNAs, found across all experiments (von Kügelgen and Chekulaeva, 2020).

Interestingly, miRs commonly found between synaptosomes and microfluidic chambers are often important for developmental processes; miR-128-3p, for example, promotes neuronal differentiation (Zhang et al., 2016). Members of the let-7 miR group are necessary to suppress cell division and to promote differentiation (Fairchild et al., 2019; Song et al., 2015; Zhao et al., 2010). The let-7 miRs are crucial to neuronal survival; their name derives from *lethal*, since loss of let-7 proved to be deadly, when it was first discovered in *C. elegans* (Reinhart et al., 2000). My findings underline this and show that neurons supply themselves with let-7 miRs, as they are present in the SNIDER samples.

Advantages of SNIDER

With SNIDER I have introduced a method to isolate post-synaptic and pre-synaptic RNAs as well as transcripts located in neurites; a feature not possible with synaptosomes.

Overall, the isolation of a chamber's RNA can be done in less than 30min, compared to several hours of ultracentrifugation necessary for synaptosomes, improving RNA quality for downstream applications. In contrast to hanging inserts, the chambers also allow visual inspection of synapse formation.

By advancing the microfluidic chamber design to be cut-able, I made it possible to retain its three hallmark features for RNA isolation:

first, one can effectively study synapses without influence of other cell types. The very narrow entrances of microgrooves prevent cells from entering and hydrostatic pressures in the chamber minimize diffusion into the microgrooves, thereby greatly reducing the amount of EVs from glia cells reaching the synapses inside. This makes filtering for putative glia RNA obsolete, allowing the detection of unexpected transcripts.

Second, the continuous perfusion flow allows the targeted treatment of synapses residing in the perfusion channel, without affecting the soma. As I have demonstrated in Chapter 2, SNIDER can thus be used for the investigation of miR inhibition in neurites.

Third, laminar flow properties and the duration of hydrostatic pressure allow for individual transduction of the two pools of neurons. We showed that KCl stimulation in the chambers results in activity-dependent changes of the local transcriptome. Using optogenetic tools in this way would help to study the local transcriptome under stimulation, as I lay out further in the *Outlook* section.

Interaction of synaptic RNAs

The regulatory loops between mRNAs and ncRNAs can either lead to inhibition of translation or degradation of the mRNAs. In part, this depends on the endogenous binding competition between ncRNAs. Certain RNA types, such as circRNAs or some lncRNAs are known to sponge miRs, essentially lifting their inhibition on neurons.

RNA sequencings always present a snapshot of the transcriptome; to state the exact nature of each RNA interaction, experiments have to focus on single candidates.

We still have to imagine the local transcriptome to be quite dynamic; RNAs are being shuttled between neurites and the soma in a conveyer belt fashion, fittingly called the sushi belt model (Doyle and Kiebler, 2011). It describes how RNA granules – complexes formed of RNA binding proteins, mRNA and ncRNA – are transported via motor proteins on microtubules along the neurites. During transport, packaging is often so condensed that transported mRNAs are not available for translation (Wells, 2006).

This means that there are plenty of RNA granules passing by and through local translational hot spots constantly, possibly influencing their interactions. miRs that are transported in a granule could bind a somatic mRNA only incompletely, causing transient inhibition of translation and increasing RNA stability (Oh et al., 2013). While passing through residual RNAs, such miRs might find new targets with more complete hybridization potential, thus potentially switching from inhibition of a somatic mRNA to degradation of a synaptic one. Likewise, the other granule's components, RNA binding proteins and lncRNAs, might detach at any point in time from the granule to enrich a local transcriptome.

On the other side, RNAs are being exchanged between cells as described in Chapter 3. Even axon terminals themselves can actively secrete miRs, presumably for uptake at the postsynapse (Xu et al., 2013). It was further demonstrated that those miRs are bound with different affinities to Ago2 – some miRs were bound almost completely to it, such as miR-26a-5p, mir-128-3p, 99a-5p, 30a-5p while other miRs just to a certain extent (Xu et al., 2013). Thus, the type of interaction of uptaken and localized RNA might be determined by how the donor cells packages the secreted RNA.

It would be of great interest to see if there are differences among the isoforms of synaptic transcript in terms of their 3' UTR and the resulting impact on miR binding.

Likewise, secondary structures of mRNA could reveal available stretches for regulation as well as other parts that are shielded by self-hybridization. Notably, I showed longer 3' UTR regions in transferred RNAs, indicative of neurite located RNAs and of additional forms of regulation compared to cytosol mRNAs (Tushev et al., 2018).

Intercellular origin of synaptic RNAs

Neurons are capable of supplying themselves with RNAs for local translation; otherwise, *in vitro* experiments could not show the establishing of functional synapses under the exclusion of other cell-types (Taylor et al., 2010). However, cell cultures differ substantially from the actual *in vivo* situation.

Neurons *in vitro* only have around 100-200 synapses, even after three weeks in culture (Cullen et al., 2010). Furthermore, neurobasal medium contains 25mM of glucose, whereas in healthy humans the concentration is a tenth of that (Bardy et al., 2015). Neurons are primarily fueled by glucose; it thus stands to reason that such an unphysiological amount of glucose could prompt them to overproduce RNAs and proteins greatly beyond any *in vivo* situation. While I worked on the InSUREns method, I saw a vast increase in transferred RNAs only after I switched to BrainPhys medium, which contains physiological glucose levels (Bardy et al., 2015).

Finally, there are time-constraints a self-sufficient neuron would face in trying to support its several thousand synapses constantly with RNAs;

transport of somatic mRNAs into dendrites happens at a slow pace of around 0.03mm/h (Akbalik et al., 2017). Consequently, a recent computer simulation calculated that it would take a whole day to replace the transcriptome of the dendritic tree (Fonkeu et al., 2019). Similarly, axonal transport can be rather slowly with around 0.05mm/h (Terada et al., 1996) - although there is also fast axonal transport with around 10mm/h (Jasmin et al., 1988).

Through the architecture of the tripartite synapse, astrocytes could supply local RNA pools much faster and more time-sensitive than the neuron itself (Fig 1).

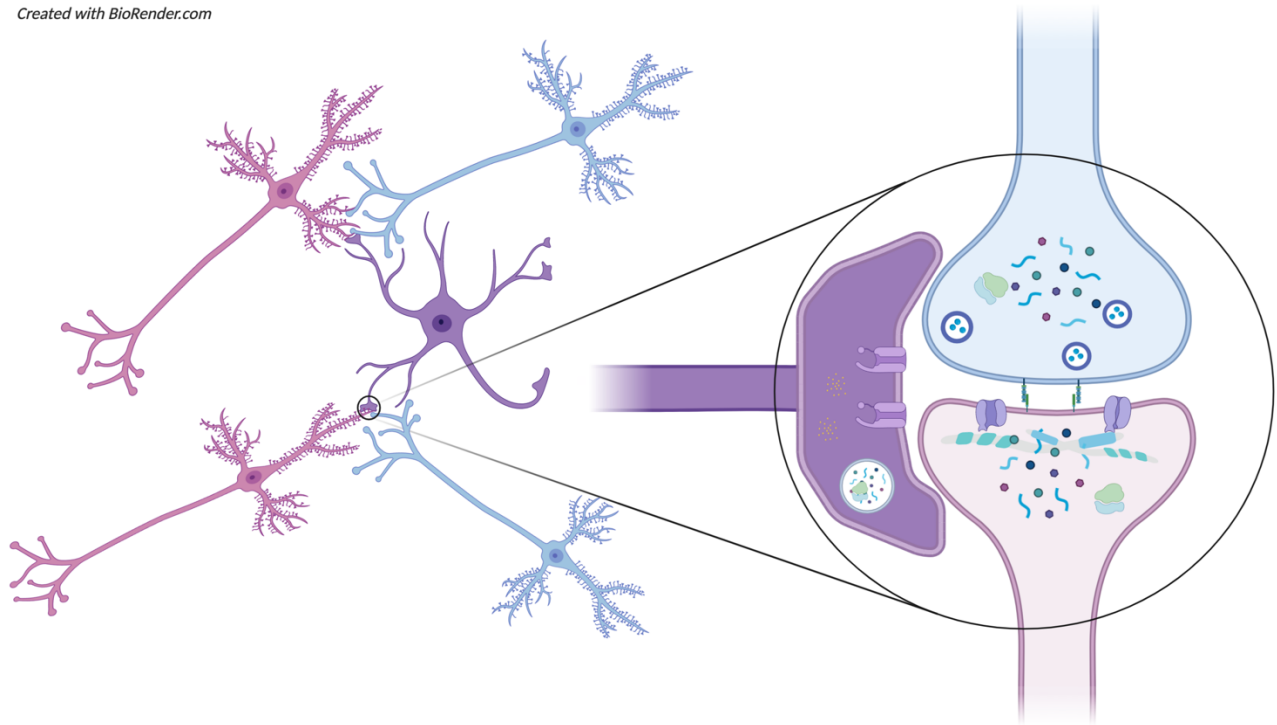


Fig 1: Anatomy of tripartite synapses. Astrocytes possess multiple endfeet that are in close contact with synapses, where they influence synapses, e.g., by glutamate uptake, secretion of gliotransmitter and ATP.

For all these reasons, I suggest that intercellular RNA transport could be essential for proper synaptic function. Transport of astrocytic RNAs to neurons has been shown in Chapter 3. Even though we have not directly proven transfer at the synapse level, our results point strongly towards a cell-wide uptake of astrocytic RNAs, including at dendrites and axons. We saw ribotag protein expressed throughout the soma and the neurites. We also observed the uptake of EVs along neurites with two staining strategies. And a third of the most frequently transferred RNAs were found in dendrites and axons (Fig 3D, Chapter 3).

At the same time, we have observed in total several thousands of RNAs being transferred, many more than found at the synapse. Therefore, I propose at least two purposes of RNA transfer; to support neurons with a broad range of RNAs, potentially for homeostasis - and to specifically supply local translation pools. Depending on the immediate vicinity to subparts of neurons, subparts of astrocytes could behave differently. Astrocytic membrane patches closer to the neuronal cytosol might secrete ADEVs that carry primarily transcripts regulating DNA transcription, whereas astrocytic end feet would secrete ADEVs with transcripts for RNA processing and splicing genes. As laid out in Chapter 3's discussion, astrocytic end-feet are highly responsive to synaptic activity and contain multiple mRNAs. Additionally, there are mechanisms in place to keep pre-packed EVs at specific parts of the astrocytic membrane.

InSUREns

To study the contribution of glial RNAs to the neuronal transcriptome I developed a technique that allows the identification of astrocytic RNAs that are shipped to neurons to be translated. I combined and optimized protocols for both pulldowns respectively, improving yields and signal-to-noise ratios greatly.

The modularity of InSUREns makes it applicable to any two cell-types and any proteins for pulldown, as laid out further in the *Outlook* section.

There were other conceivable ways to obtain transferred RNAs, yet InSUREns has advantages over all of them. One way would have been to let neurons express a reporter and astrocytes express UPRT. It would then be possible to FACS-sort the neurons based on their fluorescence and subsequently perform the 4TU-pulldown. Similarly, synaptosomes could have been generated, with a prior AAV injection for astrocytic UPRT expression. Then a 4TU-pulldown would also leave only astrocytic RNAs that ended up in synaptosomes.

However, both those alternatives would lose information: before neurons can be FACS-sorted, they have to undergo rough protease and tissue disruption protocols, during which most neurites get lost. In synaptosomes all RNAs uptaken outside of the axon terminal would be lost. And although both alternatives would require only one pulldown, they would not allow statements about the fate of transferred RNAs; it could be that some transferred RNAs end up in lysosomes for degradation. With InSUREns on the other hand, we know the uptaken RNA is about to be translated, as we detect it only if it is loaded onto ribosomes.

Means of RNA transport

We present strong evidence here that RNAs are trafficked via lipid vesicles. Yet, there are several other mechanisms how cells could exchange RNAs.

Gymnosis, a process in which RNAs without packaging are internalized in their naked form (Stein et al., 2010), has not been widely described for vertebrate neurons and would bode severe danger; in case of neuronal injury, dying nerve cells would leak their RNAs in an unregulated manner, thereby throwing off the transcriptome of nearby neurons completely and suddenly.

The widescale RNA transfer over large cell-cell contacts, called tunneling nanotubes (Ariazi et al., 2017) could be problematic, too. Nanotubes at synaptic membranes would dilute changes in electric potential. Moreover, tunneling nanotubes are less flexible. They need to be constructed first, with many parallel running cytoskeletal fibers, hence they could not react to quick synaptic events. Nonetheless, miR transport through much smaller gap junctions has been described before (Mayorquin et al., 2018).

Conclusively, it is possible that RNAs detected by InSUREns were partially transferred via different routes, though these alternative passages pose restrictions.

ADEVs as a way to transfer RNAs

We observed an increase of RNA concentration in the medium of long-term cultures. This led us to believe that extracellular vesicles could constitute the main way of shipping RNAs. Neuroprotective proteins like neuroglobin, are already known to be transported in such fashion from astrocytes to neurons (Venturini et al., 2019). Also, an increasing number of studies, as recently reviewed (Gomes et al., 2020), highlight ADEVs as a widely-used way to signal among cells in the nervous system.

Ribosomal proteins have been detected in EVs before (Morhayim et al., 2015) and by tracking labelled ribosomes in ADEVs we observed their internalization by neurons, parallel to what has been shown for ribosome transfer from Schwann cells into axons (Müller et al., 2018).

We substantiated ADEV uptake by a second imaging experiment with a membrane-labeling dye. Moreover, we confirmed the majority of InSUREns genes to be present in ADEVs, strongly suggesting ADEV-mediated transfer. The cargo of ADEVs varies depending on the stimulation of astrocytes, ranging from miRs that are detrimental to neurons under IL-1 β influence, to neuroprotective proteins under oxidative stress (Upadhyaya et al., 2020). ATP stimulation enhances ADEV secretion (Datta Chaudhuri et al., 2020) and releases protein and factors for neurite outgrowth and dendritic branching (Upadhyaya et al., 2020). The ADEVs we obtained can thus only partially resemble the physiological state; especially since they were cultured without neurons. It would be intriguing to research the changes of ADEV RNAomes depending on different stimuli and how those RNAs change recipient neurons' properties.

It was not necessary for our initial hypothesis to differentiate between the different types of EvV. For a deeper understanding a differentiated analysis would be helpful in order to understand possible uptake routes.

Extracellular vesicle internalization mechanisms

The uptake mechanism of ADEVs and thereby the uptake mechanism of InSUREns was not addressed in my experiments and remains an open question. As it has been shown, there is a plethora of possibilities for cells to absorb molecules; macropinocytosis, phagocytosis and the many forms of endocytosis (mediated by clathrin, lipid-raft, or caveolae), while each of those paths alters the way the cell uses the internalized molecules (Conner and Schmid, 2003). Still, the ADEV uptake examined here most likely happens through clathrin-dependent endocytosis, a process found in every mammalian cell (Conner and Schmid, 2003).

One study researching oligodendrocytic exosomes found that neuronal uptake works via clathrin-dependent endocytosis; when neurons were treated with Pitstop-2 and dynasore, thus suppressing dynamin activity and clathrin-mediated endocytosis, their uptake of oligodendrocytic exosomes was strongly impaired. Inhibiting clathrin-independent endocytosis by withdrawal of membrane cholesterol, conversely, had no such effect (Frühbeis et al., 2013).

Another study produced similar findings in neuroblastoma cells with siRNA knockdown of TSG101 and VPS4A, two important proteins in exosome secretion, cutting down the exosome secretion by over 75% (Sardar Sinha et al., 2018).

The EV uptake patterns we observed look similarly to other works (Czernek et al., 2015; Morales-Kastresana et al., 2017; Yuyama et al., 2012) with the strongest signals visible around the nucleus, but also strong uptake of 100nm-sized EVs at the neurites (Ibáñez et al., 2019). Similarly, in P12 cells, a cell line originating from the neuronal crest, CFSE-labeled exosomes are internalized throughout the whole cell, including processes (Tian et al., 2014). ADEVs from the Ribotracker mouse line contained labeled ribosomes (RPL4) and were uptaken by neurons in a similar pattern to the CFSE labeled ADEVs. If ADEVs contain mRNAs and ribosomes, most likely some mRNAs are already loaded on ribosomes and await translation after being endocytosed.

lncRNAs in ADEVs

Here we present datasets for synaptic, transferred and ADEV-contained lncRNAs, presented in Chapter 1 and 3 respectively, providing a great resource for further studies.

The area of lncRNA research is still in its infancy, with many functions still unresolved. Strikingly, 40% of all lncRNAs are present exclusively in the central nervous system (Briggs et al., 2015). The high amount of lncRNAs in ADEVs is strongly pointing towards a tight interplay between coding and non-coding cargo, as to inhibit RNAs translation (Muslimov et al., 1998), potentially akin to RNA granules during transport in EVs. In accordance, the dendritic abundance of lncRNAs is partly dependent on the neuron's activity (Lipovich et al., 2012).

The huge networks of interactions that we described between transferred lncRNAs and synaptic mRNAs (Fig S2, S3, Chapter 3) demonstrates how many RNAs could be affected by the addition of a single lncRNAs.

Apart from direct RNA-RNA interaction, lncRNAs can inhibit enzymatic activity through allosteric binding (Wang and Guo, 2008). They can even induce longer lasting epigenetic changes in recipient cells, for instance by activating histone methyltransferases (Kaneko et al., 2013; van Werven et al., 2012). Certain lncRNAs, e.g., Malat1 - the second most abundant lncRNA we found in chambers - are known to regulate synapse formation (Bernard et al., 2010).

Synaptic Tagging

Once a synapse receives a stimulus strong enough to trigger late LTP (L-LTP) it requires supply of proteins and other molecules from the soma. As this process of retrograde signaling from synapse to soma and then the transport back requires several hours, the synapse-to-be-changed must be tagged for the intracellular cargo to arrive at the right place, otherwise unspecific synapses would see their weight increased (Frey and Morris, 1997, 1998). To this day, the exact molecule that functions as the synaptic tag remains elusive.

In Chapter 3 I argued that the synaptic tagging and capturing problem could be addressed by horizontal RNA shuttling from astrocytes to neurons. Here, I provide a more in-depth discussion.

Certain criteria must be fulfilled by candidate molecules in order to be considered synaptic tags (Okuda et al., 2020). Namely the tag has to be, A) locally restricted, B) independent of protein translation and C) able to capture - that is to bind anterogradely transported proteins from the soma.

Transferred RNAs would fulfill all these criteria:

A) Their uptake can be spatially controlled through tripartite synapses, B) they do not need translation, rather they allow and enhance protein synthesis and C) they can easily capture RBP and other RNAs by being part of bigger complexes.

The fourth criterion D) demands the tag to be reversible to a certain extent. When synapses are only weakly stimulated, the increase of synaptic weight results in the protein-synthesis-independent early LTP (E-LTP-stimulus) that is transient and lasts only a couple of hours.

However, even in E-LTP the tag is present, thus criterion D) demands that the tag cannot turn an E-LTP into L-LTP without any additional stimulation. This could be easily achieved through many dose-dependent RNA-regulatory pathways. For instance, only when enough ncRNA have been transferred to sponge all transcripts of a specific miR, local translation would take place due to lifted inhibition. Similarly, only L-LTP inducing stimulation could cause enough ADEVs to be transferred, that the tag RNA can be either translated in sufficient amounts or bind sufficient molecules from the soma.

The last criterion E) states, that an E-LTP synapse can still undergo L-LTP, if another nearby synapse of the same neuron receives a L-LTP inducing stimulus shortly before or after the E-LTP stimulus at the first synapse. We can imagine three ways how that could be achieved with transferred RNAs.

With the synaptic tag coming from the outside, a few ADEVs might stay in the extracellular space for some time after secretion – those could then be internalized by the weaker stimulated synapse.

If, instead, synaptic tagging is dose-dependent, we suggest an intracellular transport of astrocytic RNA after uptake; if that transport happens from stronger to weaker stimulated synapses, this could tip the scale for the weaker synapse to undergo L-LTP.

Lastly, astrocytes have intracellular Ca^{2+} signaling, based on surrounding synaptic activity (Guerra-Gomes et al., 2018; Wang et al., 2009); if Ca^{2+} is already elevated in the end feet that is part of the E-LTP tripartite synapses and another Ca^{2+} increase is triggered by the end feet at an L-LTP synapse then this could drive Ca^{2+} levels at the E-LTP end feet high enough to release more ADEVs, even without further activity at the E-LTP synapse, resulting in L-LTP at the E-LTP synapse.

Strikingly, a study demonstrated how human astrocytes, which are larger and have more complex calcium signalling, vastly improved learning and LTP when implanted in mouse brains (Han et al., 2013). The authors inserted an engraftment of human glial progenitor cells into neonatal mice, where human cells dispersed evenly into hippocampus and cortex. In all tested learning paradigms, Barnes' maze, fear conditioning and memorizing object location, those mice scored much better than controls, who received mouse glial progenitor cells.

Neurites have been shown to be surprisingly void of ribosomes, yet after LTP induction polyribosomes were found right at stimulated spines (Ostroff et al., 2018). Excitingly many enriched as well as most abundant InSUREns RNAs were involved in ribosome biogenesis (Fig 3E). And since ribosome assembly happens in the cytoplasm (Nerurkar et al., 2015), InSUREns RNAs could allow ribosome assembly right at the synapse. In line with that would be that primarily monosomes are observed at the post-synapse (Biever et al., 2020), hinting at spontaneous small-scale genesis.

Additionally, we have tracked RPL4-RFP, a ribosomal protein, being transferred in the AWESAM ADEV experiment. It is unclear, whether or not RPL4-RFP was part of a complete ribosome during transfer, yet if ADEVs contain incomplete ribosomes as well as mRNAs for the missing parts, ribosome completion might happen after uptake of ADEVs by the neuron.

To summarize, our findings, in light with other research, build a case how astrocytic RNAs could be the elusive synaptic tags. This would further argue against a single tag molecule and in favor of the interplay of proteins and RNAs, neuronal as well as glial, to tag a synapse and capture L-LTP related proteins.

Outlook and possible improvements

1) InSUREns modifications and use cases

In light of the monosome or polysome preference of mRNAs (Biever et al., 2020) experiments with new Ribotag versions could provide interesting insights: if some ribosomal proteins mainly appear in monosomes, they might bind divergent sets of genes. Different ribosomal proteins for HA-pulldown could be used to this end; e.g., Rpl11, Rpl5 and Rpl4, all of which have been shown to be found more often in monosomes than in polysomes (Slavov et al., 2015).

Intercellularly transferred small ncRNAs could be obtained with InSUREns; one would simply have to switch the protein to which the HA-tag is attached; to isolate miRs, AGO2 could be expressed with attached HA-epitopes; to isolate piRNAs, one would use PIWI.

To increase yield and allow a more precise calculation of labeling efficiency, the TU-pulldown approach could be changed to SLAM-ITseq (Matsushima et al., 2018). By converting thiouracil bases into cytosine, effectively by-passing the necessity of a pulldown, much more RNA could be sequenced, allowing higher gene coverage.

There are no reasons why the InSUREns method would not work *in vivo* as well; 4-TU can cross the blood brain barrier (Tomorsky et al., 2017). So, by injecting both viruses in the same brain area, e.g., the hippocampus, and then having the animal perform memory tasks, one could readily investigate the extent of intercellular RNA transfer from astrocyte to neuron in the living brain during real engram formation.

2) ADEVs - open questions

Imaging studies would be very valuable to further to follow up ADEV internalization. Of special interest would be the extent to which internalized ADEVs stay at a synapse, or if they are transported inside neurites as well. In order to track ADEVs, one can use cell lines where the exosomal marker gene CD63 is coupled to GFP (Men et al., 2019), which would enable the investigating of subcellular properties of RNA transfer and the fate of EVs after uptake.

Likewise, single-molecule experiments would answer these questions for a candidate transcript; labeling here would be done with MS2-halotags (Wu et al., 2016) or mango aptamers (Autour et al., 2018).

Ideally one would combine this with CaMPARI, where recently-activated synapses are fluorescently labeled (Ebner et al., 2019).

Understanding the mechanisms, by which RNAs become ADEV cargo would be quite intriguing, especially how external stimuli might change cargo loading, if transcript isoforms change packaging and which mechanisms of loading exist for each type of ADEV. Given the vast number of transcripts we found, as well as the several thousand transcripts from other studies (Skog et al., 2008) it is likely that many different cargo-signals exist. Indeed, one pioneering study identified already three eight-base motifs for RNAs inside exosomes (Batagov et al., 2011). It appears that such motifs can form stemloops, affecting also miR binding (Bolukbasi et al., 2012).

3) Extending the regulatory network with more ncRNAs

There are two intriguing types of ncRNAs that could not be studied in this thesis, yet would complete the regulatory picture:

Before miRs mature they exist as pre-miRs, a hairpin structure, which is then cleaved by Dicer to yield both mature miR-arms. Maturation can also take place in neurites, sometimes upon activity (Sambandan et al., 2017), providing a further regulatory mechanism. Due to their size, pre-miRs were elusive in the data presented in this thesis and would require a different library preparation protocol (personal communication with manufacturers).

During the last couple of years circRNAs have been gaining interest; several are known to be located at synapses and sponging miRs seems to be one of their major functions (Memczak et al., 2013; Panda, 2018). Furthermore, their circular structure grants them long half-lives, hence they could influence local RNA pools, even in small quantities. To sequence circRNAs paired-end sequencing would be necessary.

4) Combining 4TU tagging and SNIDER

The combination of SNIDER with the 4TU-tagging method offers ways to investigate more detailed questions. For example, it would be possible for the first time to obtain pure post-synaptic RNAs, since as of now they are not obtainable without also including either glia remnants (neuropil) or pre-synaptic RNAs (hanging inserts).

I provided a pipetting scheme (Fig A2) with which pools of neurons can be transduced individually (data not shown). Neuronal pools of the chamber either extend axons into the microgrooves when distances to the perfusion channel is long (axonal side), or dendrites when that distance is short. To enhance this neurite - specificity, a coating-gradient of Laminin and PDL can be used, ensuring pure dendrites at the short site (Virlogeux et al., 2018).

Only the dendritic site would be transduced with UPRT, either continuously or, one day prior to SNIDER isolation, 4TU would be added to label all post-synaptic RNAs. Since the synaptic RNA amount is rather low, instead of a pulldown, the SLAM-Seq approach of base conversion could be used instead of a pulldown.

To take it one step further, also the axonal side could be transduced, yet with an optogenetic construct to stimulate the dendritic side. Thereby stimulation would occur in a more natural fashion, with action potential transduction taking place from pre- to post-synapses only inside the microgrooves. By applying different stimulation protocols, one could for instance test the transcriptomic differences, when either an E-LTP or L-LTP stimulation is given. Likewise, long term depression (LTD) could be induced and investigated.

Another interesting approach would be the perfusion with 4TU labelled ADEVs. Here one would prepare AWESAM cultures and transduce them with UPRT. By adding 4TU, ADEV RNAs would be labelled. Subsequently synapses in the chambers could be perfused with them. Afterwards synapses would be cut via SNIDER and transferred ADEV RNAs inside could be isolated and sequenced.

The strength of modern molecular biology lies in its rapidly developing methodology; protocols are becoming faster, more precise and modular. The future of dissecting the inner workings of synapses may lie within the clever combination of these tools.

I hope that my contributions to this toolbox will be a small stepping stone towards achieving this goal.

List of Abbreviations

AAV	Adeno-associated viruses
A β	Amyloid beta
ADEV	Astrocyte derived extracellular vesicles
ATP	Adenosine triphosphate
CA1	Cornus ammonis 1
circRNA	Circular RNA
CNS	Central nervous system
DAPI	4',6-diamidino-2-phenylindole
DIV	Day in vitro
DMEM	Dulbecco's Modified Eagle's Medium
DNA	Deoxyribonucleic acid
E-LTP	Early LTP
EPSP	excitatory postsynaptic potential
EV	Extracellular vesicles
FBS	Fetal Bovine Serum
6FAM	6-Carboxyfluorescein
GC	guanine-cytosine
GFAP	Glial fibrillary acidic protein
GFP	Green fluorescent protein
GO	Gene Ontology
HA	Human influenza hemagglutinin
KEGG	Kyoto Encyclopedia of Genes and Genomes
lncRNA	Long non-coding RNA
LNP	Lipid nano particle
LTD	Long-term depression
LTP	Long-term potentiation
miR	microRNA
mRNA	Messenger RNA
NB	Neurobasal
NGS	Next Generation Sequencing
PBS	Phosphate-buffered saline
PDMS	Polydimethylsiloxane
PS	Penicillin/Streptomycin
qPCR	Quantitative polymerase chain reaction
RBP	RNA binding protein
RNA	Ribonucleic acid
STED	Stimulated emission depletion
trfRNA	transfer RNA fragments
UPRT	Uracil phosphoribosyltransferase

Bibliography (for Introduction, Chapter 2 and 2.1 and Discussion)

Abcam Immunocytochemistry and immunofluorescence staining protocol:

<https://www.abcam.com/protocols/immunocytochemistry-immunofluorescence-protocol>

Akbalik, G., Langebeck-Jensen, K., Tushev, G., Sambandan, S., Rinne, J., Epstein, I., Cajigas, I., Vlatkovic, I., and Schuman, E.M. (2017). Visualization of newly synthesized neuronal RNA in vitro and in vivo using click-chemistry. *RNA Biol* 14, 20–28.

Araque, A., Parpura, V., Sanzgiri, R.P., and Haydon, P.G. (1999). Tripartite synapses: glia, the unacknowledged partner. *Trends Neurosci* 22, 208–215.

Arendt, T. (2009). Synaptic degeneration in Alzheimer's disease. *Acta Neuropathol* 118, 167–179.

Ariazi, J., Benowitz, A., De Biasi, V., Den Boer, M.L., Cherqui, S., Cui, H., Douillet, N., Eugenin, E.A., Favre, D., Goodman, S., et al. (2017). Tunneling Nanotubes and Gap Junctions—Their Role in Long-Range Intercellular Communication during Development, Health, and Disease Conditions. *Front. Mol. Neurosci.* 10, 333.

Autour, A., C. Y. Jeng, S., D. Cawte, A., Abdolazadeh, A., Galli, A., Panchapakesan, S.S.S., Rueda, D., Ryckelynck, M., and Unrau, P.J. (2018). Fluorogenic RNA Mango aptamers for imaging small non-coding RNAs in mammalian cells. *Nat Commun* 9, 656.

Baleriola, J., Walker, C.A., Jean, Y.Y., Crary, J.F., Troy, C.M., Nagy, P.L., and Hengst, U. (2014). Axonally Synthesized ATF4 Transmits a Neurodegenerative Signal across Brain Regions. *Cell* 158, 1159–1172.

Bardy, C., van den Hurk, M., Eames, T., Marchand, C., Hernandez, R.V., Kellogg, M., Gorris, M., Galet, B., Palomares, V., Brown, J., et al. (2015). Neuronal medium that supports basic synaptic functions and activity of human neurons in vitro. *Proc Natl Acad Sci USA* 112, E2725–E2734.

Bartol, T.M., Bromer, C., Kinney, J., Chirillo, M.A., Bourne, J.N., Harris, K.M., and Sejnowski, T.J. (2015). Nanoconnectomic upper bound on the variability of synaptic plasticity. *ELife* 4, e10778.

Batagov, A.O., Kuznetsov, V.A., and Kurochkin, I.V. (2011). Identification of nucleotide patterns enriched in secreted RNAs as putative cis-acting elements targeting them to exosome nano-vesicles. *BMC Genomics* 12, S18.

Bernard, D., Prasanth, K.V., Tripathi, V., Colasse, S., Nakamura, T., Xuan, Z., Zhang, M.Q., Sedel, F., Jourden, L., Couplier, F., et al. (2010). A long nuclear-retained non-coding RNA regulates synaptogenesis by modulating gene expression. *EMBO J* 29, 3082–3093.

Biever, A., Glock, C., Tushev, G., Ciirdaeva, E., Dalmay, T., Langer, J.D., and Schuman, E.M. (2020). Monosomes actively translate synaptic mRNAs in neuronal processes. *Science* 367, eaay4991.

Bolukbasi, M.F., Mizrak, A., Ozdener, G.B., Madlener, S., Ströbel, T., Erkan, E.P., Fan, J.-B., Breakefield, X.O., and Saydam, O. (2012). miR-1289 and “Zipcode”-like Sequence Enrich mRNAs in Microvesicles. *Mol Ther Nucleic Acids* 1, e10.

Bosch, M., Castro, J., Saneyoshi, T., Matsuno, H., Sur, M., and Hayashi, Y. (2014). Structural and Molecular Remodeling of Dendritic Spine Substructures during Long-Term Potentiation. *Neuron* 82, 444–459.

Briggs, J.A., Wolvetang, E.J., Mattick, J.S., Rinn, J.L., and Barry, G. (2015). Mechanisms of Long Non-coding RNAs in Mammalian Nervous System Development, Plasticity, Disease, and Evolution. *Neuron* 88, 861–877.

- Cajigas, I.J., Tushev, G., Will, T.J., tom Dieck, S., Fuerst, N., and Schuman, E.M. (2012). The Local Transcriptome in the Synaptic Neuropil Revealed by Deep Sequencing and High-Resolution Imaging. *Neuron* 74, 453–466.
- Campenot, R.B. (1977). Local control of neurite development by nerve growth factor. *Proc Natl Acad Sci U S A* 74, 4516–4519.
- Chang, F., Zhang, L.-H., Xu, W.-P., Jing, P., and Zhan, P.-Y. (2014). microRNA-9 attenuates amyloid β -induced synaptotoxicity by targeting calcium/calmodulin-dependent protein kinase kinase 2. *Mol Med Rep* 9, 1917–1922.
- Conner, S.D., and Schmid, S.L. (2003). Regulated portals of entry into the cell. *Nature* 422, 37–44.
- Cullen, D.K., Gilroy, M.E., Irons, H.R., and Laplaca, M.C. (2010). Synapse-to-neuron ratio is inversely related to neuronal density in mature neuronal cultures. *Brain Res* 1359, 44–55.
- Czernek, L., Chworos, A., and Duechler, M. (2015). The Uptake of Extracellular Vesicles is Affected by the Differentiation Status of Myeloid Cells. *Scand J Immunol* 82, 506–514.
- Datta Chaudhuri, A., Dasgheyb, R.M., DeVine, L.R., Bi, H., Cole, R.N., and Haughey, N.J. (2020). Stimulus-dependent modifications in astrocyte-derived extracellular vesicle cargo regulate neuronal excitability. *Glia* 68, 128–144.
- Doyle, M., and Kiebler, M.A. (2011). Mechanisms of dendritic mRNA transport and its role in synaptic tagging. *EMBO J* 30, 3540–3552.
- Ebner, C., Ledderose, J., Zolnik, T.A., Dominiak, S.E., Turko, P., Papoutsis, A., Poirazi, P., Eickholt, B.J., Vida, I., Larkum, M.E., et al. (2019). Optically Induced Calcium-Dependent Gene Activation and Labeling of Active Neurons Using CaMPARI and Cal-Light. *Front. Synaptic Neurosci.* 11, 16.
- Endo, R., Takashima, N., and Tanaka, M. (2020). Abnormal Local Translation in Dendrites Impairs Cognitive Functions in Neuropsychiatric Disorders. In *Make Life Visible*, Y. Toyama, A. Miyawaki, M. Nakamura, and M. Jinzaki, eds. (Singapore: Springer Singapore), pp. 179–186.
- Epple, R., Krüger, D., Berulava, T., Brehm, G., Islam, R., Köster, S., and Fischer, A. (2020). The Coding And Small-Non-Coding Hippocampal Synaptic RNAome (Neuroscience). *BioRxiv*: 10.1101/2020.11.27.401901
<https://www.biorxiv.org/content/10.1101/2020.11.27.401901v1.full>
- Fairchild, C.L.A., Cheema, S.K., Wong, J., Hino, K., Simó, S., and La Torre, A. (2019). Let-7 regulates cell cycle dynamics in the developing cerebral cortex and retina. *Sci Rep* 9, 15336.
- Fonkeu, Y., Kraynyukova, N., Hafner, A.-S., Kochen, L., Sartori, F., Schuman, E.M., and Tchumatchenko, T. (2019). How mRNA Localization and Protein Synthesis Sites Influence Dendritic Protein Distribution and Dynamics. *Neuron* 103, 1109–1122.e7.
- Fornasiero, E.F., Mandad, S., Wildhagen, H., Alevra, M., Rammner, B., Keihani, S., Opazo, F., Urban, I., Ischebeck, T., Sakib, M.S., et al. (2018). Precisely measured protein lifetimes in the mouse brain reveal differences across tissues and subcellular fractions. *Nat Commun* 9, 4230.
- Frey, U., and Morris, R.G. (1997). Synaptic tagging and long-term potentiation. *Nature* 385, 533–536.
- Frey, U., and Morris, R.G. (1998). Synaptic tagging: implications for late maintenance of hippocampal long-term potentiation. *Trends Neurosci* 21, 181–188.
- Frühbeis, C., Fröhlich, D., Kuo, W.P., Amphornrat, J., Thilemann, S., Saab, A.S., Kirchhoff, F., Möbius, W., Goebbels, S., Nave, K.-A., et al. (2013). Neurotransmitter-Triggered Transfer of Exosomes Mediates Oligodendrocyte–Neuron Communication. *PLoS Biol* 11, e1001604.

- Gharbi, T., Zhang, Z., and Yang, G.-Y. (2020). The Function of Astrocyte Mediated Extracellular Vesicles in Central Nervous System Diseases. *Front. Cell Dev. Biol.* *8*, 568889.
- Giuditta, A., Dettbarn, W.D., and Brzin, M. (1968). Protein synthesis in the isolated giant axon of the squid. *Proceedings of the National Academy of Sciences* *59*, 1284–1287.
- Giuditta, A., Cupellot, A., and Lazzarini, G. (1980). Ribosomal RNA in the Axoplasm of the Squid Giant Axon. *J Neurochem* *34*, 1757–1760.
- Giuditta, A., Eyman, M., and Kaplan, B.B. (2002). Gene expression in the squid giant axon: neurotransmitter modulation of RNA transfer from periaxonal glia to the axon. *The Biological Bulletin* *203*, 189–190.
- Giuditta, A., Chun, J.T., Eyman, M., Cefaliello, C., Bruno, A.P., and Crispino, M. (2008). Local gene expression in axons and nerve endings: the glia-neuron unit. *Physiological Reviews* *88*, 515–555.
- Giusti, S.A., Vogl, A.M., Brockmann, M.M., Vercelli, C.A., Rein, M.L., Trümbach, D., Wurst, W., Cazalla, D., Stein, V., Deussing, J.M., et al. (2014). MicroRNA-9 controls dendritic development by targeting REST. *ELife* *3*, e02755.
- Gomes, A.R., Sangani, N.B., Fernandes, T.G., Diogo, M.M., Curfs, L.M.G., and Reutelingsperger, C.P. (2020). Extracellular Vesicles in CNS Developmental Disorders. *IJMS* *21*, 9428.
- Guerra-Gomes, S., Sousa, N., Pinto, L., and Oliveira, J.F. (2018). Functional Roles of Astrocyte Calcium Elevations: From Synapses to Behavior. *Front. Cell. Neurosci.* *11*, 427.
- Haimovich, G., Ecker, C.M., Dunagin, M.C., Eggan, E., Raj, A., Gerst, J.E., and Singer, R.H. (2017). Intercellular mRNA trafficking via membrane nanotube-like extensions in mammalian cells. *PNAS* *114*, E9873–E9882.
- Han, X., Chen, M., Wang, F., Windrem, M., Wang, S., Shanz, S., Xu, Q., Oberheim, N.A., Bekar, L., Betstadt, S., et al. (2013). Forebrain engraftment by human glial progenitor cells enhances synaptic plasticity and learning in adult mice. *Cell Stem Cell* *12*, 342–353.
- Hanus, C., and Schuman, E.M. (2013). Proteostasis in complex dendrites. *Nat Rev Neurosci* *14*, 638–648.
- Hayashi-Takagi, A. (2017). Synapse pathology and translational applications for schizophrenia. *Neurosci Res* *114*, 3–8.
- Higa, G.S.V., de Sousa, E., Walter, L.T., Kinjo, E.R., Resende, R.R., and Kihara, A.H. (2014). MicroRNAs in neuronal communication. *Mol. Neurobiol.* *49*, 1309–1326.
- Huber, K.M., Kayser, M.S., and Bear, M.F. (2000). Role for rapid dendritic protein synthesis in hippocampal mGluR-dependent long-term depression. *Science* *288*, 1254–1257.
- Ibáñez, F., Montesinos, J., Ureña-Peralta, J.R., Guerri, C., and Pascual, M. (2019). TLR4 participates in the transmission of ethanol-induced neuroinflammation via astrocyte-derived extracellular vesicles. *J Neuroinflammation* *16*, 136.
- Jasmin, B.J., Lavoie, P.A., and Gardiner, P.F. (1988). Fast axonal transport of labeled proteins in motoneurons of exercise-trained rats. *Am J Physiol* *255*, C731-736.
- Jovičić, A., and Gitler, A.D. (2017). Distinct repertoires of microRNAs present in mouse astrocytes compared to astrocyte-secreted exosomes. *PLoS One* *12*, e0171418.
- Kaneko, S., Son, J., Shen, S.S., Reinberg, D., and Bonasio, R. (2013). PRC2 binds active promoters and contacts nascent RNAs in embryonic stem cells. *Nat Struct Mol Biol* *20*, 1258–1264.
- Kang, H., and Schuman, E.M. (1996). A Requirement for Local Protein Synthesis in Neurotrophin-Induced Hippocampal Synaptic Plasticity. *Science* *273*, 1402–1406.

Kerrigan, T.L., and Randall, A.D. (2013). A New Player in the “Synaptopathy” of Alzheimer’s Disease – Arc/Arg 3.1. *Front. Neur.* 4.

Koenig, E. (1967). Synthetic mechanisms in the axon - IV. In Vitro incorporation of [³H] precursors into axonal protein and RNA. *J Neurochem* 14, 437–446.

Kosik, K.S. (2016). Life at Low Copy Number: How Dendrites Manage with So Few mRNAs. *Neuron* 92, 1168–1180.

von Kügelgen, N., and Chekulaeva, M. (2020). Conservation of a core neurite transcriptome across neuronal types and species. *Wiley Interdiscip Rev RNA* 11, e1590.

Lazzara (2020). Protocol for Puncta, Edge Intensity, Area and Shape Measurements.

Li, H., Wu, C., Aramayo, R., Sachs, M.S., and Harlow, M.L. (2015). Synaptic vesicles contain small ribonucleic acids (sRNAs) including transfer RNA fragments (trfRNA) and microRNAs (miRNA). *Scientific Reports* 5, 14918.

Lipovich, L., Dachet, F., Cai, J., Bagla, S., Balan, K., Jia, H., and Loeb, J.A. (2012). Activity-dependent human brain coding/noncoding gene regulatory networks. *Genetics* 192, 1133–1148.

Lisman, J., Buzsáki, G., Eichenbaum, H., Nadel, L., Ranganath, C., and Redish, A.D. (2017). Viewpoints: how the hippocampus contributes to memory, navigation and cognition. *Nat Neurosci* 20, 1434–1447.

Liu, K.K.L., Hagan, M.F., and Lisman, J.E. (2017). Gradation (approx. 10 size states) of synaptic strength by quantal addition of structural modules. *Phil. Trans. R. Soc. B* 372, 20160328.

López-Erauskin, J., Tadokoro, T., Baughn, M.W., Myers, B., McAlonis-Downes, M., Chillon-Marinhas, C., Asiaban, J.N., Artates, J., Bui, A.T., Vetto, A.P., et al. (2018). ALS/FTD-Linked Mutation in FUS Suppresses Intra-axonal Protein Synthesis and Drives Disease Without Nuclear Loss-of-Function of FUS. *Neuron* 100, 816-830.e7.

Matsushima, W., Herzog, V.A., Neumann, T., Gapp, K., Zuber, J., Ameres, S.L., and Miska, E.A. (2018). SLAM-ITseq: sequencing cell type-specific transcriptomes without cell sorting. *Development* 145, dev164640.

Mayorquin, L.C., Rodriguez, A.V., Sutachan, J.-J., and Albarracín, S.L. (2018). Connexin-Mediated Functional and Metabolic Coupling Between Astrocytes and Neurons. *Front. Mol. Neurosci.* 11, 118.

Memczak, S., Jens, M., Elefsinioti, A., Torti, F., Krueger, J., Rybak, A., Maier, L., Mackowiak, S.D., Gregersen, L.H., Munschauer, M., et al. (2013). Circular RNAs are a large class of animal RNAs with regulatory potency. *Nature* 495, 333–338.

Men, Y., Yelick, J., Jin, S., Tian, Y., Chiang, M.S.R., Higashimori, H., Brown, E., Jarvis, R., and Yang, Y. (2019). Exosome reporter mice reveal the involvement of exosomes in mediating neuron to astroglia communication in the CNS. *Nat Commun* 10, 4136.

Morales-Kastresana, A., Telford, B., Musich, T.A., McKinnon, K., Clayborne, C., Braig, Z., Rosner, A., Demberg, T., Watson, D.C., Karpova, T.S., et al. (2017). Labeling Extracellular Vesicles for Nanoscale Flow Cytometry. *Sci Rep* 7, 1878.

Morhayim, J., Peppel, J., Demmers, J.A.A., Kocer, G., Nigg, A.L., Driel, M., Chiba, H., and Leeuwen, J.P. (2015). Proteomic signatures of extracellular vesicles secreted by nonmineralizing and mineralizing human osteoblasts and stimulation of tumor cell growth. *FASEB j.* 29, 274–285.

Müller, K., Schnatz, A., Schillner, M., Woertge, S., Müller, C., von Graevenitz, I., Waisman, A., van Minnen, J., and Vogelaar, C.F. (2018). A predominantly glial origin of axonal ribosomes after nerve injury. *Glia* 66, 1591–1610.

Muslimov, I.A., Banker, G., Brosius, J., and Tiedge, H. (1998). Activity-dependent Regulation of Dendritic BC1 RNA in Hippocampal Neurons in Culture. *Journal of Cell Biology* 141, 1601–1611.

- Nerurkar, P., Altwater, M., Gerhardy, S., Schütz, S., Fischer, U., Weirich, C., and Panse, V.G. (2015). Eukaryotic Ribosome Assembly and Nuclear Export. In *International Review of Cell and Molecular Biology*, (Elsevier), pp. 107–140.
- Oh, J.-Y., Kwon, A., Jo, A., Kim, H., Goo, Y.-S., Lee, J.-A., and Kim, H.K. (2013). Activity-dependent synaptic localization of processing bodies and their role in dendritic structural plasticity. *Journal of Cell Science* *126*, 2114–2123.
- Okuda, K., Højgaard, K., Privitera, L., Bayraktar, G., and Takeuchi, T. (2020). Initial memory consolidation and the synaptic tagging and capture hypothesis. *Eur J Neurosci* *ejn.14902*.
- Ostroff, L.E., Watson, D.J., Cao, G., Parker, P.H., Smith, H., and Harris, K.M. (2018). Shifting patterns of polyribosome accumulation at synapses over the course of hippocampal long-term potentiation. *Hippocampus* *28*, 416–430.
- Panda, A.C. (2018). Circular RNAs Act as miRNA Sponges. *Adv Exp Med Biol* *1087*, 67–79.
- Park, J.W., Vahidi, B., Taylor, A.M., Rhee, S.W., and Jeon, N.L. (2006). Microfluidic culture platform for neuroscience research. *Nat Protoc* *1*, 2128–2136.
- Peng, Y., Wang, X., Guo, Y., Peng, F., Zheng, N., He, B., Ge, H., Tao, L., and Wang, Q. (2019). Pattern of cell-to-cell transfer of micro RNA by gap junction and its effect on the proliferation of glioma cells. *Cancer Sci* *110*, 1947–1958.
- Perea, G., Navarrete, M., and Araque, A. (2009). Tripartite synapses: astrocytes process and control synaptic information. *Trends Neurosci* *32*, 421–431.
- Ramachandran, S., and Palanisamy, V. (2012). Horizontal Transfer of RNAs: Exosomes as mediators of intercellular communication. *Wiley Interdiscip Rev RNA* *3*, 286–293.
- Rangaraju, V., Tom Dieck, S., and Schuman, E.M. (2017). Local translation in neuronal compartments: how local is local? *EMBO Rep.* *18*, 693–711.
- Regehr, K.J., Domenech, M., Koepsel, J.T., Carver, K.C., Ellison-Zelski, S.J., Murphy, W.L., Schuler, L.A., Alarid, E.T., and Beebe, D.J. (2009). Biological implications of polydimethylsiloxane-based microfluidic cell culture. *Lab Chip* *9*, 2132.
- Reinhart, B.J., Slack, F.J., Basson, M., Pasquinelli, A.E., Bettinger, J.C., Rougvie, A.E., Horvitz, H.R., and Ruvkun, G. (2000). The 21-nucleotide let-7 RNA regulates developmental timing in *Caenorhabditis elegans*. *Nature* *403*, 901–906.
- Sambandan, S., Akbalik, G., Kochen, L., Rinne, J., Kahlstatt, J., Glock, C., Tushev, G., Alvarez-Castelao, B., Heckel, A., and Schuman, E.M. (2017). Activity-dependent spatially localized miRNA maturation in neuronal dendrites. *Science* *355*, 634–637.
- Sardar Sinha, M., Ansell-Schultz, A., Civitelli, L., Hildesjö, C., Larsson, M., Lannfelt, L., Ingelsson, M., and Hallbeck, M. (2018). Alzheimer’s disease pathology propagation by exosomes containing toxic amyloid-beta oligomers. *Acta Neuropathol* *136*, 41–56.
- Savas, J.N., Ma, B., Deinhardt, K., Culver, B.P., Restituto, S., Wu, L., Belasco, J.G., Chao, M.V., and Tanese, N. (2010). A role for huntington disease protein in dendritic RNA granules. *J Biol Chem* *285*, 13142–13153.
- Skog, J., Würdinger, T., van Rijn, S., Meijer, D.H., Gainche, L., Curry, W.T., Carter, B.S., Krichevsky, A.M., and Breakefield, X.O. (2008). Glioblastoma microvesicles transport RNA and proteins that promote tumour growth and provide diagnostic biomarkers. *Nat Cell Biol* *10*, 1470–1476.
- Slavov, N., Semrau, S., Airoidi, E., Budnik, B., and van Oudenaarden, A. (2015). Differential Stoichiometry among Core Ribosomal Proteins. *Cell Reports* *13*, 865–873.
- Song, J., Cho, K.J., Oh, Y., and Lee, J.E. (2015). Let7a involves in neural stem cell differentiation relating with TLX level. *Biochemical and Biophysical Research Communications* *462*, 396–401.

- Sotelo, J.R., Canclini, L., Kun, A., Sotelo-Silveira, J.R., Calliari, A., Cal, K., Bresque, M., Dipaolo, A., Farias, J., and Mercer, J.A. (2014). Glia to axon RNA transfer. *Developmental Neurobiology* 74, 292–302.
- Stein, C.A., Hansen, J.B., Lai, J., Wu, S., Voskresenskiy, A., Høg, A., Worm, J., Hedtjörn, M., Souleimanian, N., Miller, P., et al. (2010). Efficient gene silencing by delivery of locked nucleic acid antisense oligonucleotides, unassisted by transfection reagents. *Nucleic Acids Res* 38, e3.
- Taylor, A.M., Dieterich, D.C., Ito, H.T., Kim, S.A., and Schuman, E.M. (2010). Microfluidic local perfusion chambers for the visualization and manipulation of synapses. *Neuron* 66, 57–68.
- Terada, S., Nakata, T., Peterson, A.C., and Hirokawa, N. (1996). Visualization of slow axonal transport in vivo. *Science* 273, 784–788.
- Tian, T., Zhu, Y.-L., Zhou, Y.-Y., Liang, G.-F., Wang, Y.-Y., Hu, F.-H., and Xiao, Z.-D. (2014). Exosome Uptake through Clathrin-mediated Endocytosis and Macropinocytosis and Mediating miR-21 Delivery. *J. Biol. Chem.* 289, 22258–22267.
- Tomorsky, J., DeBlander, L., Kentros, C.G., Doe, C.Q., and Niell, C.M. (2017). TU-Tagging: A Method for Identifying Layer-Enriched Neuronal Genes in Developing Mouse Visual Cortex. *ENeuro* 4.
- Topol, A., Zhu, S., Hartley, B.J., English, J., Hauberg, M.E., Tran, N., Rittenhouse, C.A., Simone, A., Ruderfer, D.M., Johnson, J., et al. (2016). Dysregulation of miRNA-9 in a Subset of Schizophrenia Patient-Derived Neural Progenitor Cells. *Cell Reports* 15, 1024–1036.
- Tushev, G., Glock, C., Heumüller, M., Biever, A., Jovanovic, M., and Schuman, E.M. (2018). Alternative 3' UTRs Modify the Localization, Regulatory Potential, Stability, and Plasticity of mRNAs in Neuronal Compartments. *Neuron* 98, 495-511.e6.
- Upadhyaya, R., Zingg, W., Shetty, S., and Shetty, A.K. (2020). Astrocyte-derived extracellular vesicles: Neuroreparative properties and role in the pathogenesis of neurodegenerative disorders. *Journal of Controlled Release* 323, 225–239.
- Valadi, H., Ekström, K., Bossios, A., Sjöstrand, M., Lee, J.J., and Lötvall, J.O. (2007). Exosome-mediated transfer of mRNAs and microRNAs is a novel mechanism of genetic exchange between cells. *Nat Cell Biol* 9, 654–659.
- van Werven, F.J., Neuert, G., Hendrick, N., Lardenois, A., Buratowski, S., van Oudenaarden, A., Primig, M., and Amon, A. (2012). Transcription of Two Long Noncoding RNAs Mediates Mating-Type Control of Gametogenesis in Budding Yeast. *Cell* 150, 1170–1181.
- Venturini, A., Passalacqua, M., Pelassa, S., Pastorino, F., Tedesco, M., Cortese, K., Gagliani, M.C., Leo, G., Maura, G., Guidolin, D., et al. (2019). Exosomes From Astrocyte Processes: Signaling to Neurons. *Front. Pharmacol.* 10, 1452.
- Vickers, C.A., Dickson, K.S., and Wyllie, D.J. (2005). Induction and maintenance of late-phase long-term potentiation in isolated dendrites of rat hippocampal CA1 pyramidal neurones. *The Journal of Physiology* 568, 803–813.
- Virlogeux, A., Moutaux, E., Christaller, W., Genoux, A., Bruyère, J., Fino, E., Charlot, B., Cazorla, M., and Saudou, F. (2018). Reconstituting Corticostriatal Network on-a-Chip Reveals the Contribution of the Presynaptic Compartment to Huntington's Disease. *Cell Reports* 22, 110–122.
- Walters, B.J., Mercaldo, V., Gillon, C.J., Yip, M., Neve, R.L., Boyce, F.M., Frankland, P.W., and Josselyn, S.A. (2017). The Role of The RNA Demethylase FTO (Fat Mass and Obesity-Associated) and mRNA Methylation in Hippocampal Memory Formation. *Neuropsychopharmacology* 42, 1502–1510.
- Wang, B., and Bao, L. (2017). Axonal microRNAs: localization, function and regulatory mechanism during axon development. *J Mol Cell Biol* 9, 82–90.
- Wang, X., and Guo, L. (2008). Effect of tetramethyl ammonium hydroxide on rheological properties of aqueous zirconia suspensions with polyacrylate. *Colloids and Surfaces A: Physicochemical and Engineering Aspects* 324, 126–130.

- Wang, X., Takano, T., and Nedergaard, M. (2009). Astrocytic calcium signaling: mechanism and implications for functional brain imaging. *Methods Mol Biol* *489*, 93–109.
- Wang, X., Bukoreshtliev, N.V., and Gerdes, H.-H. (2012). Developing Neurons Form Transient Nanotubes Facilitating Electrical Coupling and Calcium Signaling with Distant Astrocytes. *PLOS ONE* *7*, e47429.
- Wang, X., Kery, R., and Xiong, Q. (2018). Synaptopathology in autism spectrum disorders: Complex effects of synaptic genes on neural circuits. *Prog Neuropsychopharmacol Biol Psychiatry* *84*, 398–415.
- Wells, D.G. (2006). RNA-binding proteins: a lesson in repression. *J Neurosci* *26*, 7135–7138.
- Wu, B., Eliscovich, C., Yoon, Y.J., and Singer, R.H. (2016). Translation dynamics of single mRNAs in live cells and neurons. *Science* *352*, 1430–1435.
- Xu, J., Chen, Q., Zen, K., Zhang, C., and Zhang, Q. (2013). Synaptosomes secrete and uptake functionally active microRNAs via exocytosis and endocytosis pathways. *Journal of Neurochemistry* *124*, 15–25.
- Yuyama, K., Sun, H., Mitsutake, S., and Igarashi, Y. (2012). Sphingolipid-modulated Exosome Secretion Promotes Clearance of Amyloid- β by Microglia. *J. Biol. Chem.* *287*, 10977–10989.
- Zhang, W., Kim, P.J., Chen, Z., Lokman, H., Qiu, L., Zhang, K., Rozen, S.G., Tan, E.K., Je, H.S., and Zeng, L. (2016). MiRNA-128 regulates the proliferation and neurogenesis of neural precursors by targeting PCM1 in the developing cortex. *ELife* *5*, e11324.
- Zhao, C., Sun, G., Li, S., Lang, M.-F., Yang, S., Li, W., and Shi, Y. (2010). MicroRNA *let-7b* regulates neural stem cell proliferation and differentiation by targeting nuclear receptor TLX signaling. *Proc Natl Acad Sci USA* *107*, 1876–1881.

Acknowledgements

Lieber André, vielen Dank für all die Unterstützung und die Möglichkeiten, die ich bei dir im Labor hatte. Egal, wie viele Ideen ich hatte und egal wie exotisch diese waren, ich konnte sie immer mit dir diskutieren und weiter ausfeilen. Durch die Forschungsfreiheit, die du mir ermöglicht hast, konnte ich meiner Neugier folgen und die Experimente durchführen, die mich am meisten interessiert haben.

Dear Camin, dear Tiago, I want to thank you for your continuous feedback and helpful insights.

When I started out, you, Eva, showed me the way around pipettes, protocols and problems. Your scientific genius is quite unique and if I had only heard about your efficiency, I would have to picture you with 8 arms.

Henning for prezident! Oder andersherum. Vielen Dank für deine Bereitschaft immer zu helfen, zu zuhören und mich mit Glukose zu versorgen. Dein messerscharfer Zynismus hat mir auch in den längeren Labortage ein dickes Grinsen über's Gesicht gejagt.

Ricardo, I still have to decide what impresses me more: your deep running trivia knowledge or your insane work ethic – keep rockin'!

Danke an Hendrik und Christian für die mitunter ausgedehnten, lauschigen und Frozen-Jogurt beinhaltenden Mittagsrunden.

My heart also goes out to all current and former lab members!

Sasha, Gaurav and Tea for long philosophical discussions, I wish you all the best in your future.

Thank you, Patricia and Mariia, for trusting me in supervising your master theses. You helped me immensely and without you, I would have needed probably another 4 years to finish.

Die Zeit in Göttingen war auch eine überaus gesellige. Ein sattes Prost an den Stammtisch!
Danke, Albert, Georg, Felix, Nikos and Habakuk.

An die alte Hobbithöhle: ja, wir haben jetzt alle mehr Quadratmeter, aber können wir jemals so viel lachen wie in dieser Bude? Danke an die unglaubliche Zeit, Daniel und Alex.

Myrtaki - I am ecstatic to have you in my life and by my side.
Your love carried me through the last year, and I cannot wait to secrete dopamine, serotonin and endorphines with you throughout our time to come; let's grow a hell of a lot of synapses together!

Meiner Familie möchte ich zum Schluss danken. Ohne eure Unterstützung und Ermunterungen hätte diese Arbeit nicht verfasst werden können. Ludwig, danke für deine Gelassenheit. Papa, danke, dass du mir gezeigt hast, wie man sich richtig in eine Sache reinkniet und danke Mama für deine ansteckende, positive Lebenseinstellung und dein Interesse an meinem Schaffen.

Declaration

I hereby declare that I have written the dissertation

“The Synaptic RNAome - identification, interactions and intercellular transfer”

independently with no other aids or sources than stated.

Robert Epple Göttingen, 23.01.21